Investigating novel pathways regulating mitophagy in Parkinson's Disease

Daniela Melandri

Queen Square Institute of Neurology, UCL

Doctor Of Philosophy

2022

I, Daniela Melandri, confirm that the work presented in this thesis is my own. Where information has been derived from other sources, I confirm that this has been indicated in the thesis.

Date: 26 January 2022

Signed:

Acknowledgements

First thanks goes to my supervisors, Helene and Sonia, for choosing me back ages ago after saying I was most proud of my sci comm efforts and for the support and guidance throughout these years. Thanks to their labs too! Have to particularly thank the postdocs that taught me so much, many bits of the thesis would not exist! Noemi, Minee, Amy, Eliona, Ben thank you. And the girls in the lab that were always up for a chat, Darija, Jackie, Bea, Sam, grazie.

Looking back at certain moments, I honestly don't know what I would have done without some people. My lab wife Emily, who always bet on me and got my head in the game, maestra come me nell'avere i belli problemi, and many other things. The fun office 719 for the laughs and listening to rants, Alkyoni and Mark. My art buddy Georgie. My theatre buddy Bridget. The people that were always up for a coffee and my confusion at life in England, Lorenza, Pablo. The neighbours that adopted me as an extra grandchild and cheered on Italy with me, Luisa and Bruno. London, you were wonderful too!

My new family, built in London and now all over the world, I love you all. Le coinquiline quelle belle e speciali, Giulia e Annalisa, and the flatmates that feed you when you are sick, thank you Ricardo, I nearly nailed it. Julia, look where I went from that cell culture hood in the cruciform! The old family, i molecolari sempre piu' fighi, we can nearly lift the ban on the T-word. The friends from home, quelli che ti danno la carica sempre, Bea, e quelli che studiano con te da tanto tempo, Lorenzo.

And my real family. Far away Zii but always close, you helped loads from down under. And finally, mamma, papa', Michela, Giuseppe (e Holly), non ce l'avrei mai fatta senza il vostro sostegno e incoraggiamento, non sarei neanche qui a scrivere queste ultime parole nella tesi di dottorato. Vi voglio tanto tanto bene.

Abstract

Parkinson's disease (PD) is the second most common neurodegenerative disease and no disease modifying therapy has been approved as of yet. The analysis of the familial forms of PD has led to the identification of the monogenic causes and has implicated key pathways in the pathogenesis of the diseases. Genome-wide association studies have greatly advanced our understanding of genetic risk of PD. However, identifying the causal genes and their functional significance is challenging. Mitophagy, the selective degradation of damaged mitochondria, is a key causative pathway in monogenic PD, but whether it is relevant for sporadic PD is unclear. In this thesis, I describe the setup of a high content mitophagy siRNA screen to evaluate the functional role of prioritised PD risk genes. This screen identified two novel regulators of mitophagy, KAT8 and KANSL1, part of a protein complex involved in lysine acetylation. KAT8 and KANSL1 modulate PINK1 activity and subsequent mitophagy, linking sporadic and familial PD and providing a novel pathway for therapeutic investigation. Finally, I describe the optimisation of iPSC-derived neuron and iNeuron models to study mitophagy in more physiological systems. This includes the optimisation of CRISPR interference in the iNeuron model to modulate the levels of KAT8 and KANSL1 and investigate their role in regulating mitophagy in neuronal cells.

Impact Statement

Parkinson's disease (PD) is a common neurodegenerative for which no disease modifying cure exists. The challenge in the field is finding new targets for drug development that are effective on patients. The support of genetic evidence when choosing a target to develop greatly increases the chances of success in clinical trials. Therefore, a great effort is undergoing in the field to identify and understand which genes contribute to increased risk of PD.

The genes known to cause PD have identified mitochondria as a key player in the pathogenesis of the disease. Mitochondria provide energy to all cells in the body, as well as performing a variety of essential roles, and dysfunctional mitochondria are implicated in many neurodegenerative diseases. The clearance of dysfunctional mitochondria in cells is a process called mitophagy, and this process is inefficient or absent in PD patients with mutations in certain genes. Removing dysfunctional mitochondria from cells is considered an important therapeutic avenue, but many aspects of the regulation of mitophagy are still poorly understood.

In this thesis, I developed an imaging screen to study how new PD risk genes affect mitochondria. This technique can be used to study many different genes at once, speeding up the identification of relevant candidate pathways which are relevant for PD. In particular, it helps functionally evaluate genes that are difficult to study with conventional genetic methods. It can also help link known pathways (mitophagy) to previously unknown regulators of these pathways. I describe how this screen identified two disease-relevant risk genes and how they impact mitophagy, providing

a novel therapeutic avenue. Moreover, for the first time in this pathway, risk genes are connected with causal genes, implicating that the same therapeutic strategy might be useful for different subtypes of PD patients.

Finally, PD is a disease in which the certain neurons in the brain die. For ease of use, most studies in the past have been carried out in cancer cell lines, which have very different characteristics to neurons. In the final chapter, I optimise a neuronal cell model to detect and modulate mitophagy. This is important to study how putative drug targets are regulated specifically in neurons. A consensus in the field on the parameters to use in such a model will be essential to correctly evaluate candidate genes. I describe differences in culture systems which influence mitophagy.

Table of Contents

Table of Figures

Table of Tables

Abbreviations

%CV	Percent Coefficient of Variation
AAVS1	Adeno-associated virus integration site 1
ALS	Amyotrophic lateral sclerosis
CCCP	Carbonyl cyanide m-chlorophenyl hydrazone
cDNA	complementary DNA
CFP	Cyan Fluorescent Protein
CoA	Coenzyme A
CRISPR	Clustered Regularly Interspaced Short Palindromic Repeats
CRISPRi	CRISPR interference
dCas9	dead Cas9
eQTL	expression Quantitative Trait Loci
FCCP	carbonyl cyanide 4-(trifluoromethoxy)phenylhydrazone
FTD	Frontotemporal dementia
GWAS	Genome-wide association study
HCS	High Content Screening
IMM	Inner Mitochondrial Membrane
iPSC(s)	Induced Pluripotent Stem Cell(s)
KAT	Lysine Acetyltransferase
KDAC	Lysine decetylases
KO/KD	Knockout/knockdown
LIR	LC3-interacting region
MAP2	Microtubule-associated protein 2
mDA	Midbrain Dopaminergic (neurons)

MTS	Mitochondrial Targeting Sequence
NA	Numerical aperture
NeuN	Neuronal Nuclei
NLS	Non Specific Lethal (complex)
NPC(s)	Neural Precursor Cell(s)
O/A	oligomycin/antimycin
OCR	Oxygen Consumption Rate
OGT	O-Linked N-Acetylglucosamine (GlcNAc) Transferase
OMM	Outer Mitochondrial Membrane
ORF	Open Reading Frames
PD	Parkinson's Disease
PMPCB	Mitochondrial-processing peptidase subunit beta
POE	Parkin overexpressing
PTM	Post Translational Modification
pUb(Ser65)	phospho-ubiquitin (Serine 65)
RNAi	RNA interference
ROS	Reactive Oxygen Species
SCR	Scrambled - non targeting control
sgRNA	Single Guide RNA
siRNA	small interfering RNA
SNP	Single nucleotide polymorphism
SNpc	Substantia Nigra pars compacta
TMRM	Tetramethylrhodamine, methyl ester
TOM20	Translocase of the outer membrane subunit 20kDa
UPRmt	Unfolded Protein Response (mitochondrial)

YFP	Yellow Fluorescent Protein

Introduction

Parkinson's Disease

Parkinson's disease (PD) is the second-most common neurodegenerative disease, affecting 2-3% of the population ≥ 65 years old (Poewe *et al.*, 2017). PD is relatively rare before 50 years of age, but its incidence rises sharply with age and it is more common in men than women (Dorsey *et al.*, 2018). The incidence and prevalence of PD has greatly increased in the past decades, and it has been suggested that it might be the fastest growing neurodegenerative disease worldwide (Feigin *et al.*, 2019). This rapid growth, together with the long disease progression in an ageing population, makes PD a relevant socioeconomical problem. Therefore, there is an urgent need to develop novel therapeutic strategies to modify or slow the disease.

The classical clinical features of PD are the so-called parkinsonian motor symptoms, such as bradykinesia, muscle rigidity, postural instability, rest tremor. However, patients also present a variety of non-motor symptoms, such as sleep disorders, cognitive impairment, psychiatric disorders, autonomic dysfunction, hyposmia, pain and, with disease progression, dementia (Kalia and Lang, 2015), which severely impact quality of life. The non-motor symptoms can manifest long before the onset of motor symptoms, in the prodromal phase in which the pathological changes and neurodegeneration start taking place (Armstrong and Okun, 2020). Both motor and non-motor symptoms progressively worsen as the neurodegeneration becomes more widespread. However, PD is a heterogeneous disease, with different identifiable subtypes of patients, which impacts the type of

symptoms they experience, the speed of the progression of the disease and their response to treatment (Thenganatt and Jankovic, 2014).

PD is neuropathologically characterised by the loss of dopaminergic (DA) neurons in the substantia nigra pars compacta (SNpc) and by the intracellular deposition of aggregates containing α-synuclein, called Lewy bodies, in the surviving neurons. Both of these pathologies are required for a definite diagnosis of idiopathic (or sporadic) PD post-mortem (Dickson *et al.*, 2009). The loss of DA neurons, which is visible as a reduction of the neuromelanin pigmentation in the brain, leads to a reduction in dopamine levels in the striatum, causing the motor symptoms. The decrease in the number of DA neurons is progressive and at least half of them are dead or dysfunctional by the time symptoms emerge (Kordower *et al.*, 2013). The Lewy pathology, which can also be in the shape of neurites, consists mainly of aggregated, insoluble α-synuclein fibrils (Spillantini *et al.*, 1997), but can also contain fragmented membranes, organelles such as mitochondria, and vesicles (Shahmoradian *et al.*, 2019). Lewy pathology can be found not only in the SN, but also in the peripheral nervous system, supporting the idea of PD as a multisystem disease (Goedert *et al.*, 2013). The Lewy pathology progresses throughout different areas of the brain, from a localised area to widespread distribution across regions, in stages that correlate to the severity of the disease in the patients, from non-motor to motor symptoms and eventually dementia (Braak *et al.*, 2003).

Current treatments for PD only provide temporary symptom relief. Motor symptoms are treated by supplementing the missing dopamine with drugs such as the dopamine precursor L-DOPA or dopamine agonists. A combination of other

drugs is also prescribed to manage non motor symptoms. However, these solutions can have serious side effects, some patients are L-DOPA resistant or develop resistance and no therapy is treating the underlying causes of the disease (Poewe *et al.*, 2017). In particular, the heterogeneity of the disease suggests that several different approaches will be necessary. Therefore, there is an urgent need to identify and characterise novel targets to develop alternative disease-modifying therapies.

The genetics of Parkinson's disease

PD was long considered to be an environmental disease. Increased risk of PD has been associated with age, exposure to pesticides, prior head injury, while smoking, caffeine use and alcohol have been linked to reduce risk of PD (Ascherio and Schwarzschild, 2016). The discovery of causal mutations in *SNCA* (Polymeropoulos *et al.*, 1996, 1997), which encodes α-synuclein, through family studies, has opened the way to further investigations of the genetics of PD. Since then, the discovery of many Mendelian and risk genes has shown that PD is a genetically heterogeneous, multifactorial disorder arising through a complex interaction of genes and environment (Trinh and Farrer, 2013).

Through classic linkage analyses and next generation sequencing, researchers have identified PD loci (assigned a *PARK* designation in the order of their discovery) which cause autosomal dominant or recessive PD (Table 1). These are the so called forms of familial PD, in that they are inheritable, which make up 5-10% of all PD cases (Del Rey *et al.*, 2018). To date, mutations in *SNCA* (*PARK1/4*), *LRRK2* (*PARK8*), *VPS35* (*PARK17*) and *DNAJC13* (*PARK21*) have been shown to

cause autosomal dominant PD. These mutations generally cause late-onset PD, which is mostly undistinguishable from idiopathic PD and responsive to L-DOPA treatment, with Lewy pathology. On the other hand, mutations in the following loci have been shown to cause autosomal recessive PD: *PRKN* (*PARK2*), *PINK1* (*PARK6*), *DJ1* (*PARK7*), *ATP13A2* (*PARK9*), *PLA2G6* (*PARK14*), *FBXO7* (*PARK15*), *DNAJC6* (*PARK19*), *SYNJ1* (*PARK20*), *VPS13C* (*PARK23*). Mutations in *PINK1* and *PRKN* cause early onset (<50 years old) and juvenile PD (<20 years old), are generally characterised by severe but localised degeneration of nigral neurons but rare Lewy pathology and slow progression. In particular, mutations in *PRKN* are the most common cause of recessive, early onset PD and of sporadic PD with early onset (Hernandez, Reed and Singleton, 2016). Mutations in these Mendelian genes for PD are very rare in the population but are causal for the disease.

Gene	Protein encoded	Inheritance and onset	Function	Parkinsonism	Pathology	References
SNCA (PARK1/4)	α-synuclein	Dominant, early onset and sporadic	Synaptic activity, trafficking, vesicle fusion	Classic PD, dementia	Lewy bodies	(Polymeropoulos *et al.*, 1997; Singleton *et al.*, 2003)
PRKN (PARK2)	Parkin	Recessive, juvenile, early onset and sporadic	Mitophagy	Slow progression, dystonia	Very rare Lewy Bodies	(Kitada *et al.*, 1998)
PINK1 (PARK6)	PINK1	Recessive, early onset	Mitophagy	Slow progression, dystonia psychiatric features	Rare Lewy bodies	(Valente *et al.*, 2004)
DJ1 (PARK7)	DJ-1	Recessive, early onset	Redox-sensing, Mitophagy?	Dystonia, psychosis	Lewy bodies	(Bonifati *et al.*, 2003)
LRRK2 (PARK8)	LRRK2	Dominant, late onset and sporadic	Autophagy, Lysosomes	Classic PD	Lewy bodies	(Zimprich *et al.*, 2004)
ATP13A2 (PARK9)	ATP13A2	Recessive, early onset	Autophagy, Lysosomes	Atypical parkinsonism with complex phenotype, including dementia	Unknown	(Ramirez *et al.*, 2006)
PLA2G6 (PARK14)	PLA2G6	Recessive, early onset	Lipid metabolism	Atypical parkinsonism, dystonia	Lewy bodies	(Paisan-Ruiz *et al.*, 2009)
FBXO7 (PARK15)	FBXO7	Recessive, early onset	Mitophagy	Atypical parkinsonism with complex phenotype	Unknown	(Fonzo *et al.*, 2009)
VPS35 (PARK17)	VPS35	Dominant, late onset	Endosomes	Classic PD	Unknown	(Vilariño-Güell *et al.*, 2011; Zimprich *et al.*, 2011)

DNAJC6 (PARK19)	DNAJC6 (auxilin)	Recessive, early onset	Endosomes	Slow progression	Lewy bodies	(Olgiati *et al.*, 2016)
SYNJ1 (PARK20)	Synaptojanin 1	Recessive, early onset	Synaptic vesicles, endosomes	Parkinsonism, dystonia, cognitive decline	Unknown	(Quadri *et al.*, 2013)
VPS13C (PARK23)	VPS13C	Recessive, early onset	Mitophagy	Rapid progression	Lewy bodies	(Lesage *et al.*, 2016)

Table 1. Mendelian genes for PD, known function and clinical features.

List of genes considered causal for PD with high confidence (Blauwendraat, Nalls and Singleton, 2020). Adapted from Poewe *et al.*, 2017; Singleton and Hardy, 2019; Blauwendraat, Nalls and Singleton, 2020.

However, the great majority of PD cases have no known genetic cause. Analysis of common variability in PD-associated genes and, in the last decade, Genome Wide Association Studies (GWAS) have helped identify novel common variants which contribute to risk of disease and are common in the population (Nalls *et al.*, 2014, 2019; Chang *et al.*, 2017). These studies have identified genetic variants which confer high risk of disease in *SNCA* and *LRRK2,* already Mendelian genes for PD, as well as in the Gaucher's disease linked glucocerebrosidase (*GBA*) gene and *MAPT*. Over 90 loci are currently associated with modest risk of disease (Nalls *et al.*, 2019) (Fig 1), but identifying the causal risk genes on these loci remains challenging (See Introduction of Chapter 1).

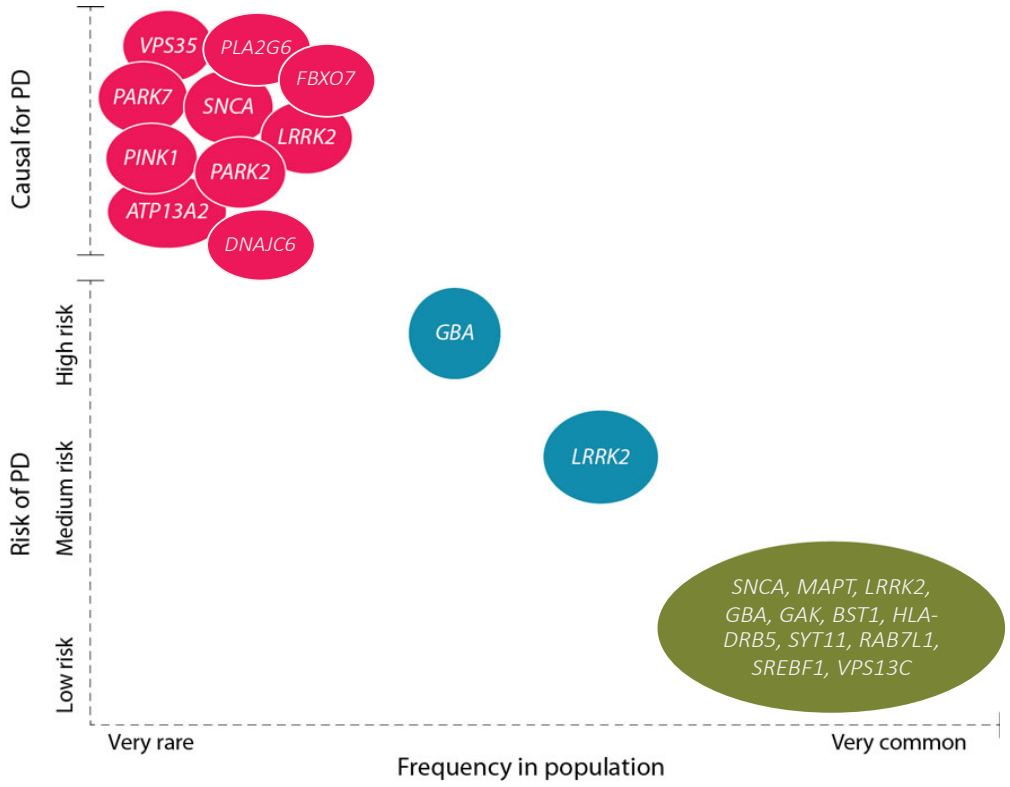

Figure 1. Genetic architecture of PD

Genes associated with PD: Mendelian (red), strong risk factors (blue), low risk factors from GWASs (green) (adapted from Van Der Brug *et al.*, 2015).

The genetics of PD has helped identify key mechanisms involved in the aetiology of the disease. Indeed, PD-associated genes are enriched in specific pathways (Singleton and Hardy, 2019): protein aggregation (*SNCA*), autophagy/lysosomal degradation (*LRRK2*, *GBA*, *ATP13A2),* mitochondrial function and quality control (*PRKN, PINK1*, *DJ1*, *FBXO7, PLA2GC*), vesicle trafficking (*SNCA*, *VPS35, DNAJC6, VPS13C, RAB7L1*) and the adaptive immune system (*HLA*). It is therefore probable that any newly identified risk genes could also map to these pathways.

Parkinson's disease and mitochondrial dysfunction

Mitochondrial dysfunction has been long associated with PD. Evidence for a mitochondrial role in the aetiology of sporadic PD was discovered in the 80s, when exposure to 1-methyl-4-phenyl-1,2,3,6-tetrahydropyridine (MPTP), a Complex I inhibitor, was shown to cause rapid parkinsonism and nigral degeneration (Langston *et al.*, 1983). Exposure to pesticides with Complex I inhibitory activity, such as rotenone and paraquat, also causes SN degeneration and parkinsonism and are often used to generate rodent models of the disease (Dawson, Ko and Dawson, 2010; Tanner *et al.*, 2011). Analysis of post-mortem PD brains found Complex I deficiency in the SN and frontal cortex, evidence of oxidative damage and accumulation of mitochondrial DNA (mtDNA) mutations and reduced levels of PGC1α, the key master regulator for mitochondrial biogenesis (reviewed in Bose and Beal, 2016). Recently, knockout of a catalytic subunit of Complex I in mice was found to cause progressive PD-like symptoms (González-Rodríguez *et al.*, 2021). Furthermore, some studies suggest that α-synuclein may be partially located at the

mitochondria, leading to deficits in respiration, impaired mitochondrial protein import and increased oxidative stress as well as playing a role in the opening of the mitochondrial permeability transition pore leading to cell death (Banerjee *et al.*, 2009; Ludtmann *et al.*, 2018).

The link between PD and mitochondria was further strengthened by the analysis of the monogenetic forms of the disease and, more recently, of the common risk variants. Indeed, many of the disease associated genes, such as *PINK1*, *PRKN* and *DJ1*, map to mitochondrial quality control and function pathways. A role for these genes in mitochondrial dysfunction was first identified in *Drosophila*, as PINK1 and Parkin knockout (KO) flies showed abnormal mitochondria and DA neuron degeneration (Greene *et al.*, 2003; Whitworth *et al.*, 2005; Clark *et al.*, 2006; Park *et al.*, 2006; Yang *et al.*, 2006). Early studies in neurons and fibroblasts found reduced mitochondrial membrane potential, impaired calcium buffering capacity, increased oxidative damage and cell death in PINK1- (Wood-Kaczmar *et al.*, 2008; Gandhi *et al.*, 2009; Morais *et al.*, 2009), and DJ-1-deficient cells (Krebiehl *et al.*, 2010). Parkin was also found to be able to localise at the mitochondria with protective effects, although the role of Parkin was unclear at the time (Darios *et al.*, 2003; Kuroda *et al.*, 2006). Recently, mitochondrial specific polygenic risk score analysis for PD revealed that the cumulative effect of common variation in mitochondrial genes is associated with increased risk of PD, further underlying the importance of mitochondrial dysfunction in the pathogenesis of the disease (Billingsley *et al.*, 2019). The genetic evidence of the importance of mitochondria in PD could partially explain the selective vulnerability of the DA neurons in the SN. DA neurons have an extensive morphology with thousands of synapses (Matsuda *et al.*, 2009; Bolam and

Pissadaki, 2012), and a pace making firing activity which requires high levels of energy and effective calcium buffering (Surmeier *et al.*, 2011), and therefore would be more susceptible to any mutation or damage that would reduce mitochondrial function (Pacelli *et al.*, 2015).

Mitochondrial Quality Control

Mitochondria are highly dynamic, complex, double membrane organelles which perform a variety of key roles within the cell. Mitochondria are formed of a porous outer membrane (OMM) and an ion selective inner membrane (IMM), separated by an intermembrane space, and a matrix bound by the IMM (Kühlbrandt, 2015).

Mitochondria are the main source of energy in the cell in the form of ATP, which is produced via the Krebs cycle in the matrix and via oxidative phosphorylation through the 5 electron transport chain complexes embedded in the IMM. The selectivity of the IMM to ion diffusion creates a mitochondrial membrane potential and the transfer of electrons across the respiratory chain and movement of protons from the matrix to the intermembrane space creates a pH gradient. This electrochemical gradient across the IMM drives ATP synthesis through the ATP synthase (or Complex V). The mitochondrial membrane potential is not only essential to produce ATP, but is also playing a role in the import of proteins into the mitochondria (Schmidt, Pfanner and Meisinger, 2010) and in calcium buffering (Giorgi, Marchi and Pinton, 2018). Depolarisation of the mitochondria thus impairs a

variety of key functions, and is commonly considered an indicator of mitochondrial health.

Mitochondria are not only important for generating ATP, they are also involved in many crucial pathways. Mitochondria are involved in lipid and amino acid metabolism, regulate apoptosis, generate reactive oxygen species (ROS) and have been linked to immune response regulation (Murphy and Hartley, 2018; Spinelli and Haigis, 2018). All these functions are especially important for postmitotic tissues with high energy and calcium buffering requirements, and extensive morphology, such as neurons. Mitochondrial dysfunction is indeed associated with ageing and a variety of diseases, such as cancer, cardiovascular diseases and neurodegeneration (Sorrentino, Menzies and Auwerx, 2018). Given their essential role, it is necessary for cells to maintain mitochondrial homeostasis. Indeed, several, partially overlapping, mitochondrial quality control pathways have evolved.

Mitochondrial protein quality control

Misfolded and oxidised proteins within the mitochondria are constantly correctly folded or degraded by mitochondrial chaperones and proteases, such as the family of AAA proteases (Quirós, Langer and López-Otín, 2015). Damaged proteins on the OMM instead can get ubiquitylated and degraded via the cytoplasmic ubiquitin-proteasome system (Taylor and Rutter, 2011). If the amount of damaged proteins is overwhelming, mitochondria can trigger their own mitochondrial unfolded protein response and upregulate expression of nuclear-encoded mitochondrial chaperones and proteases (Zhao *et al.*, 2002).

Mitochondrial Derived Vesicles

When the impairment is more extensive, small vesicles containing damaged cargo can bud off the OMM and be trafficked to peroxisomes (Neuspiel *et al.*, 2008; Braschi *et al.*, 2010) or to late endosomes/lysosomes (Soubannier, McLelland, *et al.*, 2012; Matheoud *et al.*, 2016; Ryan *et al.*, 2020) for degradation (mitochondrial derived vesicles – MDVs). MDVs selectively incorporate oxidised mitochondrial proteins, the identity of which appears to be related to the type of mitochondrial stress the cells are subjected to, and their formation is upregulated during conditions of stress (Soubannier, Rippstein, *et al.*, 2012; Roberts *et al.*, 2021). MDVs are thought to be an early response to stress (Sugiura *et al.*, 2014), as their formation increases before long before activation of mitophagy and their trafficking to lysosomes is independent of the activation of the autophagy machinery (Soubannier, McLelland, *et al.*, 2012; McLelland *et al.*, 2014). Several PD-associated proteins are required in MDV formation and trafficking. PINK1 and Parkin, two key mitophagy proteins (See next Section), promote MDV formation and in particular their targeting to the lysosomes for degradation (McLelland *et al.*, 2014; Ryan *et al.*, 2020). Furthermore, they have been linked to mitochondrial antigen presentation in the context of immunity (Matheoud *et al.*, 2016). VPS35 is instead involved in the trafficking of MDVs to peroxisomes (Braschi *et al.*, 2010).

Mitophagy

When mitochondrial damage is global, the whole organelle is targeted for selective degradation through the process of mitophagy. Mitophagy is a particularly relevant pathway in PD, as it involves two proteins encoded by genes mutated in autosomal recessive early onset PD, PRKN (Parkin) and PINK1. Loss of function

mutations in PINK1 and Parkin lead to deficient mitophagy. PINK1 and Parkin were first discovered to act within the same conserved pathway, with PINK1 acting upstream of Parkin, in *Drosophila*. The phenotype in PINK1 KO flies was rescued by overexpression of Parkin but not vice versa (Greene *et al.*, 2003; Clark *et al.*, 2006; Park *et al.*, 2006; Yang *et al.*, 2006). Subsequent cell-based studies have further deepened our understanding of the process, described in the following sections.

PINK1

PINK1 is a mitochondrial Serine/Threonine kinase, encoded by the *PINK1(PARK6)* gene on chromosome 1. Mutations in PINK1 cause are the second most common cause of autosomal recessive early-onset PD, and were the first genetic evidence supporting a role for mitochondrial dysfunction in the disease (Valente *et al.*, 2004). PINK1 is a 581 amino acid protein, with an N-terminal mitochondrial targeting sequence and transmembrane domain, a conserved kinase domain and conserved C-terminal domain. The majority of the pathogenic mutations in PINK1 occur in the kinase domain, affecting the structure and the activity of the protein (Kumar *et al.*, 2017; Schubert *et al.*, 2017) (Fig 2A).

In basal steady-state conditions, PINK1 is constitutively imported into the mitochondria, where it is cleaved by the mitochondrial proteases MPP and PARL (Jin *et al.*, 2010; Deas *et al.*, 2011; Meissner *et al.*, 2011; Greene *et al.*, 2012). Cleaved PINK1 is retrotransported to the cytosol and degraded via the N-end rule pathway by the ubiquitin proteasome system (Yamano and Youle, 2013), thus only very low levels of PINK1 are detectable in healthy cells.

Parkin

Parkin is a cytosolic E3-ubiquitin ligase, encoded by the *PRKN (PARK2)* gene on chromosome 6. Mutations in Parkin are the most common cause of autosomal recessive early onset PD and Parkin was the second gene linked to PD (Kitada *et al.*, 1998). Parkin is a 465 amino acid protein, with an N-terminal ubiquitin-like domain followed by four zinc-coordinating RING-like domains. Parkin mutations include rearrangements, deletions and duplications of exons and missense, nonsense or splice site mutations and have been identified along the whole expanse of the protein, affecting its structure, activation and enzymatic activity (Kasten *et al.*, 2018; Yi *et al.*, 2019) (Fig 2B).

The cellular localisation of Parkin and its significance was originally debated. Early studies reported Parkin in vesicles, Golgi and the cytosol (Shimura *et al.*, 1999; Kubo *et al.*, 2001), while later studies reported its presence on the OMM (Darios *et al.*, 2003) or partially imported in the mitochondria (Kuroda *et al.*, 2006). A seminal paper from the Youle lab discovered instead the translocation of Parkin to impaired mitochondria as part of mitochondrial degradation (Narendra *et al.*, 2008) (See following Section).

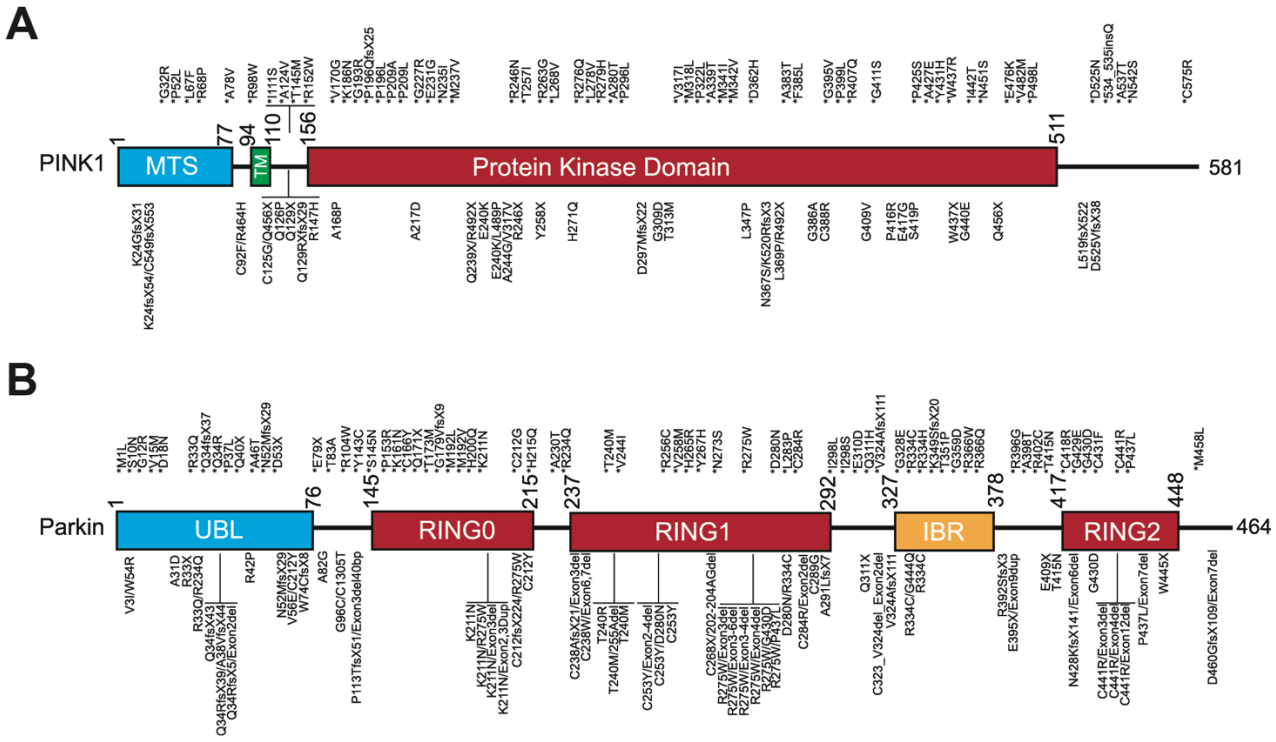

Figure 2. Structure of PINK1 (A) and Parkin (B), with the location of mutations found in PD patients (from Pickrell and Youle, 2015)

MTS: mitochondrial targeting sequence, TM: transmembrane domain, UBL: ubiquitin-like domain, RING: really interesting new gene domain, IBR: in between RING domain; ins: insertion, dup: duplication, del: deletion, fs: frame shift.

PINK1/Parkin-dependent mitophagy

When mitochondria become globally impaired, PINK1 accumulates selectively on the dysfunctional mitochondria initiating the process that leads to their degradation. The block of mitochondrial import due to the depolarisation of the mitochondria (Jin *et al.*, 2010; Narendra, Jin, *et al.*, 2010; Meissner *et al.*, 2011) or the accumulation of unfolded proteins in the matrix (Jin and Youle, 2013), causes PINK1 to accumulate at the surface of damaged mitochondria. PINK1 on the OMM phosphorylates pre-existing ubiquitin molecules on Ser65 (Kane *et al.*, 2014; Kazlauskaite *et al.*, 2014; Koyano *et al.*, 2014). It is currently unclear which, if any,

E3 ubiquitin ligase is responsible for the deposition of these ubiquitin seeds on the OMM and how they are regulated. Several mitochondrial E3 ubiquitin ligases, such as MARCH5/MITOL, MUL1/MULAN and HUWE1, have been proposed to ubiquitylate proteins on the mitochondrial surface, such as proteins involved in mitochondrial dynamics, the mitochondrial translocon and mitochondrial import substrates (Li *et al.*, 2008; Michel *et al.*, 2017; Koyano *et al.*, 2019; Phu *et al.*, 2020), providing the initial substrate for PINK1 activity. However, knockout of either MARCH5 or MUL1 alone did not affect the accumulation of pUb(Ser65) (Ordureau *et al.*, 2020), suggesting a possible redundancy of the ubiquitin ligases to provide basal ubiquitylation.

PINK1 also recruits to the mitochondria (Matsuda *et al.*, 2010; Narendra, Jin, *et al.*, 2010; Vives-Bauza *et al.*, 2010) and phosphorylates Parkin on the highly conserved Ser65 residue in the ubiquitin-like domain (Kondapalli *et al.*, 2012; Shiba-Fukushima *et al.*, 2012). Parkin exists in the cytosol in an inactive, autoinhibited state (Chaugule *et al.*, 2011; Wauer and Komander, 2013) and is activated both by binding to phosphorylated ubiquitin (pUb(Ser65)) and by phosphorylation on Ser65 (Kondapalli *et al.*, 2012; Kazlauskaite *et al.*, 2015; Kumar *et al.*, 2015; Sauvé *et al.*, 2015; Wauer *et al.*, 2015; Gladkova *et al.*, 2018). Active Parkin further ubiquitylates other mitochondrial proteins, mostly on the OMM, forming polyubiquitin chains linked mostly on lysine 48 or 63 (K48 and K68), as well as on K6 and K11 (Chan *et al.*, 2011; Sarraf *et al.*, 2013; Ordureau *et al.*, 2014), although the role of each chain type is still unclear (Harper, Ordureau and Heo, 2018). These ubiquitin molecules also get phosphorylated by PINK1, leading to further Parkin recruitment and activation, generating a feed forward amplification loop (Ordureau *et al.*, 2014; Shiba-Fukushima *et al.*, 2014; Okatsu *et al.*, 2015). Phosphorylated ubiquitin chains recruit

autophagy receptors, such as p62/SQSTM1, NDP52, OPTN, NBR1 and TAX1BP1, although some studies suggest that only NDP52 and OPTN are required for mitophagy (Narendra, Kane, *et al.*, 2010; Heo *et al.*, 2015; Lazarou *et al.*, 2015). These autophagy receptors have an LC3-interacting domain, which is able to recruit LC3, which in turn recruits the autophagy machinery. This leads to the formation of autophagosomes around the damaged organelles, leading to fusion with the lysosomes and degradation (Fig 3).

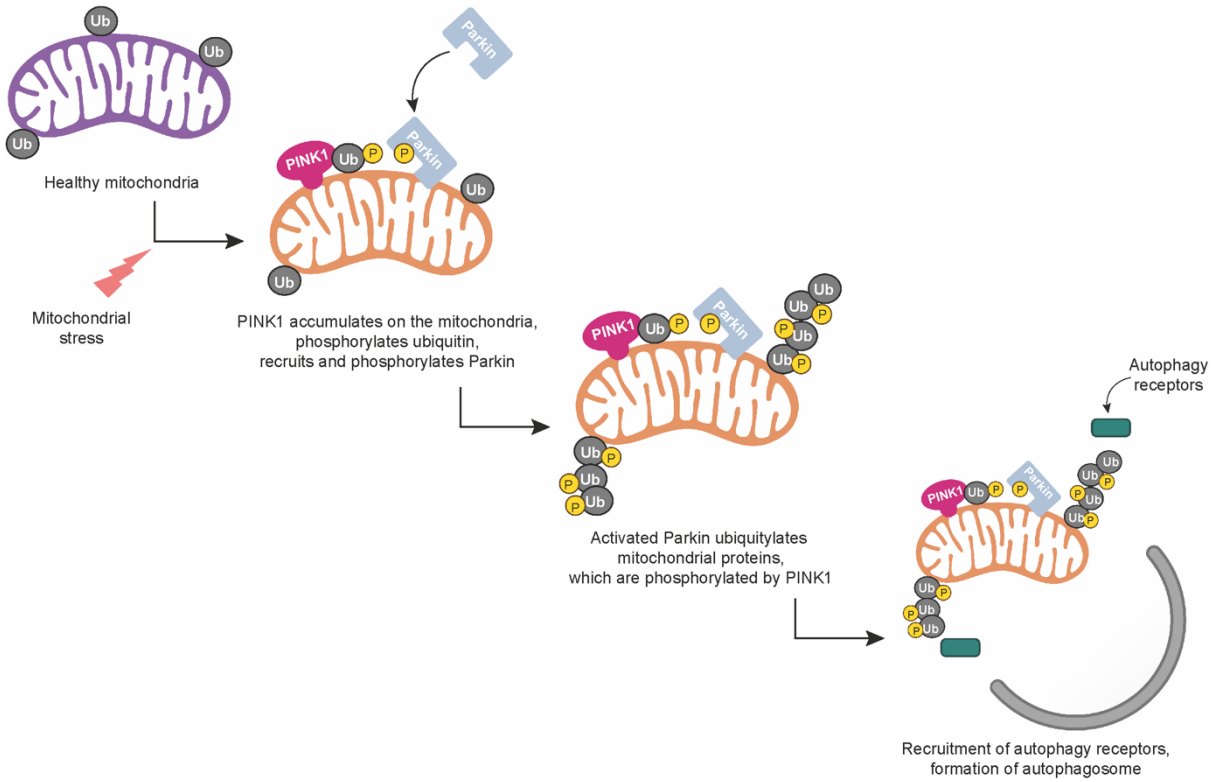

Figure 3. Diagram of PINK1-dependent mitophagy.

PINK1/Parkin-independent mitophagy

Mitochondrial degradation is not achieved exclusively by PINK1-dependent mitophagy, and other mechanisms have been described, often referred to as

PINK1/Parkin-independent mitophagy. These pathways depend on other key proteins and are activated in response to different types of stresses.

NIX-dependent mitophagy is the clearance of mitochondria mediated by two autophagy receptors, NIX and the related BNIP3 (Zhang and Ney, 2009). NIX and BNIP3 are OMM proteins, whose expression is upregulated by hypoxia (Bruick, 2000; Sowter *et al.*, 2001; Bellot *et al.*, 2009). Activated NIX and BNIP3 lead to the recruitment of LC3 and GABARAPs via their LIR and formation of the autophagosome (Hamacher-Brady *et al.*, 2007; Schwarten *et al.*, 2009; Novak *et al.*, 2010; Zhu *et al.*, 2013). NIX-dependent mitophagy has been shown to play a role in particular in erythrocyte maturation (Schweers *et al.*, 2007; Sandoval *et al.*, 2008). Several studies have reported a potential cross talk between the NIX/BNIP3 and the PINK1/Parkin pathways. Parkin has been shown to ubiquitylate NIX (Gao *et al.*, 2015) and PINK1 to interact with BNIP3 promoting the recruitment of Parkin to the mitochondria (Zhang *et al.*, 2016). Expression of NIX was found to restore mitophagy in PD patient fibroblasts with Parkin mutations (Koentjoro, Park and Sue, 2017), however the relevance of BNIP3 and NIX in the pathophysiology of PD remains unclear (Onishi *et al.*, 2021).

FUNDC1, another OMM protein with a LIR motif, has been also linked to hypoxia-induced mitophagy (Liu *et al.*, 2012). Dephosphorylation of the FUNDC1 LIR domain in hypoxic conditions increases affinity of the receptor for LC3, leading to the recruitment of the autophagy machinery (Liu *et al.*, 2012; Chen *et al.*, 2014).

Methods to detect mitophagy

Induction of mitophagy

Mitophagy in mammalian cells is generally induced by depolarising the mitochondria, as a drop in membrane potential leads to the accumulation of PINK1 on the OMM. This is usually necessary because of the low levels of basal mitophagy in healthy cells (Narendra, Jin, *et al.*, 2010; McWilliams and Muqit, 2017). Depolarisation can be achieved by chemical treatments with compounds that can be more or less specific for the mitochondria. The early studies on mitophagy used high concentrations of uncoupling compounds that dissipate the mitochondrial membrane potential, such as carbonyl cyanide m-chlorophenyl hydrazone (CCCP) and carbonyl cyanide 4-(trifluoromethoxy)phenylhydrazone (FCCP). However, these agents can have non-specific effects on other organelles, such as lysosomes (Padman *et al.*, 2013), and are used at excessive concentrations than needed to depolarise mitochondria. Similarly, the potassium ionophore valinomycin can be used as an uncoupler to depolarise mitochondria, but can target other cellular compartments (Rakovic *et al.*, 2019). To avoid the off targets effects, mitochondrial-specific compounds, such as the ATP synthase inhibitor oligomycin and the Complex III inhibitor antimycin A, have been used more recently to induce mitophagy at comparable levels to the CCCP/FCCP treatments (Ordureau *et al.*, 2014). Overall, these compounds allow fast and effective initiation of mitophagy at levels that are detectable in experimental setups. However, a global disruption of the mitochondrial network is unlikely to reflect physiological induction of mitophagy in cell lines, especially neurons, and also raises the question of what is the trigger of mitophagy *in vivo* (Whitworth and Pallanck, 2017). The accumulation of unfolded proteins in the matrix has been described to activate PINK1-dependent mitophagy in cell lines (Jin

and Youle, 2013), as well as the localised production of ROS at the mitochondria using the photoactivatable fluorescent protein mtKillerRed in primary neurons (Ashrafi *et al.*, 2014). More recently, mitophagy has been studied by using mild levels of oxidative stress caused by removing antioxidants from the culture medium (Evans and Holzbaur, 2020).

Detection of mitophagy

Co-localisation of mitochondria and autophagosomes or lysosomes

Mitophagy can be detected in cells by measuring different stages of the pathway (Klionsky *et al.*, 2021). One common way is to detect the engulfment of the mitochondria by the autophagy machinery or the fusion with the lysosomes. This can be done by measuring the co-localisation of mitochondrial markers and the autophagy receptors, such as p62, markers of the autophagosome, such as LC3, or markers of the lysosomes, such as LAMP1, by immunofluorescence or by fluorescently tagging the proteins of interest. Similarly, it can be done in live cells using fluorescent dyes for the mitochondria and the lysosomes. However, it is important to test beforehand the dependence of the dye on functional aspects, such as the mitochondrial membrane potential, which could affect proper loading. Finally, co-localisation can be assessed using electron microscopy, to identify mitochondrial structures within the lysosomes or autophagosomes.

Activation of PINK1-dependent mitophagy and degradation of mitochondrial proteins

The early steps of mitophagy can be measured by detecting PINK1 and Parkin mitochondrial accumulation and recruitment/phosphorylation, respectively. PINK1 accumulation at the mitochondria can be measured by mitochondrial

fractionation/enrichment and Western blotting, and PINK1 activity at the mitochondria can be monitored by staining or blotting for pUb(Ser65) (Fig 4A) and pParkin(Ser65). Other targets of PINK1 activity that can be probed for by blotting also are PINK1 itself, which can be autophosphorylated (Okatsu *et al.*, 2012), and Rab8A, whose phosphorylation on Ser111 is dependent on, but not a direct target of, PINK1 (Lai *et al.*, 2015). Parkin recruitment can be measured by blotting the mitochondrial fraction for Parkin (Fig 4B) or by imaging and measurement of the translocation from the cytosol to the mitochondrial mask.

The end result of the activation of mitophagy is the degradation of mitochondrial proteins, which can be detected by measuring the decrease of mitochondrial markers by Western blotting or immunofluorescence (Fig 4). The effect of Parkin activation, that is the ubiquitylation of the mitochondrial proteins on the outer membrane, can also be detected by Western blotting as a higher molecular weight smear or bands over the protein of interest (Fig 4B - MFN1), or by probing for ubiquitin. However, given that outer mitochondrial membrane proteins, such as TOM20, can be degraded by other quality control systems, it is important to measure proteins from different mitochondrial compartments.

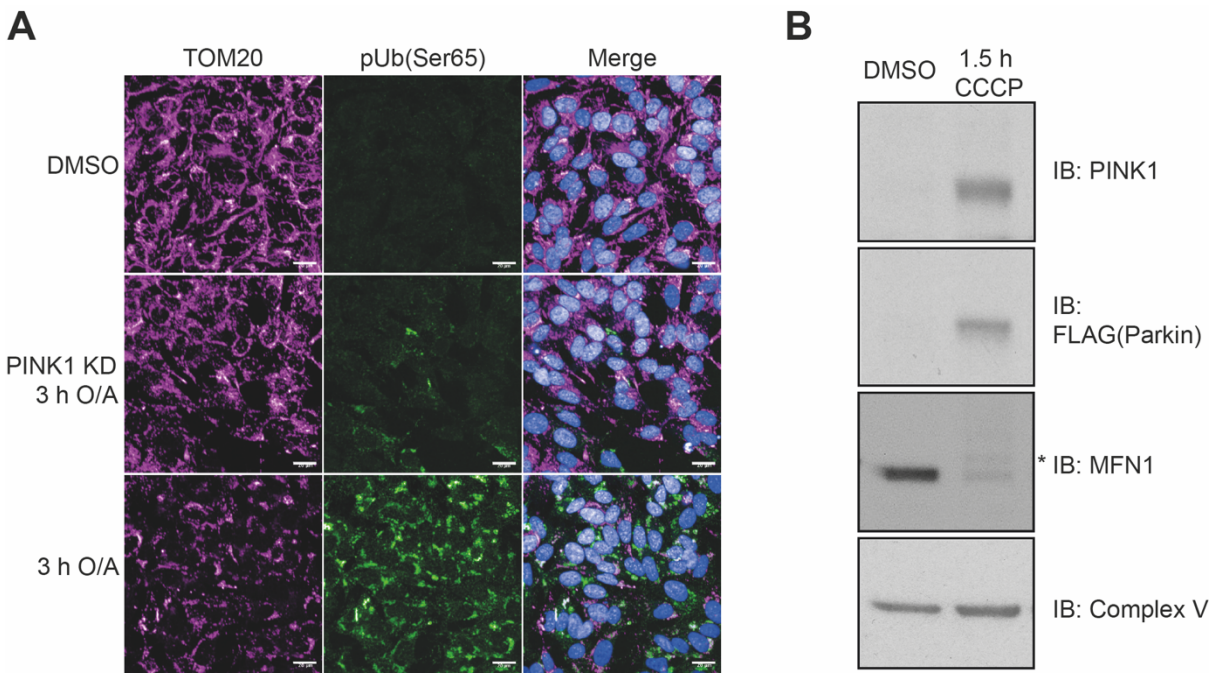

Figure 4. Methods to detect PINK1-dependent mitophagy.

A. Parkin-overexpressing SHSY5Y cells were transfected with siRNA against PINK1 or control for 72 h before inducting mitophagy by treating with 1 μM Oligomycin/Antimycin A for 3 h. Cells were fixed and stained for TOM20 and pUb(Ser65) before imaging on the Opera Phenix. **B.** Parkin-overexpressing SHSY5Y cells were treated with 10 μM CCCP for 1.5 h, before being lysed and enriched for the mitochondrial fraction. Lysates were blotted for PINK1, Parkin (FLAG), Mitofusin 1 and Complex V (WB by Dr Marc Soutar). * indicates higher molecular weight band due to the ubiquitylation of MFN1. Treatment with CCCP reflects the early standard in the field to induce mitophagy. Comparable results are obtained by Western blotting after O/A treatment (see for example Chapter 3 Fig 31 and Fig 36, with the accumulation of PINK1 after the induction of mitophagy and higher molecular weight band indicating ubiquitylation of MFN2).

Mitophagy reporters

Blotting or imaging specific markers only capture a limited portion of the mitophagic flux, and Western blotting in particular requires global damage to the network to be able to detect mitophagy. To follow the degradation of mitochondria, from the activation of mitophagy to the fusion with the lysosomes, several fluorescent

reporters have been developed over the years, taking advantage of the different properties of fluorescent proteins in acidic or neutral environments.

Mito-QC is a tandem mCherry - GFP fluorescent protein which is targeted to the mitochondria via the mitochondrial targeting sequence (MTS) of the outer mitochondrial membrane protein FIS1 (Allen *et al.*, 2013). This construct exploits the different acid sensitivity of the two fluorescent proteins, as only the fluorescence of GFP is quenched in acidic environments, such as lysosomes. In basal conditions the mitochondrial network will be tagged by both green and red signals, while mitochondria in lysosomes will be only tagged red. Therefore, activation of mitophagy can be measured by counting the red mCherry dots. Mito-QC has the advantage of being a fixable reporter, and transgenic mice models have been developed to study mitophagy in vivo (McWilliams *et al.*, 2016). However, mito-QC is targeted to the outer mitochondrial membrane, and is therefore subject to degradation by the ubiquitin proteasome system independently of the degradation of the whole organelle, making it a less sensitive reporter than the mt-Keima and mito-SRAI (Katayama *et al.*, 2020; Liu *et al.*, 2021). Evolutions of this construct, for example by substituting the FIS MTS with the MTS of the matrix protein COX VIII (Ordureau *et al.*, 2020), will be useful.

Mt-Keima is a pH-sensitive, mitochondrially targeted dual fluorescence protein, whose excitation spectrum shifts from a green wavelength in neutral environments (such as the cytoplasm), to a red wavelength in acidic environments (such as the lysosome), while the emission wavelength is not pH dependent (Katayama *et al.*, 2011). Mt-Keima is targeted to the mitochondrial matrix via the

MTS of COX VIII. Using this reporter, mitophagy can be measured as a ratio of the area of red (lysosomal mitochondria) to red plus green (total mitochondria) signals (Katayama *et al.*, 2011; Sun *et al.*, 2015). The mt-Keima reporter is resistant to lysosomal proteases, which enables measurement of the mitophagic flux over time, but can only be imaged in live cells, as fixing samples abolishes the pH gradient across the lysosomal membrane. As for the mito-QC, transgenic animal models have been developed (Sun *et al.*, 2015).

Recently, two new reporters have been developed. Mito-SRAI (Katayama *et al.*, 2020), a tandem fluorescent construct made of an acid-resistant CFP and an acid-sensitive YPF that can be degraded by lysosomal proteases. This reporter is targeted to the mitochondrial matrix by a tandem COX VIII MTS, and mislocalisation is prevented by the presence of a C-terminal degron for degradation of any remaining construct in the cytoplasm. The overlap between the CFP emission spectrum and the YFP excitation spectrum allows the fluorescence resonance energy transfer (FRET) between the two fluorescent proteins, with CFP being the donor and YFP the acceptor. When the YFP is degraded in the lysosomal environment, the CFP is unquenched and appears as an increase punctate fluorescence. The ratio between the lysosomal CFP signal and total signal can be used as an index of mitophagy, similarly to the mt-Keima measurement. Unlike mt-Keima, mito-SRAI is a fixable reporter, which will allow easier measurement of mitophagy in fixed tissues, as well as be more amenable to high throughput screening. The most recent reporter to have been developed is the mito-Pain, a ratiometric fluorescent sensor to measure mitochondrial stress (Uesugi *et al.*, 2021). This reporter is a ratiometric fluorescent sensor, composed by GFP-tagged PINK1, a

degron sequence to promote degradation, a cleavage sequence, and RFP, with the transmembrane domain of the outer mitochondrial membrane protein Omp25. In basal conditions, the construct is cleaved at the cleavage sequence, allowing PINK1-GFP-degron to be targeted to the healthy mitochondria, processed and degraded. In depolarised mitochondria, PINK1-GFP accumulates on the outer mitochondrial membrane. In both cases, RFP-Omp25 is localised to the mitochondria, and the ratio of GFP-RFP can be used to measure the presence of impaired mitochondria. While this reporter does not measure mitophagy, as it does not measure the targeting of damaged mitochondria to the lysosomes, it takes advantage of PINK1 as a sensor of mitochondrial stress and is fixable.

Mitochondrial quality control and neurodegeneration: beyond PD

Overall, mitochondrial quality control is a key pathway in PD. Not only PINK1 and Parkin play a role in mitophagy and MDV formation, but other PD-associated proteins have been linked to mitochondrial quality control pathways. FBOX7 (*PARK15*) interacts with Parkin and PINK1 to mediate mitophagy (Burchell *et al.*, 2013). VPS35 (*PARK17*) interacts with Parkin and may play a role in MDV trafficking (Malik, Godena and Whitworth, 2015; Williams *et al.*, 2018), while silencing of VPS13C (*PARK23*) increases PINK1-dependent mitophagy (Lesage *et al.*, 2016). PINK1 and Parkin have been proposed to be able to rescue mitochondrial defects deriving from loss of DJ-1 (*PARK7*) (Irrcher *et al.*, 2010; Thomas *et al.*, 2011), but whether DJ-1 can induce or regulate mitophagy is unclear. Other studies have linked LRRK2 (*PARK8*) to impaired mitophagy (Bonello *et al.*, 2019; Korecka *et al.*, 2019;

Wauters *et al.*, 2020), although it is uncertain whether it is due mainly to defects in bulk autophagy and lysosomal function (Singh and Ganley, 2021).

However, PINK1-dependent mitophagy is being increasingly linked to ageing and other neurodegenerative diseases. Elevated levels of pUb(Ser65) have been found not only in PD patient brains, but also in older brains (Hou *et al.*, 2018). PINK1-dependent mitophagy has been recently linked to Alzheimer's disease (Du *et al.*, 2017; Sorrentino *et al.*, 2017), to Huntington's disease (Khalil *et al.*, 2015) and to frontotemporal dementia (FTD) (Zhou *et al.*, 2019). Mutations in OPTN, one of the key autophagy receptors for mitophagy, cause amyotrophic lateral sclerosis (ALS) and affect mitochondrial clearance (Wong and Holzbaur, 2014). Phosphorylation of OPTN by TBK1, which is required for mitophagy, is disrupted by mutations in TBK1 that cause ALS and FTD (Moore and Holzbaur, 2016; Harding *et al.*, 2021). Mutations in VCP/p97, also associated with ALS and FTD, impair mitochondrial function (Bartolome *et al.*, 2013) and PINK1-dependent mitophagy (Tanaka *et al.*, 2010; Kim *et al.*, 2013). Therefore, a better understanding of mitochondrial quality control pathways is necessary in order to develop potential global strategies to treat neurodegenerative diseases.

Objectives of this thesis

The genetics of the familial forms of PD have shed light on some of the key pathogenic mechanisms of the disease, but no disease modifying therapy is as of yet available. The clinical success of drug discovery is improved by the presence of genetic data supporting the choice of target (Nelson *et al.*, 2015), but mutations in the Mendelian PD genes are rare in the general population and do not explain the great majority of cases. Insight in the genes that increase risk of developing PD has come from the large GWAS analysis of the last decade, however the identification of the causal gene in a risk locus and how this impacts disease is complex.
One of the main pathogenic pathways identified by the Mendelian genes is mitochondrial dysfunction, and in particular mitophagy. Therefore, the aim of this project is to determine whether and how the GWAS risk gene candidates could also affect mitophagy.

To functionally assess the GWAS genes and their effect on mitophagy, I developed a high content loss of function mitophagy screen, measuring mitophagy activation and mitochondrial degradation after knockdown of a selection of gene candidates. The first chapter will describe the assay development, from the selection of the phenotype to the running of the screen. The second chapter will investigate how the hit from the screen, KAT8, and a protein part of the same complex, KANSL1, which is also a GWAS hit for PD, affect mitophagy in SHSY5Y cells. Finally, the role of KAT8 and KANSL1 was investigated in disease-relevant cell lines, iPSC-derived neurons. In the third chapter, I will describe the setup of a model to induce and detect mitophagy in iPSC-derived neurons using lines from a family of PD patients with a novel mutation in PINK1. Finally, to model the effect of a

reduction of KAT8 and KANSL1 in neurons, I optimised a system to perform CRISPR interference in iPSC-derived induced neurons before studying mitophagy.

Materials and methods

Cell Culture

Mammalian cell culture

POE SHSY5Y cells are a kind gift from H. Ardley (Ardley *et al.*, 2003). SHSY5Y were purchased from ATCC. The mt-Keima POE SHSY5Y cells were a kind gift of C. Luft (Soutar *et al.*, 2019). The Lenti HEK293 cells were a kind gift of O. Lazo (Lazo and Schiavo, 2021). Cells were cultured in Dulbecco's Modified Eagle (DMEM, Gibco, 11995-065) and supplemented with 10% heat-inactivated foetal bovine serum (FBS, Gibco, 10500064) in a humidified chamber at 37 °C with 5% CO_2. Cells were grown to about 90% confluency before splitting. To split the cells, the media was aspirated off the flask before washing the cells once with PBS. The PBS was then removed before adding 0.25% trypsin - EDTA (Sigma-Aldrich,T4049) and incubating for 5 min at 37 °C to lift the cells. After checking that the cells had detached, they were collected by adding fresh prewarmed media and transferred into a 15 ml tube. Cells were centrifuged for 3 min at 300g before removing the supernatant and resuspending the cell pellet in 1ml of fresh media. The cells were then counted using the Countess II automated cell counter (Invitrogen, AMQAF1000). For routine maintenance, 4 x 10^6 cells were seeded into a new flask topped up with 25 ml of media.

siRNA transfection

To knock down the genes of interest, cells were reverse transfected with small interfering RNAs (siRNA). All siRNAs were purchased as pre-designed siGENOME

SMARTpools from Dharmacon: non-targeting (D-001206-13), PINK1 (M-004030-02), PLK1 (L-003290-00), KAT8 (M-014800-00), KANSL1 (M-031748-00), KANSL2 (M-020816-01), KANSL3 (M-016928-01), HCFC1 (M-019953-01), MCRS1 (M-018557-00), OGT (M-019111-00), PHF20 (M-015234-02), WDR5 (M-013383-01). siRNAs were resuspended in RNase-free water for a final concentration of 20 µM, aliquoted and stored at -20 °C.

For transfections in a 96-well plate, the transfection mix was prepared so to add 25 µl of mix per well. For one well, 4.8 µl/ml of DharmaFECT1 transfection reagent (Dharmacon, T-2001-03) was added to cold serum free DMEM. siRNAs were added at a concentration of 0.25 µM, to achieve a final concentration in the well (once added the cells) of 50 nM. The transfection mix was added to the appropriate wells and incubated for 30 min at room temperature. In the meanwhile, the cells were harvested as described above and counted. Cells were plated by adding 100 µl/well of a cell suspension mix prepared to achieve 15000 cells/well in DMEM + 10% FBS. Cells were incubated for 72 h before use.

Induction of mitophagy

To induce mitophagy, cells were treated with 1 µM Oligomycin, a mitochondrial complex V inhibitor (Cayman Chemicals, 11341 and Sigma, O4876), and 1 µM antimycin A, a mitochondrial complex III inhibitor (Sigma, A8674). Both compounds were individually diluted in DMSO to make a 25 mM stock, and then combined to make a 1 mM working stock. To treat cells plated in 96-well plates after a siRNA transfection (125 µl volume/well), a treatment mix was prepared in fresh DMEM + 10% FBS at 6X the final concentration (i.e. 6 µM) and 25 µl were gently

added to appropriate wells. The DMSO control was prepared similarly by diluting the same volume of DMSO in fresh media.

High Content siRNA Screen

siRNA library

The siRNA library was purchased from Dharmacon as an ON-TARGETplus SMARTpool Cherry-pick siRNA library, 0.25 nmol in a 384-well plate. siRNAs were resuspended in RNase-free water for a final concentration of 20 µM. SCR, PINK1 and PLK1 controls were added to the 384-well plate at a concentration of 20 µM before dispensing into barcoded assay-ready plates.

Cell plating and siRNA transfection

siRNA was dispensed into Geltrex-coated 96-well CellCarrier Ultra plates (Perkin Elmer) at a final concentration of 30 nM using the Echo 555 acoustic liquid handler (Labcyte). For each well, 25 µl of DMEM containing 4.8 µl/ml of DharmaFECT1 transfection reagent was added and incubated for 30 min before POE SHSY5Y cells were seeded using the CyBio SELMA (Analytik Jena) at 15,000 cells per well, 100 µl per well in DMEM + 10% FBS. Cells were incubated for 72h before treatment with 10 µM oligomycin/10 µM antimycin for 3 h to induce mitophagy.

Immunofluorescence and Image Capture and Analysis

Cells were fixed with 4% PFA (Sigma, F8775), then blocked and permeabilised with 10% FBS, 0.25% Triton X-100 (Sigma, 93443) in PBS for 1h, before immunostaining with pUb(Ser65) and TOM20 primary antibodies (in 10% FBS/PBS) for 2 h at room temperature. After 3x PBS washes, AlexaFluor 568 anti-mouse and 488 anti-rabbit secondary antibodies and Hoechst 33342 (Thermo Scientific, 62249)

were added (in 10% FBS/PBS, 1:2000 dilution for all) and incubated for 1 h at room temperature. Following a final 3x PBS washes, plates were imaged using the Opera Phenix (Perkin Elmer). 5x fields of view and 4x 1 µm Z-planes were acquired per well, using the 40X water objective, NA1.1. Images were analysed in an automated way using the Columbus 2.8 analysis system (Perkin Elmer) to measure the integrated intensity of pUb(Ser65) and TOM20 within the whole cell.

Screen quality control, data processing and candidate selection

Screen plates were quality controlled based on the efficacy of the PINK1 siRNA control and O/A treatment window (minimum 3-fold). Data was checked for edge effects using Dotmatics Vortex visualization software. Raw data was quality controlled using robust Z prime > 0.5. Data was processed using Python for Z score calculation before visualization in Dotmatics Vortex. Candidates were considered a hit where Z score was ≥ 2 or ≤ -2, and where replication of efficacy was seen both within and across plates.

iPSC culture and differentiation

iPSC culture

The PINK1 and Control 1 human induced pluripotent stem cells (iPSCs) were obtained by reprogramming of patient fibroblasts at the Queen Square Institute of Neurology (lab of S. Gandhi). The human dCas9 iPSCs, with stably integrated inducible Ngn2 and CRISPRi cassettes, were a kind gift of M. Ward (Tian *et al.*, 2019). The iPSCs were cultured on Geltrex (Gibco, A1413302)-coated 6-well plates in Essential 8 medium (ThermoFisher, A1517001) (PINK1 iPSCs) or in mTesr Plus (STEMCELL Technologies, 100-0276) (dCas9 iPSCs). Media was fully replaced

daily (E8 cells) or every two or three days (mTesr Plus cells). Cells were grown until 70-80% confluency, and checked daily to ensure the presence of stem cell like colonies and absence of spontaneous differentiation. To passage the cells, the medium was removed before washing the wells with 1 ml of PBS. To lift the cells, 1 ml of 0.5 mM EDTA in PBS (Invitrogen, 15575020) was added to each well before incubating the plate at 37 °C with 5% CO_2 for 5 min. During the incubation with EDTA, Geltrex was aspirated from the new wells and replaced with 1.5 ml of warm media. The EDTA was removed from the cells, before forcefully adding 3 ml of fresh warm media to the wells, to lift the cells. The iPSCs were briefly resuspended to collect as many cells as possible, but taking care to keep them in clumps. 0.5 ml of the resuspended cells were then added dropwise to the new wells, to achieve a 1 in 6 split. The plate was then gently rocked to ensure even distribution of the cells before incubating in a humidified chamber at 37 °C with 5% CO_2.

Cortical neuron differentiation using the dual SMAD inhibition protocol

Differentiation of the PINK1 iPSCs into cortical neurons was induced by dual SMAD inhibition according to the Shi protocol (Shi, Kirwan and Livesey, 2012). Inhibition of SMAD signalling using the combined action of two small molecule inhibitors, Dorsomorphin and SB431542, is sufficient to induce efficient differentiation of stem cells to the anterior central nervous system lineage (Chambers *et al.*, 2009; Shi *et al.*, 2012). iPSCs were grown to 100% confluence in Geltrex-coated 6 well plates before switching the cells to neural induction media, which was prepared by supplementing the neural maintenance media N2B27 (Table 2) with 1 µM dorsomorphin (Tocris, 3093) and 10 µM SB431452 (Tocris, 1614). The N2B27

media was prepared by mixing the media containing N2 and media containing B27 in a 1:1 ratio and stored at 4 °C for up to three weeks.

Reagent	**Supplier and Cat. Number**	**Volume of stock to add for 50 ml**
N2 containing medium		
DMEM/F-12 GlutaMAX	Thermofisher, 31331028	48.5 ml
N2 supplement (100X)	Thermofisher, 17502048	500 µl
Insulin (10 mg/ml)	Sigma, I9278-5ML	25 µl
Non-essential amino acids (100X)	Thermofisher, 11140050	500 µl
2-mercaptoethanol (50 mM)	Thermofisher, 31350-010	90.9 µl
Penicillin/streptomycin (10000 U/ml)	Thermofisher, 15140122	500 µl
B27-containing medium		
Neurobasal	Thermofisher, 12348017	48 ml
B27 Supplement (50X)	Thermofisher, 17504044	1 ml
L-glutamine (200 mM) or GlutaMAX	Thermofisher, 25030024 or 35050061	500 µl
Penicillin/streptomycin (10000 U/ml)	Thermofisher, 15140122	500 µl

Table 2. Neural Maintenance Medium (N2B27).

The induction media was changed on a daily basis for 10 days before lifting the neuroepithelial layer using dispase (Thermofisher, 17105041) and replating the cells onto laminin (Sigma, L2020-1MG) - coated plates (prepared overnight at 37 °C). Neural precursor cells (NPCs) were maintained in N2B27 medium and split using accutase (Thermofisher, A1110501), before final plating in Geltrex-coated CellCarrier Ultra 96 well plates or 12 well plates at day 50. Cells were maintained in N2B27 until at least day 70 after the start of differentiation before use.

Rapid differentiation of the dCas9 iPSCs and maintenance of the CRISPRi - i^{3}Neurons

Rapid differentiation of the dCas9 iPSCs into cortical neurons was obtained by inducing overexpression of the stably integrated Ngn2, as described by Fernandopulle et al. 2018.

dCas9 iPSCs were grown as described above to 70-80 % confluency. The iPSCs were checked to assess the absence of spontaneous differentiation and the presence of healthy colonies. The iPSCs were harvested by accutase dissociation to obtain single cells as follows: cells were washed with PBS until no debris was visible, before adding 0.5 ml of pre warmed accutase and incubating the plate at 37˚C for 5 minutes (or until most cells had detached, maximum up to 15 min). Once the cells had detached, the accutase solution was used to wash the well to break apart the clumps, before transferring the cells to a 15 ml conical tube. The surface of the well was then rinsed with warm induction media (Table 3) to collect and transfer all remaining cells.

Reagent	**Supplier and Cat. Number**	**Amount to add for 50 ml**
DMEM/F12, HEPES	Thermofisher, 11330032	48.5 ml
N2 Supplement (100x)	Thermofisher, 17502048	500 µl
Non-essential amino acids (100x)	Thermofisher, 11140050	500 µl
GlutaMAX (100x)	Thermofisher, 35050061	500 µl

Table 3. Induction Medium for dCas9 iPSCs.

Cells were then centrifuged at 300x g for 5 min. In the meanwhile, the recipient Geltrex-coated 6 well plates were prepared by aspirating the Geltrex solution and adding 1 ml/well of induction media supplemented with 2 µg/ml Doxycycline (from a 2 mg/ml stock prepared in PBS - Sigma, D9891), to induce Ngn2 expression, and 10 µM ROCK inhibitor Y-27632 (Miltenyi Biotec, 130-106-538), to promote survival of the iPSC when dissociated in single cells. After the spin, the supernatant was aspirated as much as possible and the cell pellet was gently resuspended in 2 ml of supplemented induction media. Cells were then counted with the Countess II automated cell counter and plated at a density of 4 x 10^5 cells/well. The wells were then topped up to 2 ml with supplemented induction media and incubated overnight in a humidified chamber at 37 °C with 5% CO_2.

The following day, which was designated as day 1, the cells were checked under the microscope for nascent neuritic extensions. Fresh prewarmed induction media was then supplemented with 2 µg/ml Doxycycline only and a full media change was performed. If significant cell debris was present, the wells were washed with PBS once before replacing with 2 ml of fresh induction media. The same process was repeated on day 2. On day 3, 72 h after doxycycline exposure, the cells were assessed to check they were healthy and had evident neurites, and were final plated. For final plating, the iNeurons were harvested via accutase dissociation as described above, counted, and plated on Geltrex-coated vessels or laminin-coated glass coverslips at the following densities (Table 4):

Plate type	Number of cells/well	Volume of media/well
12 well plate (for biochemistry or qPCR)	4 x 10^5	1 ml
96 well plate (for imaging - inner 60 wells, outer wells filled with PBS)	3 - 5 x 10^4	100 µl
24 well plate (for imaging on glass coverslips)	2 x 10^5	500 µl
µ-Slide 8 Well (Ibidi, 80806)	2.5 - 5 x 10^4	250 µl

Table 4. Cell density for final plating of the iNeurons on day 3.

At final plating stage, the cells were gently resuspended and plated in maintenance media. For experiments comparing the maturity of the iNeurons and its impact on mitophagy induction, the iNeurons were cultured in either N2B27 (Table 2 minus the penicillin/streptomycin) or in Brainphys (Table 5).

Reagent	Supplier and Cat. Number	Amount to add for 50 ml
Brainphys Neuronal Culture Medium	STEMCELL Technologies, 05790	49 ml
B27 Supplement (50X)	Thermofisher, 17504044	1 ml
BDNF (reconstituted in 0.1% BSA in PBS to 10 µg/ml)	PeproTech, 450-02	50 µl (final concentration 10 ng/ml)
NT-3 (reconstituted in 0.1% BSA in PBS to 10 µg/ml)	PeproTech, 450-03	50 µl (final concentration 10 ng/ml)

Table 5. Brainphys Neural Maintenance medium.

After plating, the plates were gently rocked to ensure even distribution of the iNeurons and incubated at 37 °C with 5% CO_2. For maintenance of the cultures, the media was half changed twice a week (i.e. every 3-4 days) by slowly aspirating half the volume and very gently replacing it with fresh media, pipetting on the side of the well, to avoid detachment of the cells.

Induction of mitophagy in iPSC-derived neurons and iNeurons

To induce mitophagy, the neurons were treated with 1 µM Oligomycin and 1 µM antimycin A (O/A). For neurons cultured in 96 well plates, the treatment mix was prepared in maintenance media at 3X the final concentration (i.e. 3 µM) and 50 µl were added to appropriate wells gently on the side of the well. For neurons cultured in 12 well plates, O/A was added directly to the wells so to have a final concentration of 1 µM. For Western blot mitophagy experiments in the PINK1 cortical neurons, the cells were switched to maintenance medium without antioxidants (N2B27 medium without 2-mercaptoethanol and with B-27 no antioxidant supplement) 1 h before treatment with 1 µM O/A, as removing antioxidants has been suggested to improve detection of mitophagy (Joselin et al, 2012; Grenier et al, 2013). Every 12 h 50% of the medium was replaced with fresh antioxidant free medium supplemented with 1 µM O/A until lysis (Soutar *et al.*, 2018).

Lentivirus production for sgRNA delivery

Single guide RNAs (sgRNAs) against KAT8, KANSL1 and PINK1 were selected from the human CRISPRi-v2.1 library (Horlbeck *et al.*, 2016). The 5 guides with the highest predicted target activity were selected for KANSL1 and PINK1, while the top 3 guides for each transcription start site were selected for KAT8 (Table 6).

Lentivirus CRISPR vector containing the chosen sgRNAs were purchased from VectorBuilder.

Target Gene and Sequence number	Target Sequence (5'-3')
PINK1_Seq1	GGGCCGCGGCGCCACCATGG
PINK1_Seq2	GCCGGGCCGCGGCGCCACCA
PINK1_Seq3	GGCCTGTCGCACCGCCATGG
PINK1_Seq4	GAGTTTGTTGTGACCGGCGG
PINK1_Seq5	GCGCCAGCCCGGCCACCGAC
KANSL1_Seq1	GCCGCCGCGGCGAGACGAGT
KANSL1_Seq2	GAGACGAGTCGGCTTCGCTA
KANSL1_Seq3	GCCCCCCGCCCGGAAAGTCA
KANSL1_Seq4	GCCGGCTCGGCGAGCGGTGG
KANSL1_Seq5	GCCGCTTCAGATTAAAGGGG
KAT8_Promoter 1_Seq1	GGTTGCGGCGGGGACTTCAG
KAT8_Promoter 1_Seq2	GACTTCCCTTCCCGCGATGG
KAT8_Promoter 1_Seq3	GGCACAGGGAGCTGCTGCGG
KAT8_Promoter 2_Seq1	GTCAGGATGTAAAAGACGAA
KAT8_Promoter 2_Seq2	GGGTTCTGACAGTAAATCTA
KAT8_Promoter 2_Seq3	GCTGCAGGAGAAGGAGTCCC

Table 6. Single guide RNA sequences for CRISPRi, from Horlbeck et al.

The sgRNA containing lentiviruses were generated using a 2nd-generation system in Lenti HEK293 cells, by transfecting the sgRNA vectors, the VSV-G envelope plasmid (Addgene plasmid #12259) and the PAX packaging plasmid

(Addgene plasmid #22036) using Lipofectamine 3000 (Thermofisher, L3000008). Cells were seeded at $1x10^6$ cells/well in a 6-well plate, so to reach 80% confluence at the time of transfection. After 24 h, media was fully changed 1 h prior to transfection. For one transfection in one well, two tubes were prepared: in the first tube (DNA tube), 1 μg of sgRNA plasmid, 0.7 μg of PAX plasmid and 0.3 μg of VSV-G plasmid were added to 125 μl of OptiMEM (Thermofisher, 31985062) and 6 μl of p3000 reagent. In the second tube (lipofectamine tube), 6 μl of lipofectamine 3000 were added to 125 μl of OptiMEM. The DNA mixture was then added dropwise to the lipofectamine mixture and incubated for 20 min at room temperature. The transfection mix was then added dropwise to the 6-well plate, before gently rocking the plate to mix. Cells were incubated in Containment level 2 (CL2) in a humidified chamber at 37 °C with 5% CO_2 overnight and all subsequent steps were performed in CL2 facilities.

The following day, the media was fully replaced with 2 ml of mTesr Plus, so to allow for transduction of the iPSCs. The lentivirus containing supernatant was disposed of in Virkon. Cells were again incubated overnight in a humidified chamber at 37 °C with 5% CO_2. After another 24 h, the lentiviral supernatant in mTesr Plus was collected and filtered through a 0.45 μm polyethersulfone (PES) filter. the filtered virus supernatant was diluted 1:1 in fresh mTesr Plus and supplemented with polybrene (Hexadimethrine Bromide, Sigma, H9268) at a final concentration of 10μg/ml, to improve lentiviral transduction. ROCK inhibitor Y27632 was added at a final concentration of 10 μM to improve iPSC survival after single cell dissociation while plating. The filtered and supplemented lentivirus solution was then either snap frozen in dry ice and stored at -80 °C or used immediately for transduction.

Lentivirus transduction of the dCas9 iPSCs

On the day of transduction, the diluted lentivirus solution (supplemented with ROCK inhibitor and polybrene) was thawed on ice for volumes bigger than 1 ml, or in the hood just before transduction if smaller than 1 ml. The dCas9 iPSCs were harvested with accutase as described in the differentiation section. The cells were counted and seeded at $4x10^5$ cells/well in a Geltrex-coated 6-well plate. 2ml of the diluted lentivirus solutions were added on top of the cells in the appropriate wells. The plate was gently rocked to ensure even distribution of the cells, before incubation in a humidified chamber at 37 °C with 5% CO_2.

Imaging

Immunocytochemistry (ICC)

To prepare cells for imaging, cells were first of all fixed with cold 4% PFA in PBS, after treatment to induce mitophagy or at the right confluency. Cells grown on glass coverslips were washed once with PBS before adding the PFA to cover the cell layer. Cells grown in 96 well plates were fixed by adding half the volume of media in well of 12% PFA on top of the cells directly (i.e. for wells containing 150 µl of media, 75 µl of 12 % PFA was added on top, so that the final concentration of PFA on the cells was 4%, a 1/3 dilution). This was done to avoid an additional aspiration and washing step that could impact cell attachment, especially for the neuronal cultures, and introduce extra variability and plate effects. Cells were incubated with PFA for 15 min at room temperature, before aspirating the PFA and washing once with PBS. If necessary, cells were stored at this point at 4°C in PBS before continuing with the staining.

To avoid unspecific antibody binding, reducing background fluorescence, and to allow penetration of the antibodies of interest into the cells and to the mitochondria, cells were blocked and permeabilised with 10% FBS, 0.25% Triton X-100 in PBS for 45 min - 1 h at room temperature. Cells were then immunostained with primary antibodies against the targets of interests. The antibodies were diluted in 10% FBS in PBS and well resuspended, before addition to the cells and incubation on a rocker for 2 h at room temperature. Following incubation with the primary antibodies, cells were washed 3X with PBS before the fluorophore-conjugated secondary antibodies (to detect and amplify the primary antibodies) and Hoechst 33342 (to label the nuclei) were diluted in 10% FBS in PBS and added to the wells. The plates were then incubated for 1h at room temperature in the dark. After a final 3X PBS washes, 96 well plates were filled with PBS (150 µl/well), sealed with foil seals and stored at 4°C. Coverslips were mounted on microscope slides using a drop of Prolong Gold Antifade Mountant (Thermofisher, P10144) and left to dry in the dark at room temperature overnight, to allow the mountant to set. The slides were then stored at 4°C.

High Content Imaging and analysis

All 96 well plates were imaged using the Opera Phenix confocal high content system. Images were acquired using the 40X (NA 1.1) or 63X water objective (NA1.15). Multiple fields of view with Z-planes (of 1 µm distance for the 40X objective, 0.5 µm for the 63X) were acquired for each well. The following excitation and emission filters were used for the following wavelengths:

Fluorophore	Excitation (nm)	Emission (nm)
Alexa Fluor 488	488	500-550
Alexa Fluor 568 (also used for TMRM)	561	570-630
Alexa Fluor 647	640	650-760
Hoechst 33342	375	435-480
Keima Green	488	650-760
Keima Red	561	570-630

Table 7. Wavelength specifications for high content imaging on the Opera Phenix.

Images were analysed in an automated way using the Columbus 2.8 analysis system. To measure the intensity of the mitochondrial signal (i.e. TOM20 or TMRM) and of the pUb(Ser65) signal in the SHSY5Y cells, the software first finds the nuclei on maximum projections, before defining the cytoplasm, identifying the TOM20 and pUb(Ser65) spots and measuring their intensities. The outputs of the analysis are the number of nuclei selected and the mean integrated TOM20 and pUb(Ser65) intensity, calculated as the area of the cell covered by TOM20 or pUb(Ser65) spots x corrected intensity of the spots. This script was adapted to analyse the iNeurons by defining the cytoplasm on the MAP2 signal and adding a selection step to only measure the mitochondrial and pUb(Ser65) intensities in the MAP2-positive cells.

Confocal Imaging

Cells plated on glass coverslips or in Ibidis were imaged on a Zeiss LSM 700 upright confocal, using the Zen 2009 software. Images were acquired using the 63X

NA 1.4 oil objective. Laser power and gain settings were adjusted to avoid saturation and reduce the background noise, and were kept the same across samples when imaging to quantify intensity levels. Z-stacks were acquired for at least 3 fields of view per sample.

Mitophagy measurement using the mt-Keima reporter

Mt-Keima is a pH-sensitive, mitochondrial matrix-targeted dual fluorescence protein whose excitation spectrum shifts from a green wavelength in neutral environment (such as the cytoplasm) to a red wavelength in an acidic environment (such as lysosomes). This allows to measure mitophagy as a ratio of the area of red (lysosomal mitochondria) to red plus green (total mitochondria) signals (Katayama *et al.*, 2011; Sun *et al.*, 2015). The mt-Keima reporter is resistant to lysosomal proteases, which enables measurement of the mitophagic flux over time, but can only be imaged in live cells, as fixing samples abolishes the pH gradient across the lysosomal membrane.

Stable mt-Keima expressing POE SHSY5Y cells were reverse transfected with 50 nM siRNA in 96-well CellCarrier Ultra plates as described above and incubated for 72 h. For the assay, the cell medium was fully replaced with phenol-free DMEM + 10% FBS containing Hoechst 33342 (1:10000) and either DMSO or 1 µM O/A to induce mitophagy. Cells were immediately imaged on the Opera Phenix at 37 °C with 5% CO2, acquiring 15x single plane fields of view, using the 63X water objective, NA 1.15. The following excitation wavelengths and emission filters were used: cytoplasmic Keima: 488 nm, 650–760 nm; lysosomal Keima: 561 nm, 570–630 nm; Hoechst 33342: 375 nm, 435–480 nm. Images were analysed in an automated way using the Columbus 2.8 analysis system (Perkin Elmer) to measure the mitophagy

index. Cells were identified using the nuclear signal of the Hoechst 33342 channel, before segmenting and measuring the area of the cytoplasmic and lysosomal mt-Keima. The mitophagy index was calculated as the ratio between the total area of lysosomal mitochondria and the total area of mt-Keima (sum of the cytoplasmic and lysosomal mt-Keima areas) per well.

Measurement of the mitochondrial membrane potential using TMRM

Mitochondrial membrane potential ($\Delta\Psi_m$) was measured using the fluorescent dye tetramethylrhodamine methyl ester (TMRM - Thermofisher, T668). TMRM is a cell permeant, cationic dye which accumulates in the negatively charged mitochondrial matrix in proportion to $\Delta\Psi_m$, without affecting mitochondrial function and cell health. TMRM is a single excitation, single emission dye and at low concentrations it accumulates in the matrix without aggregating and quenching the signal. Therefore, at low concentrations of dye, the fluorescence signal will be proportional in intensity to the $\Delta\Psi_m$, and decrease after depolarisation, as the dye dissipates into the cytosol (Connolly *et al.*, 2018).

Cells were plated in 96 well Cell Carrier Ultra plates, with knockdowns performed as described above. To load the dye, the cells were washed once with room temperature HBSS and incubated with 25 nM TMRM and Hoechst 33342 (1:10000) in HBSS for 40 min at room temperature in the dark. The cells were then imaged on the Opera Phenix (96 well plates), or on a Zeiss LSM 700 upright confocal microscope (Ibidis). High content imaging was performed using the 40X

water objective, NA 1.1, using the Alexa Fluor 568 settings described above. Multiple fields of view were acquired per well, with 1 µm Z-planes per field of view. TMRM fluorescence was quantified using Columbus 2.8, using the analysis for integrated intensity of the mitochondria described above.

Calcium imaging using Fura-2 AM

Cytosolic calcium is an essential second messenger in cells, and in neurons it is linked to their electrical activity. Measuring intracellular calcium transients upon stimulation can therefore be a way to determine neuronal activity and firing, which is dependent on the maturity of the neurons. To measure the intracellular concentration of calcium in the iNeurons, the ratiometric fluorescent calcium indicator Fura-2 AM (Thermofisher, F1201) was used. This dye undergoes a shift in its excitation spectrum when it binds Ca^{2+}, from 380 nm to 340 nm, maintaining the same emission wavelength at 510 nm. Therefore, the ratio of the fluorescence intensity F340/F380 can be used as an indication of cytoplasmic Ca^{2+} levels. Using a ratiometric dye has several advantages, as it corrects for uneven dye loading across samples and potential photobleaching, which would affect both channels equally.
To perform calcium imaging, the iNeurons were plated on Ibidi 8 Well µ-Slides and cultured up to day 21. The cells were then gently washed twice with HBSS and incubated with 5 µM Fura-2 AM in HBSS for 30 min at room temperature in the dark. After incubation, the iNeurons were again washed once with HBSS and imaged on an epifluorescence inverted microscope equipped with a 20x fluorite objective (Nikon Eclipse Ti-S). The excitation light was generated by a xenon arc lamp through a monochromator at 340 and 380 nm, while the emitted fluorescence light was reflected through an ET510/80 m filter to an Andor Zyla sCMOS camera (Cairn

Research) and digitised to a 16-bit resolution. The excitation light intensity was adjusted so to not saturate the signal and allow to measure increases. Images were acquired every 5 seconds. The iNeurons were imaged at basal levels for 2 min, to monitor stability of the dye and of the signal being acquired, before being treated with 5 μM glutamate to stimulate firing and imaged for up to a total of 10 min. Images were analysed using the Andor iQ2 software (Andor), by manually drawing Regions of Interest around the neuronal soma and measuring the ratio of the fluorescence intensity for the two channels.

Molecular Biology

Real Time - qPCR

To measure the expression levels of genes of interest relative to housekeeping control genes, after knockdown, treatment or during neuronal development, real time quantitative PCR (RT-qPCR) was performed. Total RNA was extracted from confluent wells of a 12 well plate using the Monarch Total RNA Miniprep Kit (New England Bioscience), with inclusion of the optional on-column DNAse treatment. The RNA was resuspended in nuclease free water, quantified using the NanoDrop One (Thermofisher) and stored at -80°C. 500 ng of the RNA was reverse transcribed with SuperScript IV reverse transcriptase (Thermofisher, 18090010) to obtain complementary DNA (cDNA) in the following way. The RNA samples were thawed on ice, and all steps were carried out on ice. 500ng were added to wells of a 96 well PCR plate and topped up to 4.875 µl with nuclease free water. At least one sample was added in duplicate to use as a no reverse transcription control. The random hexamer primers mixture was prepared by adding

(for one well) 0.25 µl of the 100 µM random hexamer stock (Thermofisher, SO142) and 0.5 µl of the 10 mM dNTP mix (Thermofisher, 18427013) to 1.25 µl nuclease free water. The mixture was then added to each well (2 µl/well), before the plate was sealed, vortexed and spun down. The plate was then heated at 65 °C for 5 min in the PCR block and snap cooled on ice. The reverse transcription mix was prepared using the SuperScript IV reverse transcriptase kit: for one well, 0.5 µl of the 100 mM DTT, 0.5 µl of the RNase OUT (Thermofisher, 10777019) and 0.125 µl of the reverse transcriptase were added to 2 µl of the buffer. The negative control was prepared in the same way but excluding the enzyme. 3.125 µl of the mix were added to each well, before sealing, vortexing and spinning down the plate. The samples were then incubated on the PCR block using the following conditions: 25 °C for 10 min, 50 °C for 40 min, 80 °C for 10 min. The cDNA was then diluted 1:60 in nuclease free water, and stored at -20°C.

The cDNA product was then used to perform RT-qPCR using the Fast SYBR™ Green Master Mix (Thermofisher, 4385612) and primers specific for the genes of interest (Table 8). The primers individually were reconstituted in nuclease free water to 100 µM. For the RT-qPCR reaction, a primer mix of 5 µM forward and 5 µM reverse primers was prepared in nuclease free water. The reaction mix was prepared by adding 5 µl of the Fast SYBR Master Mix, 1 µl of the 5 µM primer mix and 4 µl of the 1:60 diluted cDNA to each well. Each sample, including the negative control, was run in triplicate. Plates were read on the QuantStudio 7 Flex Real-Time PCR System (Applied Biosystems). The amplification curves were checked for absence of amplification of the negative control, similar threshold cycles (Ct) for the housekeeping gene in the different samples and absence of multiple melting peaks.

Relative mRNA expression levels were then calculated using the $2^{-\Delta\Delta Ct}$ method and *RPL18A* as the housekeeping gene. To do this, firstly the average Ct for *RPL18A* was subtracted from the average Ct of the gene of interest for each sample individually (ΔCt). The ΔCt of the control sample (e.g. the SCR control) was then subtracted from the ΔCt of the treatment sample to calculate the ΔΔCt.

Target Gene	Forward Primer (5'-3')	Reverse Primer (5'-3')
RPL18A	CCCACAACATGTACCGGGAA	TCTTGGAGTCGTGGAACTGC
PINK1	GTGGAACATCTCGGCAGGTT	CCTCTCTTGGATTTTCTGTAAGTGAC
KAT8	TCACTCGCAACCAAAAGCG	GATCGCCTCATGCTCCTTCT
KANSL1	ATCCTCCACACAGTCCCTTG	CCCCTTCTCCTCCTTACTGG
OCT4	CCTCACTTCACTGCACTGTA	CAGGTTTTCTTTCCCTAGCT
NANOG	GCTTGCCTTGCTTTGAAGCA	TTCTTGACCGGGACCTTGTC
NGN2	TCAAGAAGACCCGTAGACTGAAGG	GTGAGTGCCCAGATGTAGTTG
NESTIN	AGCAGGAGAAACAGGGCCTAC	CTCTGGGGTCCTAGGGAATTG
MAP2	ATAGACCTAAGCCATGTGAC	AATCTTGACATTACCACCTC
TUJ1	CATGGACAGTGTCCGCTCAG	CAGGCAGTCGCAGTTTTCAC

Table 8. Primer sequences for RT-qPCR.

Western blotting

To analyse proteins in whole cell lysates, cells were plated in either 6 or 12-well plates. To lyse SHSY5Y cells, the media was aspirated and the wells washed once with ice cold PBS, before adding 100 µl of ice cold lysis buffer (50 mM Tris-HCl pH 7.4, 0.1 mM EGTA, 1 mM EDTA, 1% Triton-X-100, 1X protease and phosphatase

inhibitor cocktails). To lyse the neurons, the media was very gently aspirated off the well and 50 µl of ice cold lysis buffer were added immediately to the cells, to prevent detachment. Plates were then stored at -80°C, to ensure complete breakdown of the cells. To harvest the proteins, plates were thawed on ice and cells were scraped off the wells using cell scrapers. The lysates were collected into chilled microcentrifuge tubes and centrifuged at 4°C at 17000xg for 10 min. The supernatant was collected into new chilled microcentrifuge tubes and the protein content was estimated using the DC protein assay. Samples were diluted to 1 mg/ml or 0.5 mg/ml in 4X LDS (10 mM DTT) buffer and heated at 70°C for 10 min.

Samples were then run on SDS-PAGE, to separate the proteins, prior to immunoblotting. 10 µg of protein per sample and a molecular weight marker (Chameleon Duo Pre-stained Protein Ladder, LI-COR Biosciences, 928-60000) were loaded in precast gradient polyacrylamide gels (NuPAGE 4-12% Bis-Tris Gels, Thermofisher). The gels were run at 180V in running buffer (NuPAGE MES SDS running buffer, Thermofisher, NP0002), until the lowest molecular weight marker reached the bottom of the gel. The proteins were then transferred onto PVDF or nitrocellulose membranes using a wet transfer system or the iBlot 2 dry blotting system (Thermofisher). Successful transfer of the proteins to the membrane was checked by staining with Ponceau S (Sigma, P7170), a dye that reversibly binds protein bands, by adding the dye to cover the membrane and rinsing it off with distilled water. At this stage, if necessary the membranes were cut at the required molecular weights to probe for multiple proteins. The membranes were blocked in 5% milk in PBST (1X PBS 0.1% Tween-20, Sigma) for 30 min at room temperature, then incubated with primary antibodies diluted in blocking buffer overnight at 4°C

(Table 9). The membranes were washed 3x in PBST, prior to being incubated with fluorophore-conjugated secondary antibodies diluted in blocking buffer for 1h at room temperature (Table 9). The membranes were again washed 3x in PBST, and a final time in PBS. Blots were then acquired on the Odyssey CLx Imager (LI-COR Biosciences), using the auto settings. The intensity of the protein bands was analysed using Image Studio ver 5.2 (LI-COR Biosciences), and normalised to the GAPDH loading control.

Antibodies

Primary antibodies				
Target	Species	Company	Cat. number	Dilution
TOM20	Mouse	Santa Cruz	sc-17764	ICC: 1:1000
TOM20	Rabbit	Santa Cruz	sc-11415 (discontinued)	ICC: 1:1000 WB: 1:5000
Phospho-ubiquitin (Ser65)	Rabbit	Cell Signaling	37642 (discontinued)	ICC: 1:1000
Phospho-ubiquitin (Ser65)	Rabbit	Cell Signaling	62802	ICC: 1:1000 WB: 1:1000
PMPCB	Rabbit	Proteintech	16064-1-AP	ICC: 1:500
ATPβ	Mouse	Abcam	ab14730	ICC: 1:500
FLAG	Rabbit	Sigma Aldrich	F7425	ICC 1:500
Phospho-Parkin(Ser65)*	Rabbit	Abcam MJFF	MJF-17-42-4	ICC: 1:500
GAPDH	Mouse	Abcam	ab110305	WB: 1:10000
PINK1	Rabbit	In House		WB: 1:1000
Mitofusin 2 (MFN2)	Rabbit	Cell Signaling	9482S	WB: 1:1000
TIM23	Mouse	BD Biosciences	611223	WB: 1:1000
MTCO2	Mouse	Abcam	ab110258	ICC: 1:500

KANSL1	Rabbit	Abcam	ab230008	ICC 1:100
KANSL1	Rabbit	Abcam	ab118187	ICC 1:100
KANSL1	Rabbit	Abcam	ab228899	ICC 1:100
KANSL1	Rabbit	Invitrogen	PA5-70090	ICC 1:100
KANSL1	Rabbit	Abnova	PAB20355	ICC 1:100
V5 tag	Goat	Abcam	ab9137	ICC 1:500
Nestin	Mouse	BD Biosciences	611658	ICC 1:500
Pax 6	Rat	Biolegend	939802	ICC 1:200
Beta 3 Tubulin	Chicken	Abcam	ab41489	ICC 1:1000
Neuronal Nuclei (NeuN)	Rabbit	Abcam	ab104225	ICC 1:500
MAP2	Chicken	Merck	AB5543	ICC 1:5000
Secondary antibodies				
Target	Species	Company	Cat. number	Dilution
AlexaFluor 488 goat anti rabbit	-	Invitrogen	A11008	1:2000
AlexaFluor 568 goat anti mouse	-	Invitrogen	A11004	1:2000
Alexa Fluor 647 goat anti chicken	-	Invitrogen	A21449	1:2000
AlexaFluor 488 goat anti rat	-	Invitrogen	A11006	1:2000
IRDye 680LT donkey anti mouse	-	LI-COR Biosciences	925-68022	1:20000
IRDye 800CW donkey anti rabbit	-	LI-COR Biosciences	925-32213	1:20000

Table 9. Antibodies used for Western blotting and immunocytochemistry.

* The pParkin(Ser65) antibody requires a preclearing step before use. To preclear the antibody, POE SHSY5Y cells were plated in two wells of a 12-well plate and grown to confluence. The cells in both wells were then fixed and blocked one at a time following the same staining protocol used for the experiment. The pParkin(Ser65) antibody was diluted 1:500 in 10% FBS, 0.25% Triton X in PBS and added to the first well for 1 h at room temperature, before being transferred to the second well for 1 h at room temperature. The cleared and diluted antibody was then either used immediately or stored at -20 °C.

Measurement of mitochondrial respiration in the iNeurons (Seahorse)

Mitochondrial respiration was measured using the Seahorse XFe96 Mito Stress Test kit (Agilent, 103708-100). This test measures mitochondrial function by measuring the oxygen consumption rate (OCR) in live cells in real time. The concentration of oxygen and the pH in a small volume of media above a monolayer of cells is measured using fluorescent probes at baseline and after sequential addition of pharmacological inhibitors of the electron transport chain. This allows the assessment of the following parameters in order: basal respiration, all the processes that consume oxygen in cells; ATP-linked respiration, by inhibiting ATP synthase with oligomycin; maximal respiration, by uncoupling the electron transport chain from the membrane potential with carbonyl cyanide 4-(trifluoromethoxy)phenylhydrazone (FCCP); non mitochondrial respiration, by inhibiting the electron transport chain with antimycin A and rotenone (complex I inhibitor). These parameters vary between cell lines and impairments in cellular respiration are detected in many diseases (Hall *et al.*, 2012).

iNeurons were final plated (on day 3) on geltrex-coated Seahorse 96-well plates at a density of 20000 cells/well, in either N2B27 or Brainphys maintenance media for a final volume of 100 µl/well. Cells were plated in all wells apart from the 4 corner wells, to use as background wells. The iNeurons were maintained as described above until day 14, when the assay was carried out.

24 h prior to the assay, the sensor cartridge was prepared by adding 200 µl/well of Seahorse XF Calibrant to the utility plate and placing the probes in the wells. The cartridge was hydrated overnight at 37 °C in a non-CO_2 incubator. On the day of the assay, 80 µl/well of the maintenance media was gently removed and the cells were washed twice by slowly adding and removing 200 µl/well of warm assay medium (XF basic medium supplemented with 10 mM glucose, 2 mM L-glutamine and 1 mM sodium pyruvate, at pH 7.4). After the washes, the wells were topped up to 180 µl/well and incubated at 37 °C in a non-CO_2 incubator for equilibration for 1 hour. During the incubation, the Mito Stress Test compounds were reconstituted in assay medium and loaded in the cartridge in the following order for sequential measurement of the OCR: oligomycin (port A - final assay concentration 1 µM), FCCP (port B - final concentration 1 µM), rotenone/antimycin A (port C - final concentration 0.5 µM). To normalise the data, Hoechst 33342 was added at a 1:10000 dilution with the rotenone/antimycin A. The sensor plate and the cell plate were then loaded in the machine and the basic Mito Stress Test protocol was run. At the end of the protocol, the cell plate was loaded on the Opera Phenix to image the Hoechst signal and the number of nuclei was quantified with Columbus and used to normalise the OCR data.

Statistical Analysis

Intensity measurements from imaging experiments were normalised to SCR O/A for each experiment and presented as percentage. WB and qPCR data were normalised to the SCR control. n numbers are shown in figure legends and refer to the number of independent, replicate experiments. Within each imaging and qPCR experiment, the mean values of every condition was calculated from a minimum of 3 technical replicates. GraphPad Prism 9 (La Jolla, California, USA) was used for statistical analyses and graph production. Data were subjected to either one-way or two-way ANOVA with Dunnett's post-hoc analysis for multiple comparisons, unless otherwise stated. All error bars indicate mean ± standard deviation (SD) from replicate experiments, unless otherwise stated.

Chapter 1

Development of a high content siRNA screen to identify modulators of mitophagy

1.1 Introduction

Genome wide association studies have greatly enhanced our understanding of the genetic basis of disease, by identifying common variants (single nucleotide polymorphisms – SNPs) that are associated with increased or decreased disease risk. However, a major challenge for GWASs is to identify the causal variant(s) and the target gene(s) causing the effect. The majority of SNPs falls in non-coding regions of the genome (both intragenic and intronic) and SNPs in strong linkage disequilibrium, that is co-inherited, cannot be statistically distinguished in their association with risk (Gallagher and Chen-Plotkin, 2018). Nevertheless, GWASs nominate a probable target gene on the risk locus, based on a variety of other available information, such as proximity of the SNP(s) to a coding region or effects of the variants on expression quantitative trait loci (eQTLs), chromatin interactions and conformation, epigenetic modifications, conservation (Edwards *et al.*, 2013). While progress has been made in honing in on the responsible variants and genes, there has been a lack of functional studies to attempt to unambiguously identify the causal gene(s) on the risk loci and their functional role in the pathogenesis of disease (Dourlen, Chapuis and Lambert, 2018). Therefore, systematic analysis of the GWAS risk loci is necessary to unambiguously identify the risk genes on the loci and understand novel disease pathways. This is particularly important also for the

development of new therapeutic strategies, as drugs with a genetic basis are more likely to succeed (Nelson *et al.*, 2015).

One way to functionally assess the GWAS loci is by performing a loss-of-function screen, taking advantage of the developments in RNA interference (RNAi) and high throughput screening technologies. siRNA screening is a powerful way to identify novel gene(s) that influence biological pathways of interest, by exploiting the conserved RNAi mechanism to selectively degrade targeted transcripts (Mohr *et al.*, 2014). This type of genetic screening can be performed in multiwell plates, where one well corresponds to one siRNA pool/target, and combined with high content imaging. High content screening (HCS) allows to capture simultaneously a variety of phenotypes (such as cell viability, protein expression, protein translocation and post translational modifications, cell morphology) at once via automated confocal imaging and automated image processing and analysis (Dorval *et al.*, 2018). This results in rich phenotypic information that does not require prior knowledge of the target of interest, in a faster, higher throughput and less biased way, compared to biochemical assays such as Western blotting.

As many Mendelian and sporadic PD genes map to the mitochondrial quality control pathways (Fig 1), it is plausible that other risk genes identified through GWAS could also act in the mitophagy pathway. RNAi screening strategies have been previously successfully employed to discover novel regulators of Parkin translocation to depolarised mitochondria (Hasson *et al.*, 2013; Lefebvre *et al.*, 2013; Ivatt *et al.*, 2014; McCoy *et al.*, 2014; Scott *et al.*, 2020). More recently, CRISPR whole genome screening has been used to identify novel regulators of Parkin expression (Potting *et*

al., 2017) and of mitophagy (Hoshino *et al.*, 2019). However, none of these screens measured a direct readout of PINK1 activity (pUb(Ser65)), in combination with mitochondrial clearance as assay endpoints, nor did they prioritise gene targets based on their genetic link to disease. Therefore, to assess whether the GWAS candidates play a role in mitophagy, I developed a robust high content siRNA screen in human neuroblastoma Parkin overexpressing (POE) SHSY5Y cells to detect modulators of PINK1-dependent phosphorylation of ubiquitin on Ser65 and/or TOM20 decrease (collaboration with Dr Amy Monaghan at the ARUK UCL Drug Discovery Institute). In the next section, I will describe the steps taken to optimise the screen and how it was used to screen a selection of prioritised GWAS candidates.

1.2 Results

1.2.1 Assay optimisation

The development of a high content siRNA screen requires the optimisation of several parameters, from the selection of the phenotype in a relevant cell model to the transfection steps, the staining and imaging parameters and the image analysis algorithm. The optimised screen can then be used to screen a siRNA library of choice and any hits will undergo rounds of validation using orthogonal methods (Fig 5).

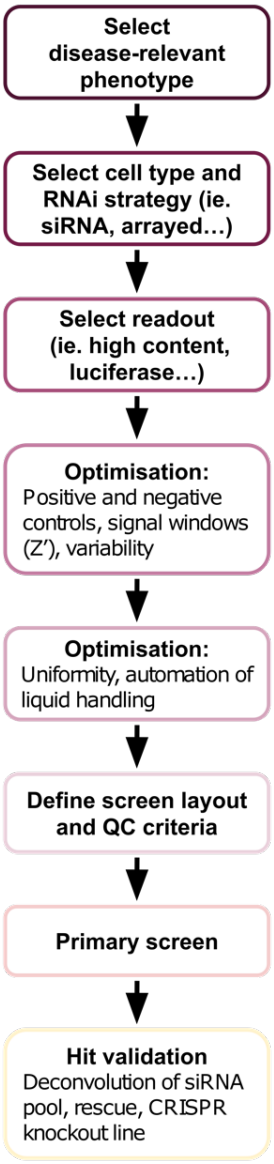

Figure 5. Flow chart of the steps necessary to optimise and run a high content siRNA screen

1.2.2 Selection of the disease relevant phenotype

The first step in the development of a high content siRNA screen is the selection of a disease relevant phenotype, which can be assessed robustly and be reproducible in an appropriate cell model. When mitochondria are damaged, such as when they are depolarised, PINK1 accumulates at the outer mitochondrial

membrane, where it phosphorylates ubiquitin on Serine 65 and it recruits and phosphorylates Parkin (See Introduction Fig 3). The chains of phosphorylated ubiquitin at the mitochondria act as signals to recruit the autophagy machinery, leading to the final degradation of the damaged mitochondria (Fig 3). Therefore, knockdown of potential modulators of mitophagy could affect the rate of mitochondrial degradation and/or the levels of PINK1-dependent phosphorylation of ubiquitin upon mitochondrial depolarisation, so two endpoint readouts were selected for the screen: the intensity of the mitochondrial marker TOM20 and the intensity of pUb(Ser65).

These mitophagy endpoints have been widely characterised in Parkin overexpressing (POE) SHSY5Y cells, a human neuroblastoma cell line. SHSY5Y cells have been extensively used to study mitochondrial mechanisms of Parkinson's disease, due to the fact that they can be differentiated to neuron-like, dopamine expressing cells (Xicoy, Wieringa and Martens, 2017). SHSY5Y cells are also well suited for high content screening, as they are easy and inexpensive to maintain, can be efficiently transfected for RNAi and are amenable to fluorescence imaging.

To characterise the mitophagy endpoints in a HCS setup, POE SHSY5Y cells were plated in a 96-well plate and mitochondria were depolarised by treatment with the ATP synthase inhibitor oligomycin and the Complex III inhibitor antimycin (O/A), before fixing, staining and imaging (Fig 6A). After 3 hours of treatment, pUb(Ser65) levels are increased 35 times (Fig 6B), while there is a 3-fold decrease in TOM20 levels (Fig 6C), as the mitochondria start being degraded. To further analyse this response, we assessed whether the pUb(Ser65) and TOM20 signals were

colocalised. As expected, more than 95% of pUb(Ser65) spots were also positive for TOM20, meaning that the phosphorylated ubiquitin is almost completely colocalised with the mitochondria in O/A treated cells (Fig 6D). This strong, rapid induction of mitophagy when mitochondria are depolarised is reduced by 70% when PINK1 is knocked down (Fig 6A,B), further confirming the central relevance of PINK1 to the mitophagy pathway and leading to the selection of PINK1 as a positive control.

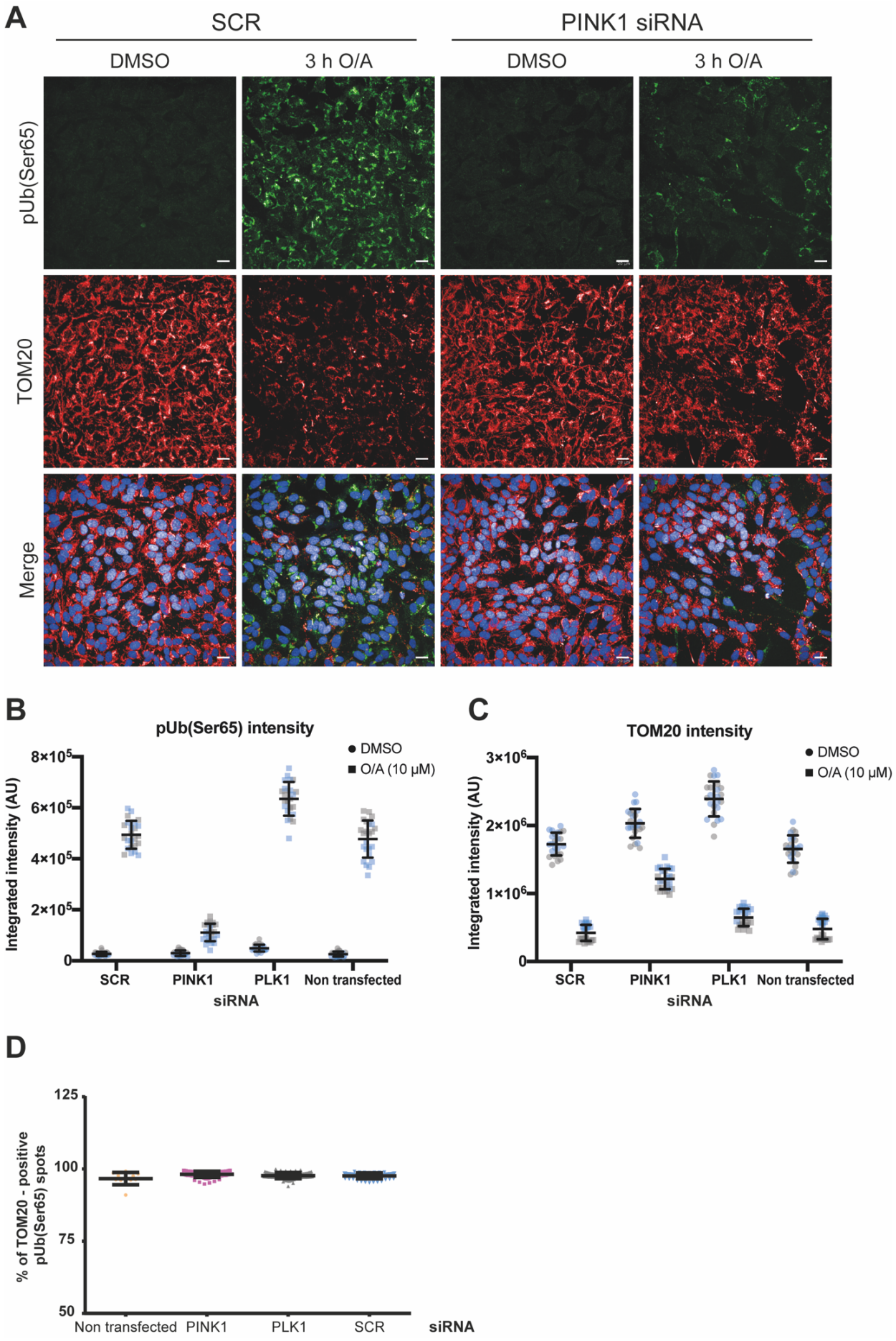
A
SCR
PINK1 siRNA
DMSO
3 h O/A
DMSO
3 h O/A
pUb(Ser65)
TOM20
Merge
B
pUb(Ser65) intensity
DMSO
O/A (10 μM)
Integrated intensity (AU)
8×10^5
6×10^5
4×10^5
2×10^5
0
SCR
PINK1
PLK1
Non transfected
siRNA
C
TOM20 intensity
DMSO
O/A (10 μM)
Integrated intensity (AU)
3×10^6
2×10^6
1×10^6
0
SCR
PINK1
PLK1
Non transfected
siRNA
D
% of TOM20 - positive pUb(Ser65) spots
125
100
75
50
Non transfected
PINK1
PLK1
SCR
siRNA

Figure 6. Selection of a disease-relevant phenotype for high content screening. **A.** Representative images of pUb(Ser65) and TOM20 in SCR and PINK1 KD POE SHSY5Y cells. Cells were transfected with siRNA for 72 h before treatment with 1 μM O/A for 3 h, fixing and staining for the indicated targets. Images were acquired on the Opera Phenix. Scale bar = 20 μm. **B.** Quantification of integrated pUb(Ser65) intensity in **A**. Each dot represents one well of a 96-well plate, the different colours indicate 2 independent plates (n=2). **C.** Quantification of integrated TOM20 intensity in **A.** Each dot represents one well of a 96-well plate, the different colours indicate 2 independent plates (n=2). **D.** Quantification of the colocalisation of TOM20 and pUb(Ser65) in **A**, calculated as the percentage of pUb(Ser65) spots that are also positive for TOM20. Each dot represents one well of a 96-well plate.

1.2.3 Optimisation of transfection efficiency

Transfection efficiency is paramount to the success of a siRNA screen, therefore a key step of assay development is the optimisation of transfection conditions. To monitor the effect of different siRNA concentrations and duration of gene silencing, knockdown of PINK1 was selected as a positive control, as efficient silencing reduces pUb(Ser65) by 70% (Fig 6B). Knockdown of polo-like kinase 1 (PLK1), which causes cell death by inhibiting proliferation and inducing apoptosis (Liu and Erikson, 2003), results in a lower number of nuclei (Fig 7A,B) and was selected as a further transfection control. Knockdown of PLK1, which should be visible at a brightfield microscope as a reduction in cell density in the PLK1 siRNA wells compared to the other control wells, indicates successful siRNA delivery in the assay plate, although it does not indicate the efficiency of transfection.

Non-targeting (scrambled, SCR) siRNA was chosen as negative control and non-transfected wells (transfection reagent only wells) were included as viability controls.

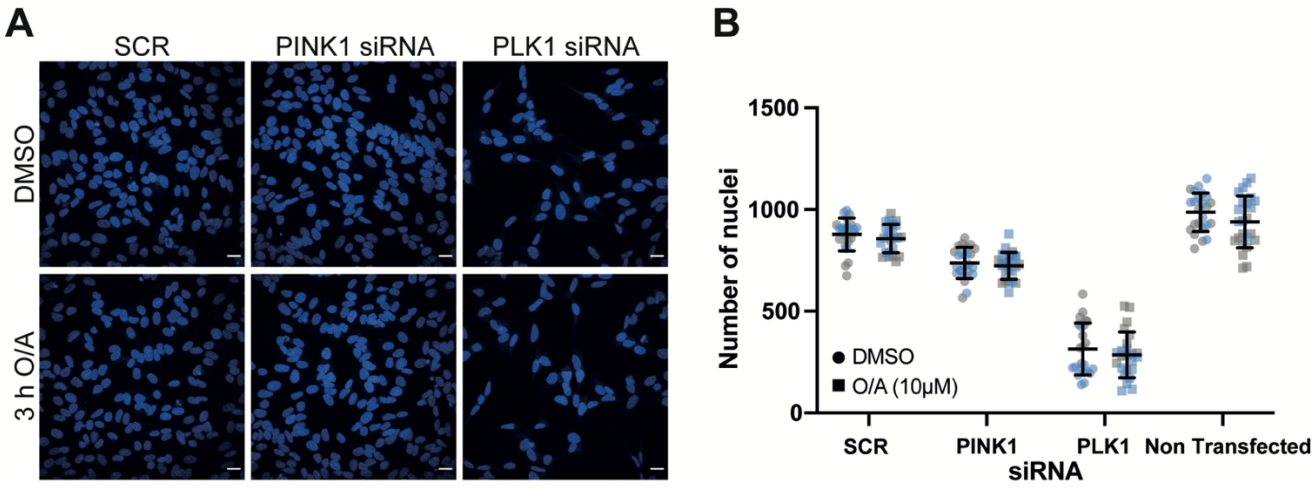

Figure 7. Knockdown of PLK1 as transfection control.

A. Representative images of Hoechst 33342 stain in SCR, PINK1 and PLK1 KD POE SHSY5Y cells. Cells were transfected with siRNA for 72 h before treatment with 1 μM O/A for 3 h, fixing and staining for the nuclei. Images were acquired on the Opera Phenix. Scale bar = 20 μm. **B.** Quantification of the number of nuclei in **A**. Each dot represents one well of a 96-well plate, the different colours indicate 2 independent plates (n=2).

To establish the optimal transfection parameters, POE SHSY5Y cells were plated at 15000 cells/well and reverse transfected with either 25 nM or 50 nM of the control siRNAs. After 48 h (Fig 8A,C) or 72 h (Fig 8B,D), cells were treated with 10 μM O/A for 3 h to induce mitophagy, before fixing and staining for pUb(Ser65) (Fig 8A,B) and TOM20 (Fig 8C,D). 72 h knockdown gave the biggest signal window, without significant plate effects. Similar knockdown efficiency was achieved with either 25 or 50 nM of siRNA, so 30 nM was chosen as final screen concentration.

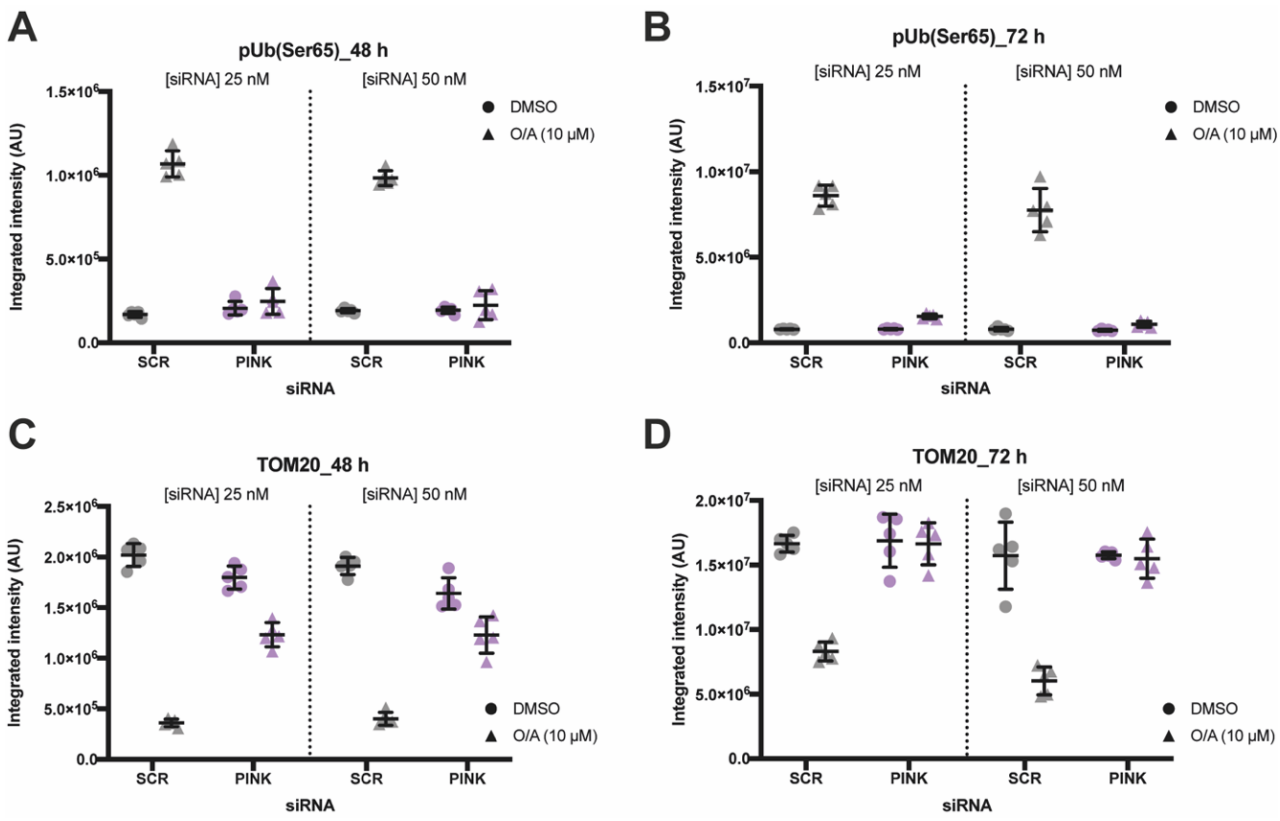

Figure 8. Optimisation of the transfection parameters: concentration and length of transfection.

A,B. Quantification of pUb(Ser65) intensity levels after 48 h **(A)** or 72 h **(B)** transfection of POE SHSY5Y cells with either 25 nM or 50 nM of SCR or PINK1 siRNA. **C,D.** Quantification of TOM20 intensity levels after 48 h **(C)** or 72 h **(D)** transfection of POE SHSY5Y cells with either 25 nM or 50 nM of SCR or PINK1 siRNA. (n=2).

1.2.4 Uniformity assessment

In order to be confident in any hits resulting from the screen, inter and intra plate variability must be assessed and lowered. This can be done by monitoring the Z' (Z prime) factor and the Coefficient of Variation (%CV) of the plates. The Z' factor is widely used to measure the quality of the assay using many replicates of the positive and negative controls. When the Z' is > 0.5, the screen is considered to have a sufficiently high signal to noise ratio and low variability to allow for confident

identification of hits (Birmingham *et al.*, 2009; Sharma and Rao, 2009). The coefficient of variation, which is the ratio between the standard deviation and the mean, measures the variability across the plate. A low %CV corresponds to low variability, therefore increasing reliability of the assay and allowing for comparisons among plates. For siRNA screening, the %CV has to be < 30 to be acceptable.

Therefore, to evaluate replicability and concordance across plates, multiple plates of control siRNAs were run at once. TOM20 and pUb(Ser65) signals were found to be concordant across runs (Fig 9A,B). Strong PINK1 knockdown was observed in both channels across plates, with O/A-treated PINK1 wells showing lower pUb(Ser65) and higher TOM20 levels compared to SCR and non transfected treated controls (Fig 9A,B). PLK1 siRNA wells showed reduced number of nuclei for both treated and untreated wells (Fig 9C). The screen was also sufficiently sensitive and robust to detect outliers, allowing us to exclude them (Fig 9B – one row in plate 4 was accidentally treated, resulting in “DMSO” signal among the PINK1 treated wells).

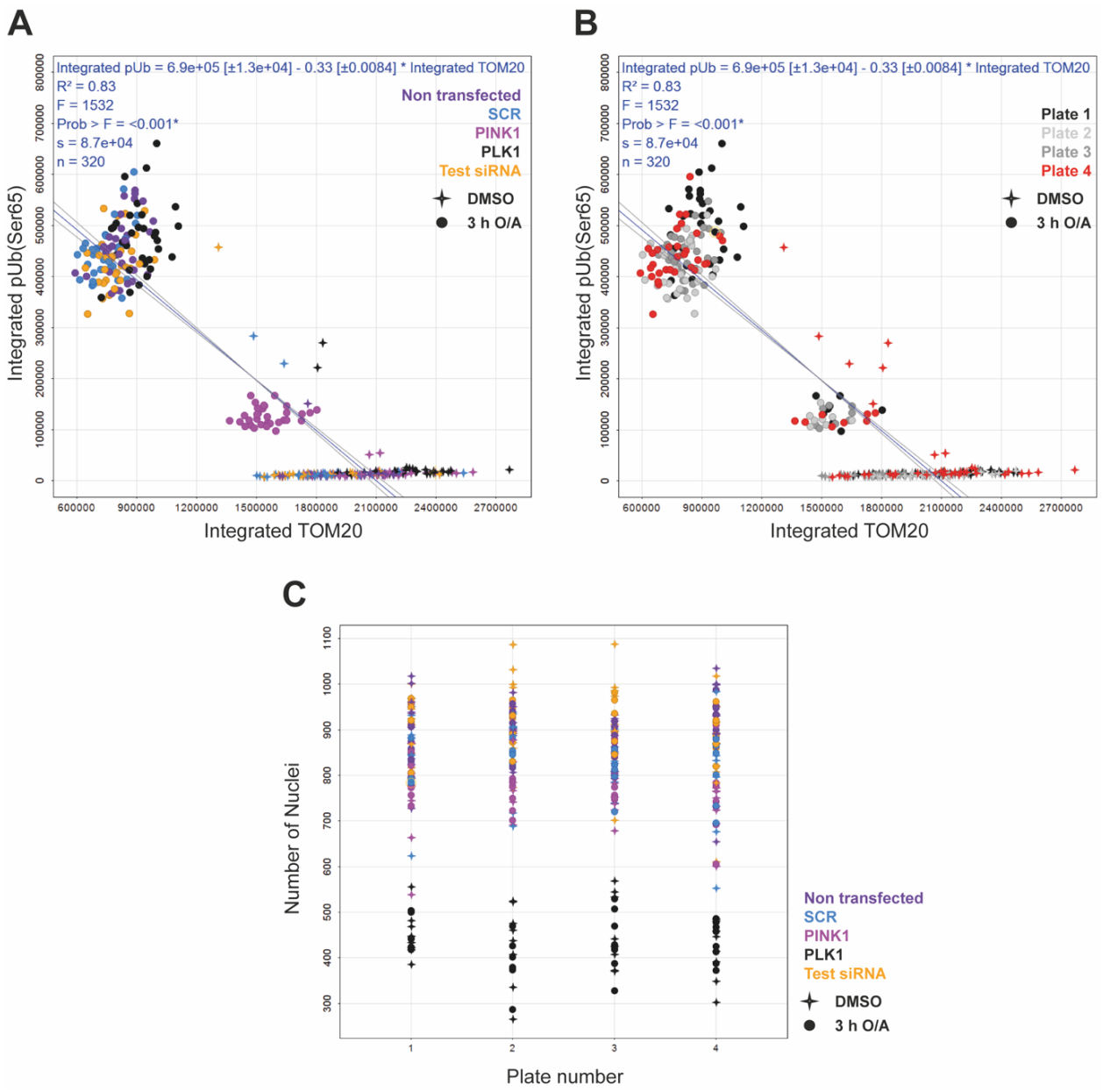

Figure 9. Evaluation of uniformity across plates.

A. Integrated pUb(Ser65) and TOM20 intensities from 4 assay development plates, highlighted by siRNA. POE SHSY5Y cells were transfected with 30 nM SCR, PINK1, PLK1, or test siRNA for 72 h before 3 h treatment with 10 µM O/A or DMSO control. Each point represents one well of a 96-well plate. **B.** Same data as in **A** but highlighted by number of the plate in the run. Note the 4 of Plate 4 among the PINK1 siRNA wells. **C.** Number of nuclei from the same plates in **A** and **B,** showing toxicity of the PLK1 KD, which causes a reduction in the number of nuclei. Graphs in this figure were generated with Dotmatics Vortex at the ARUK DDI.

1.2.5 Introduction of automated liquid handling

In order to further reduce variability and to allow for higher throughput, the siRNA and cell dispensing steps were automated, taking advantage of the equipment available in the UCL High Content Biology Laboratory. siRNAs were dispensed using the Echo 555 acoustic liquid handler, which uses sound waves to dispense nanolitres into multiwell plates. The transfection reagent DharmaFECT 1, diluted in serum free DMEM, was added to the wells using an electronic multichannel pipette. Finally, cells were plated on top of the transfection reagent-siRNA solution with the Cybio SELMA, a semiautomatic multiwell pipettor. Automated dispensing reduced variation compared to manual plating (Fig 10A,C). However, given that the Echo is not a sterile environment and siRNAs are prone to degradation, we observed reduced efficacy of the control siRNAs after one freeze-thaw cycle (Fig 10B,D – PLK1 knockdown does not reduce the number of nuclei). This led us to change our screening strategy with the aim of reducing the number of freeze/thaws of the siRNA libraries, with the control siRNAs being added fresh to the library plate just before introducing it in the Echo.

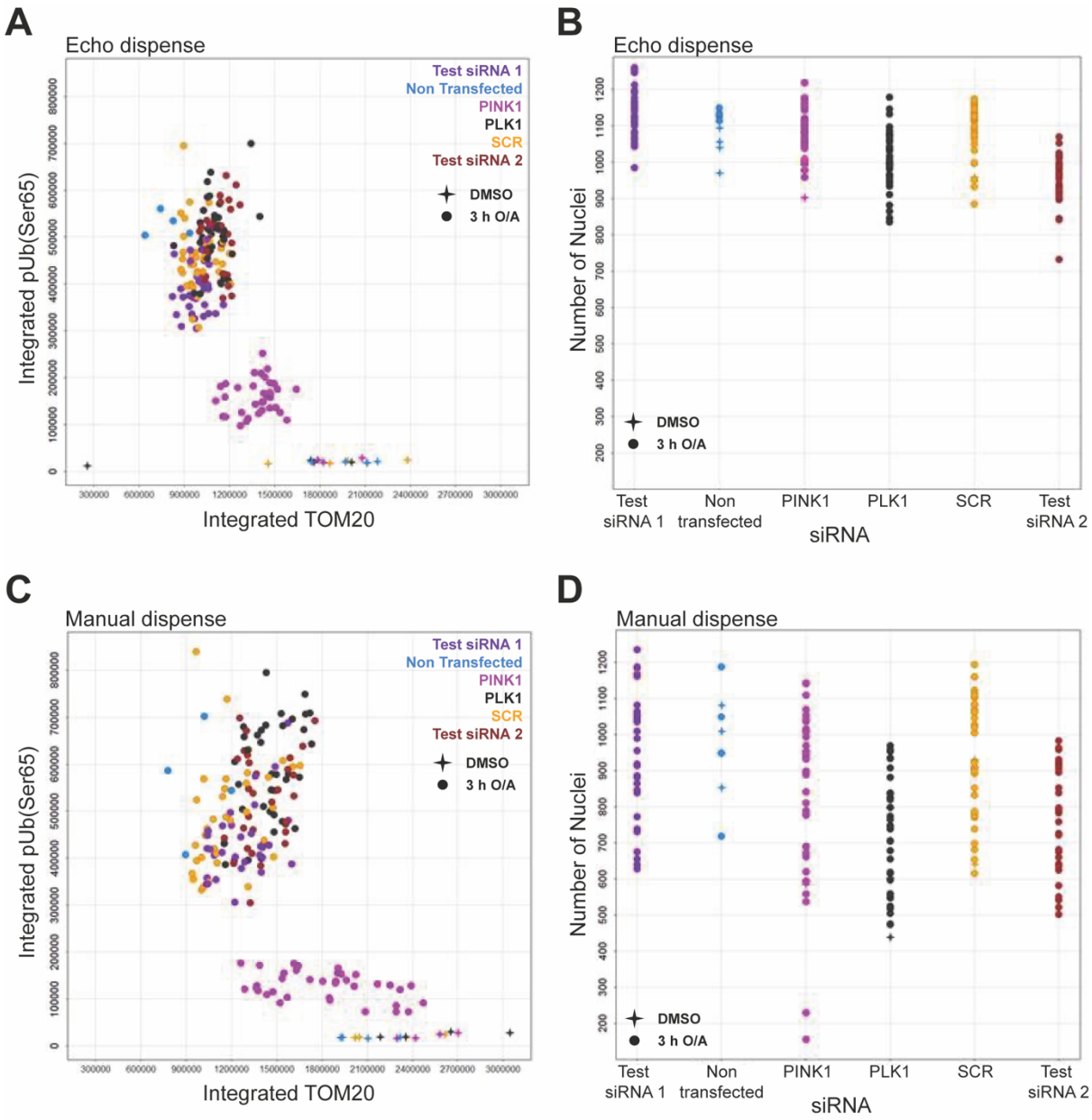

Figure 10. Liquid handling automation reduces variability compared to manual dispensing of siRNA.

A. Integrated pUb(Ser65) and TOM20 intensities from 2 assay development plates, highlighted by siRNA. POE SHSY5Y cells were transfected with 30 nM SCR, PINK1, PLK1 or test siRNA dispensed with the Echo acoustic handler. After 72 h of transfection, cells were treated for 3 h with 10 µM O/A or DMSO control. Each point represents one well of a 96-well plate. **B.** Number of nuclei from the 2 plates in **A.** Knockdown of PLK1 did not have the expected toxic effect (no reduction in the number of nuclei compared to the control siRNA). **C.** Integrated pUb(Ser65) and TOM20 intensities from 2 assay development plates, highlighted by siRNA. POE SHSY5Y cells were transfected with 30 nM SCR, PINK1, PLK1 or test siRNA dispensed manually. After 72 h of transfection, cells were treated for 3 h with

10 µM O/A or DMSO control. Each point represents one well of a 96-well plate. **D.** Number of nuclei from the 2 plates in **C.** As in B, knockdown of PLK1 did not have the expected toxic effect (no reduction in the number of nuclei compared to the control siRNA). Graphs in this figure were generated with Dotmatics Vortex at the ARUK DDI.

1.2.6 Image acquisition and analysis

Taking advantage of previous work in the lab, the screen was developed to be run on the Opera Phenix high throughput confocal system, which allows fast, high resolution, unbiased imaging. For each well of the 96 well plates, 4x 1 µm Z-planes were acquired for 5 fields of view, using the 40X water objective, NA1.1. The Hoechst 33342, Alexa Fluor 488 and Alexa Fluor 568 channels were kept separate during acquisition in order to avoid channel bleed through. Images were then exported and analysed on the Columbus 2.8 analysis system (Perkin Elmer). This platform allows users to use a series of sequential “building blocks” to write automated image analysis scripts. In order to analyse the TOM20 and pUb(Ser65) signals, the software was programmed to first find the nuclei on maximum projections, before defining the cytoplasm. It then identifies the TOM20 and pUb(Ser65) spots and measures their intensities. The outputs of the analysis are the number of nuclei selected and the mean integrated TOM20 and pUb(Ser65) intensity, calculated as the area of the cell covered by TOM20 or pUb(Ser65) spots x corrected intensity of the spots (Fig 11). The image analysis parameters were routinely checked to ensure they kept matching the assay as the screen development progressed.

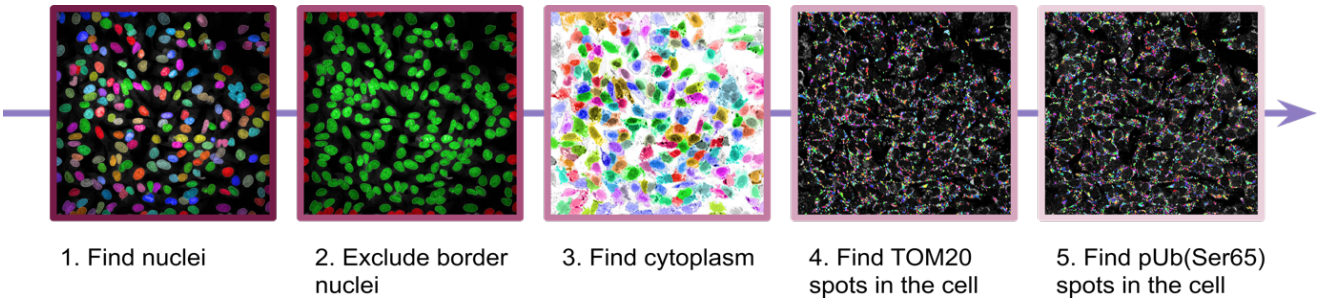

Figure 11. Flowchart of the image analysis steps.

1.2.7 Screen design and determination of the quality control criteria

To increase confidence in any hit, careful consideration was given to the design of the screen plate map. Each siRNA, including controls, would be run in duplicate on one 96 well plate. Controls would be dispensed in the first and last column of the plate, while test siRNAs would be randomly allocated to the inner 80 wells. Therefore, this design allows screening of 40 targets per plate (Fig 12A). To optimise the use of the library and reduce the number of freeze-thaw cycles, each plate would then be run in triplicate.

Concurrently, stringent quality control criteria were defined during the assay development stages. Plates would be first of all checked for plate effects, a systematic error due to the position of the well in the plate, which increases the possibility of obtaining false positive and false negative results. This bias can arise for several reasons, including errors in liquid handing (e.g. cell plating, compound dispensing) and incubation effects (e.g. uneven evaporation of the media across the wells) (Auld *et al.*, 2004). Plate effects were assessed in first instance by visualising

heat maps of the number of nuclei (Fig 12B - an example of two replicates, where blue indicates a lower number of nuclei). While the Plate 1 shows a comparable number of cells across all wells, apart from the expected toxicity of the PLK1 siRNA control (blue wells in columns 1 and 12), Plate 2 shows an uneven number of nuclei across the plate, with fewer cells in the outer wells compared to the inner wells (edge effect) and a gradient from left to right, as well as no detectable effect of the PLK1 siRNA control. Therefore, plates such as Plate 2 would be excluded from further analysis, as the variability due to the plate effect could affect the identification of a true hit. Secondly, the O/A treatment window would need to be minimum 3-fold and efficacy of the PINK1 and/or PLK1 siRNA controls would be assessed using Dotmatics Vortex visualization software. Only plates in which the raw data would yield Z' > 0.5 would then be taken forward for further processing. Finally, candidates would only be considered a hit where their Z score (the number of standard deviations from the mean) was ≥ 2 or ≤ -2, and where replication of efficacy was seen both within and across plates.

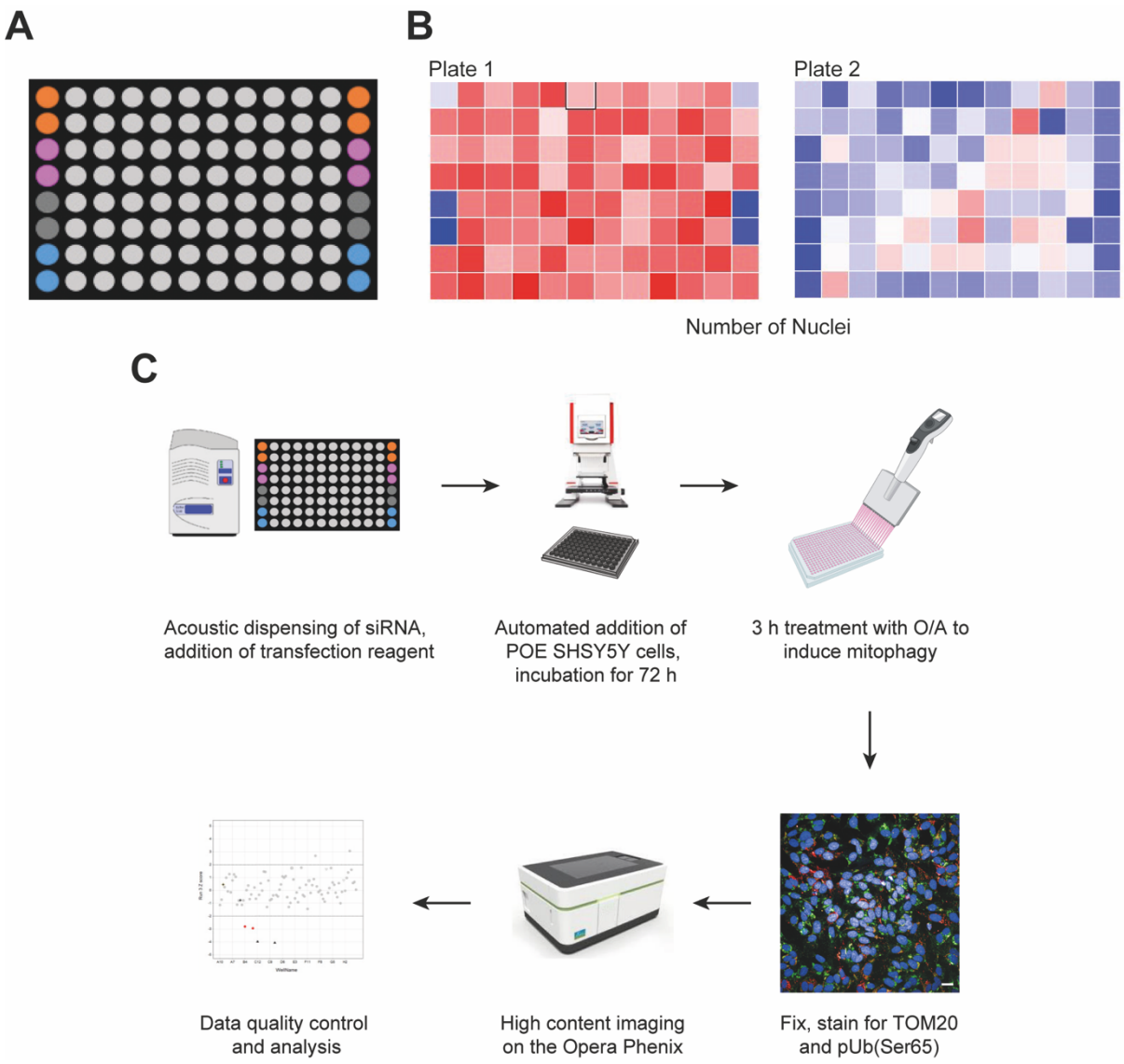

Figure 12. Plate map design, quality control criteria and final workflow.

A. Example of the plate map for the screen. Columns 1 and 12 are the control wells, with the Non trasfected, SCR, PINK1 and PLK1 controls (in duplicate). For the induction of mitophagy, column 1 is the DMSO control while the remaining 11 columns are treated with 10 μM O/A. The inner 80 wells of the plate are the test siRNA wells, in which the siRNA library to screen is dispensed, with each siRNA plated in duplicate. **B.** Example of a plate that passes QC (Plate 1) and one that failed QC (Plate 2). The heatmap shows the number of nuclei in each well, with blue being the lowest. In plate 1, the PLK1 control is visible in columns 1 and 12 as the two darker blue wells (PLK1 knockdown causes cell death). In plate 2, the number of nuclei is more variable, and it is lower around the edges of the plate. C. Final workflow of the high content mitophagy siRNA screen. siRNA is dispensed on Geltrex-coated 96 well plates using the automated liquid handler Echo. The transfection

reagent is added on top and incubated 30 min, before plating POE SHSY5Y cells using the Cybio. Cell were incubated for 72 h prior to inducing mitophagy by treating with 10 μM O/A for 3 h. Cells were then fixed and stained for TOM20 and pUb(Ser65), before imaging of the Opera Phenix and analysing the data.

1.2.8 Screening a selection of prioritised PD-linked genes

The high content siRNA mitophagy assay was then used to screen a selection of PD-linked candidate genes from GWAS studies. Due to the design of the screen plate maps (Fig 12A), a maximum of 40 genes had to be prioritised. 31 candidates from the 2014 and 2017 PD GWAS (Nalls *et al.*, 2014; Chang *et al.*, 2017) were chosen for screening (work done by our collaborators Dr Claudia Manzoni and Dr Daniah Trabzuni). Genes were prioritised based on whether the expression quantitative trait loci (eQTLs) colocalise with the PD risk SNPs (Coloc analysis, Kia *et al.*, 2019), on whether they are relevant for pathways in common with the Mendelian genes through weighted protein-protein interaction network analysis (WPPINA, Ferrari *et al.*, 2018) and on the prioritisation criteria used in the GWAS analyses. In addition, we selected 7 PD Mendelian or lysosomal storage disorder genes, as the latter are also enriched in PD (Robak *et al.*, 2017).

The candidate genes were screened in duplicate on each plate, with 3 replicate plates per run (Table 10). Except for the PINK1 control, KAT8 was identified as the only siRNA able to decrease O/A - induced phosphorylation of ubiquitin by more than 2 SD from the mean in duplicate across all plates (Fig 13A), without having a toxic effect (Fig 13C - no reduction in the number of nuclei). Knockdown of KAT8 did not have a significant effect on the levels of TOM20 (Fig 13B), possibly due to the smaller signal window for the mitochondrial marker (Fig 6C).

Gene	Coloc - B	Coloc - G	WPPINA	GWAS	MPD	MLS
ATP13A2					**X**	**X**
CAB39L		**X**				
CCNT2				**X**		
CD38	**X**	**X**		**X**		
CTSB		**X**	**X**	**X**		
DDRGK1				**X**		
DGKQ				**X**		
DJ1					**X**	
DNAJC13					**X**	
FBXO7					**X**	
GALC	**X**			**X**		**X**
GBA			**X**	**X**	**X**	**X**
GPNMB	**X**	**X**		**X**		
HSD3B7		**X**				
IDUA						**X**
INPP5F			**X**			
KAT8		**X**	**X**	**X**		
KLHL7		**X**		**X**		
LRRK2			**X**	**X**	**X**	
LSM7		**X**		**X**		
MAPT			**X**	**X**		
NCKIPSD		**X**	**X**	**X**		
NSF			**X**			
NUCKS1		**X**		**X**		
NUPL2		**X**		**X**		
PDLIM2		**X**		**X**		
PM20D1	**X**					
PRKN					**X**	
RAB7L1	**X**	**X**	**X**			

SH3GL2			**X**	**X**		
SLC41A1		**X**		**X**		
SNCA				**X**	**X**	
SPPL2B	**X**					
STK39				**X**		
VAMP4		**X**				
VPS35					**X**	
WDR6	**X**	**X**				
ZNF646				**X**		

Table 10. List of the prioritized genes that were screened.

Coloc - B = coloc analysis using Braineac, Coloc - G = coloc analysis using GTEx, WPPINA = weighted protein interaction network; GWAS = genes prioritised in the 2017 PD GWAS (Chang *et al.,* 2017), MPD = Mendelian genes associated with PD, MLS = Mendelian genes associated with lysosomal storage disorders.

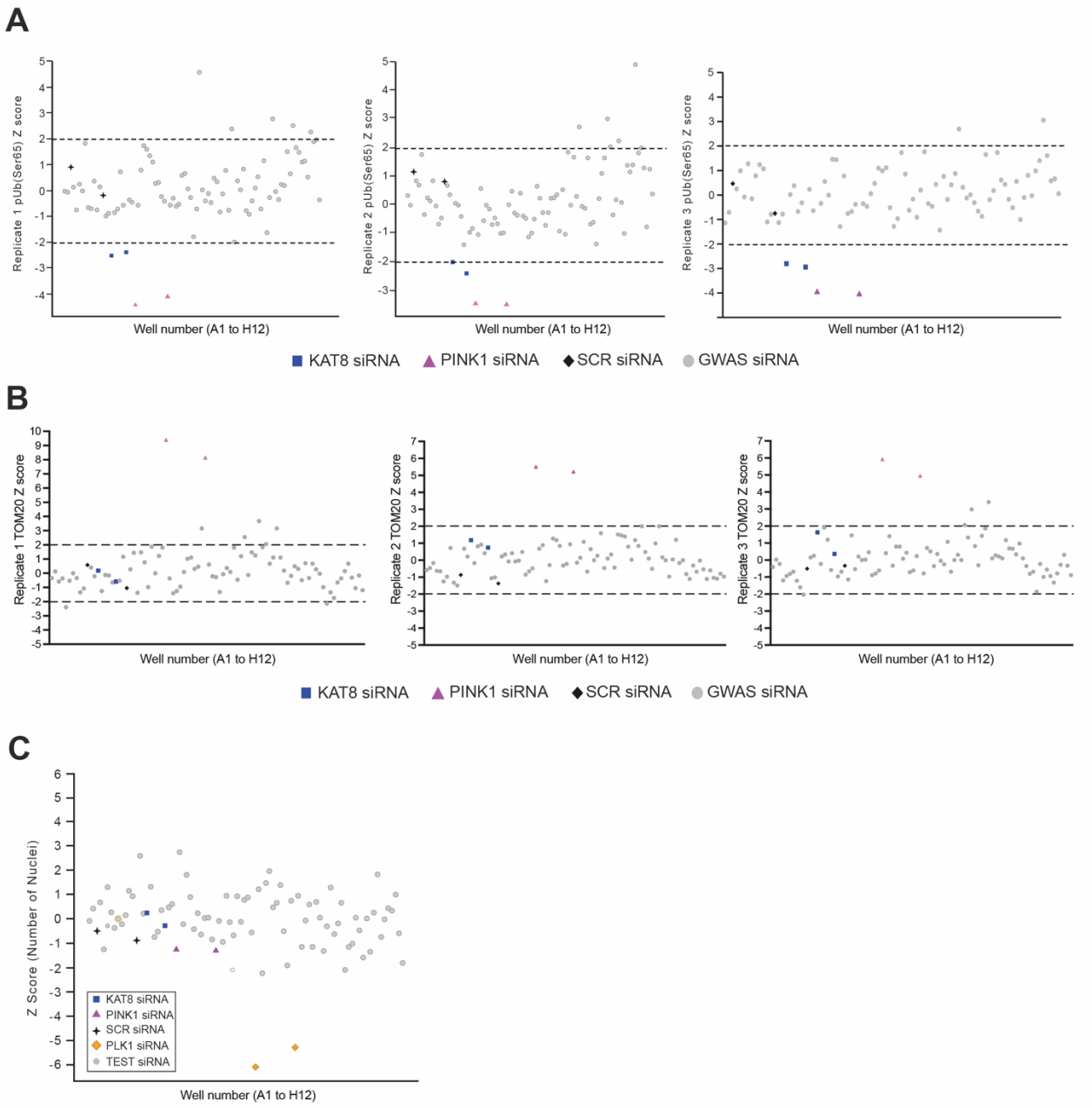

Figure 13. High content mitophagy siRNA screen of prioritised PD risk genes identifies KAT8 as a modulator of pUb(Ser65) levels.

A. pUb(Ser65) Z-scores of the three replicate screen plate. KAT8 is the only gene, together with the PINK1 control, whose knockdown reduces pUb(Ser65) intensity levels by more than 2 SD (Z-score < -2). **B.** TOM20 Z-scores of the three replicate screen plates. KAT8 knockdown does not reduce the degradation of TOM20 after O/A treatment, unlike knockdown of PINK1. **C.** Number of nuclei Z-score from Plate 1, which shows that knockdown of KAT8 does not affect cell viability, unlike the PLK1 transfection control.

1.3 Discussion

A major challenge for GWASs is the identification of the causal variant(s) and gene(s) responsible for disease risk and how they functionally contribute to the phenotype. To systematically investigate whether PD GWAS candidates could affect mitophagy, I developed a robust high content siRNA screen to identify modulators of the pathway, selecting PINK1-dependent phosphorylation of ubiquitin and clearance of the mitochondrial TOM20 as endpoints. Using this approach, we have identified one gene, *KAT8*, whose knockdown significantly reduces pUb(Ser65) levels upon mitochondrial depolarisation, linking a sporadic PD risk gene to mitochondrial quality control. Interestingly, *KAT8* was prioritised bioinformatically using all 3 criteria defined for selection, namely identification through GWAS, effect of the variant on expression (eQTL) and protein-protein interaction with PD-relevant pathways. While we did not detect a significant effect of KAT8 knockdown on TOM20 levels, this may be due to the smaller signal window upon mitochondrial depolarisation (3-fold decrease vs 35-fold for pUb(Ser65) in the SCR condition, Fig 6C). As it is unlikely that GWAS risk genes will have the same effect size as the Mendelian genes on the mitophagy pathway, better tools will be necessary to identify smaller effects on mitochondrial clearance in a screening setup.

RNAi screening is an efficient way to conduct forward genetic screens, in which alteration of one gene causes a visible phenotype. While it requires more optimisation steps and more reagents compared to classical small compound-based screens, it has the major advantage of identifying a unique target, as compounds are often promiscuous and have unknown activity. Running the RNAi screen in an

arrayed format, where one well corresponds to one siRNA, allows it to be run in a HCS format, in which you can measure simultaneously multiple phenotypes, such as in this case phosphorylation of a protein (ubiquitin) and state of the mitochondrial network. HCS depends therefore on the quality of the chosen antibodies or fluorescent reporters but results in more complete phenotypic data compared to the traditional multiwell reporter screens, such as luciferase based screens.

While RNAi-based screening approaches are very successful, they are not without their limitations. Although great progress has been made in optimising siRNA sequences, off target effects can still result in false positives. This screen was conducted with a pool of 4 siRNAs targeting different sections of the messenger RNA of each target, which increases the efficiency of the gene silencing and reduces the amount of reagents needed to run the screen. However, siRNA pools can result in off target effects and deconvolution experiments, where each siRNA in the pool in tested individually, are necessary to confirm hits from the screen. Future iterations of the screen should involve deconvolution of the hit siRNA pools, as well as validation of the efficiency and specificity of the siRNA pools by qPCR, and confirmation experiments, such as rescue of the knockdown by overexpression or the creation of knockout lines, if possible.

Moreover, the identification of true hits depends on the efficiency of the knockdown of each individual target gene. However, transfection efficiency and incubation times can only be optimised based on the positive and negative controls and screening formats do not allow to quantify individual knockdowns via biochemical means. Therefore, as assays are conducted at a fixed time point but different genes have different expression rates and half lives, it is possible to miss

disease relevant genes that might need longer incubation with siRNA. Similarly, incomplete knockdown, resulting in residual protein levels, might mask the effect of genes that require complete knockout to affect the phenotype but also allows to identify genes that might be lethal. Overall, while siRNA screening has some definite advantages, I would adapt the screen to be a gene editing, CRISPR-Cas9 based screen. Using this experimental setup, not only it is possible to analyse the effect of the total absence of protein on the chosen phenotype, but it is also possible to study both gene activation and gene repression using catalytically dead versions of Cas9 (Gilbert *et al.*, 2014). Indeed, screening GWAS candidates with a siRNA based method assumes the risk genes act via a loss of function mechanism, so it would be relevant to also be able to detect whether the risk genes might modulate mitophagy by increased expression.

Although the screen is straightforward to run and has been successful, it can be further developed into a more powerful tool. Firstly, the screen has been designed to run candidate genes in duplicate in one 96-well plate. More genes can be screened by increasing the number of plates with the same format or especially by further miniaturising the assay for a 384-well plate format. This would allow to screen bigger libraries of genes, such as a whole genome library, a druggable genome library or more GWAS-related candidates, increasing the potential to discover novel regulators. A miniaturised format would also allow to run the same genes multiple times for different O/A treatment lengths, as fewer plates would be needed. As the current screen was designed for a 3 h O/A treatment length to induce mitophagy, it is set up to identify modulators of the early stages of pathway. Screening at a later time point would allow detection of delayed responses and bigger signal windows for the

mitochondrial markers, as their level will be further decreased due to mitochondrial degradation. Moreover, the screen can be further multiplexed to detect other features of the pathway, such as Parkin recruitment to the mitochondria, due to the possibility to image a fourth channel (on top of the pUb(Ser65), TOM20 and Hoechst) on the Opera Phenix. This would depend on the availability of a reliable antibody against the phenotype of interest, but can be easily added to the current workflow. In addition, HCS results in a rich, multidimensional phenotype that can only be truly fully investigated with bioinformatic methods. While the screen is run on a “per well” basis, in which the analysis measures the fluorescence levels in the whole well and normalises by the number of nuclei, the progress in automated analysis systems allows to also obtain “per cell” results. This results in a wealth of data that could combine different types of information, such as not only intensity levels of pUb(Ser65) and TOM20, but also mitochondrial and cell morphology and location of proteins, to understand why certain cells present certain phenotypes and improve the replicability of the screen (Snijder *et al.*, 2012). Finally, screening requires cell lines that are easy to maintain and of limited variability, as well as amenable to genetic manipulations and, in this case, fluorescence imaging. However, while SHSY5Y cells are an acceptable model for mitophagy, they are still physiologically far from cell types affected in PD. Therefore, although the current screen is effective, future work should be carried out in iPSC-derived cells, both from controls and from patients. iPSC-based screening presents many challenges, due to the cost and fragility of the cultures, the length of the differentiation process and the high variability between inductions into different cell types and between individuals. However, technological advances in the optimisation of the differentiation protocols, resulting in purer neuronal cultures, and the possibility to perform CRISPR-Cas9

knockdown and knockout in iPSC lines (Tian *et al.*, 2019) mean iPSC-based screening will be more feasible and key to identify true modifiers of disease relevant phenotypes.

In conclusion, I have developed an alternative approach to identify modulators of mitophagy that has successfully identified a novel gene, *KAT8*, that links sporadic PD risk to mitochondrial quality control. In the next chapter, I will further validate and explore the mechanism by which KAT8 regulates mitophagy.

Chapter 2

The role of KAT8 and KANSL1 in the regulation of PINK1-dependent mitophagy

2.1 Introduction

In the previous chapter, KAT8 was identified as a potential novel regulator of mitophagy via functional screening of a selection of PD GWAS risk genes. KAT8 (also known as MOF or MYST1) is a lysine acetyltransferase (KAT) encoded on chromosome 16. Lysine acetyltransferases catalyse the transfer of the acetyl group from acetyl-CoA to the ε-amino group on a lysine. Lysine acetylation (and the reverse deacetylation catalysed by KDACs – lysine deacetylases) has been mostly studied as a posttranslational modification of histones, with effects on epigenetic control of transcription. Over the past decade, global proteomic analyses have revealed a wealth of acetylated non-histone proteins, thanks to advances in mass spectrometry techniques. In particular, a high percentage of all acetylated proteins have been found at the mitochondria, where the higher pH and concentration of acetyl-CoA facilitate non-enzymatic acetylation (Wagner and Payne, 2013), and where the acetylation status of proteins changes their activity in response to metabolic stimuli (Baeza, Smallegan and Denu, 2016). Overall, non-histone acetylation has been linked to the regulation of cell signalling, protein-protein interaction, protein subcellular localisation and autophagy (Narita, Weinert and Choudhary, 2019).

So far, 22 proteins have been confirmed to have KAT activity, which can be mostly grouped in three subfamilies: GCN5, CBP/p300 and MYST (Simon *et al.*, 2016; Sheikh and Akhtar, 2019). KAT8 is part of the MYST family, named after the founding members (MOZ, Ybf2/Sas3, Sas2, Tip60) and characterised by a conserved MYST catalytic domain. KAT8 is mainly responsible for acetylation of lysine 16 on histone 4, with effects on transcriptional regulation (H4K16Ac – Smith *et al.*, 2005; Taipale *et al.*, 2005). KAT8 was first reported to be essential for dosage compensation in Drosophila, an epigenetic mechanism to balance gene expression in male flies by upregulating genes on the single X chromosome (Hilfiker *et al.*, 1997; Akhtar and Becker, 2000). In those same years a human ortholog was identified (Neal *et al.*, 2000), which was subsequently linked to development (Thomas *et al.*, 2008), cell cycle regulation (Gupta *et al.*, 2005; Taipale *et al.*, 2005) and autophagy (Füllgrabe *et al.*, 2013; Hale *et al.*, 2016), although the role in the latter is still unclear.

Like other KATs, KAT8 acts within two molecular complexes, the Male Specific Lethal (MSL) and the Non Specific Lethal (NSL), which seem to confer it target specificity (Sheikh, Guhathakurta and Akhtar, 2019). Interestingly, KAT8 and some members of the NSL complex, KANSL1, KANSL2, KANSL3 and MCRS1, have been reported to localise at the mitochondria, where they can regulate mitochondrial transcription and translation (Chatterjee *et al.*, 2016), suggesting that the NSL complex may be a possible candidate for the modulation of mitophagy. In this chapter, I will explore how KAT8 and other components of the NSL complex modulate mitophagy.

2.2 Results

2.2.1 KAT8 is the only member of the KAT family able to modulate mitophagy

Given that KAT8 is one of a family of 22 lysine acetyltransferases, we firstly investigated whether the effect seen on mitophagy was due to general acetyltransferase activity or specific to KAT8. The high content mitophagy siRNA screen (Chapter 1) was used to screen the 22 confirmed KATs (Table 11). KAT8 was the only KAT able to significantly reduce pUb(Ser65) levels after mitophagy induction with O/A when knocked down using siRNA (Fig 14), suggesting a specific role for KAT8 in the modulation of mitophagy.

KAT name	Alternative name(s)
KAT1	HAT1
KAT2A	GCN5
KAT2B	PCAF
KAT3A	CREBBP, CBP
KAT3B	EP300
KAT4	TAF1, TFII250
KAT5	TIP60
KAT6A	MOZ, MYST3
KAT6B	MORF, MYST4
KAT7	HBO1, MYST2
KAT8	MOF, MYST1
KAT9	ELP3

KAT12	GTF3C4, TFIIIC90
KAT13A	NCOA1, SRC1
KAT13B	NCOA3, SRC3, ACTR
KAT13C	NCOA2
KAT13D	CLOCK
-	ACAT1
-	ATAT1
-	ATF2
-	BLOC1S1 (GCN5L1)
-	NAT10

Table 11. List of the 22 KATs genes screened.

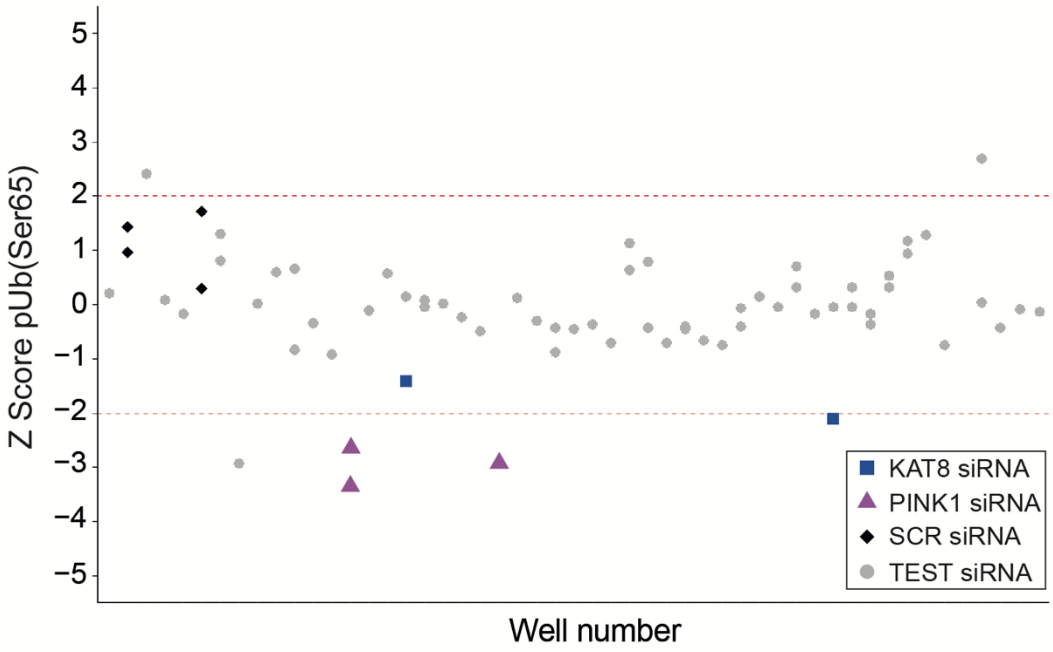

Figure 14. KAT8 is the only lysine acetyltransferase whose knockdown decreases pUb(Ser65) levels.

pUb(Ser65) Z-score of one representative screen plate of the KATs screen (n=2). KAT8 is the only KAT, together with the PINK1 control, whose knockdown reduces pUb(Ser65) intensity levels by more than 2 SD (Z-score < -2).

2.2.2 Knockdown of components of the NSL complex reduce pUb(Ser65) levels

The activity and target specificity of KAT8 is regulated by two complexes, the MSL and the NSL complexes. Since KAT8 and some members of the NSL complex were reported to localise at the mitochondria (Chatterjee *et al.*, 2016), I investigated whether any other component of the NSL complex could also play a role in mitophagy. To this end, I knocked down with siRNA the 9 components of the complex (KAT8, KANSL1, KANSL2, KANSL3, MCRS1, WDR5, PHF20, OGT, HCFC1), as well as the SCR and PINK1 controls, in the same experimental setup as the high content mitophagy screen (Chapter 1). Strikingly, after both 1.5 and 3 h of O/A treatment, a significant reduction in pUb(Ser65) intensity levels was detected when knocking down KANSL1, KANSL2, KANSL3 and MCRS1 (Fig 15A,B), which were the subunits reported by Chatterjee and colleagues to localise at the mitochondria (Chatterjee *et al.*, 2016). OGT was the only subunit whose knockdown significantly increased pUb(Ser65) levels after 3 h of O/A treatment (Fig 15B. See Chapter 2 Discussion). Of note, in this experiment, knockdown of KAT8 slightly but not significantly decreased pUb(Ser65) levels after 3 h, unlike what was seen as a result of the GWAS high content screen (Chapter 1, Fig 13), potentially due to the variability in knockdown levels.

Of the NSL subunits whose knockdown had a significant effect (KANSL1, KANSL2, KANSL3 and MCRS1), *KANSL1* was the most interesting, as it was the only gene to also be PD GWAS candidate gene (Chang *et al.*, 2017), unlike the other three. Furthermore, the *KANSL1* gene is located on the 17q21 locus, near *MAPT*, a highly relevant locus for neurodegenerative diseases (See Section 2.2.7). The effect

of knocking down KANSL1 was confirmed in an independent experiment (Fig 15C,D). Therefore, KANSL1 was prioritised to take forward for further investigation, together with KAT8.

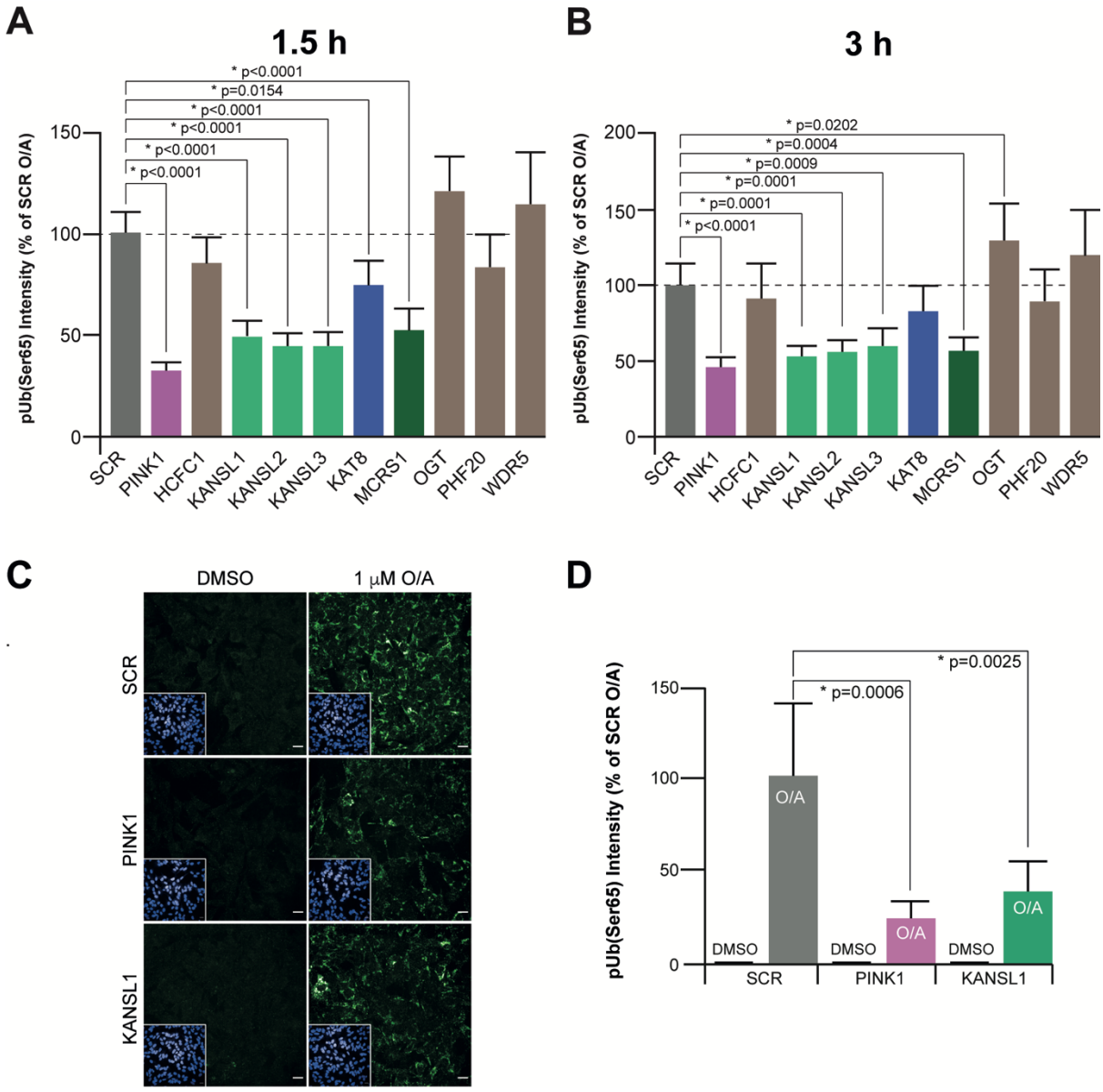

Figure 15. Several members of the NSL complex significantly reduce pUb(Ser65) levels.

A,B. Quantification of pUb(Ser65) integrated intensity levels following treatment of SCR, PINK1 or NSL components siRNA KD POE SHSY5Y cells with 1 μM O/A for 1.5 h (**A**) or 3 h (**B**). Cells were stained for pUb(Ser65) and TOM20 before imaging on the Opera Phenix and image analysis on Columbus. Bars in green indicate the subunits of the NSL complex

reported to partially localise at the mitochondria in Chatterjee *et al.* Data was normalised to the SCR control (n=6). Mean ± SD; one-way ANOVA with Dunnett's correction. **C.** Representative images of SCR, PINK1 or KANSL1 siRNA KD POE SHSY5Y cells after treatment with 1 μM O/A or DMSO control for 3 h. Cells were stained for pUb(Ser65) (in green) and Hoechst 33342 prior to imaging on the Opera Phenix. Insets show the nuclei (Hoechst 33342, in blue) for the same fields. Scale bars = 20 μm **D.** Quantification of the integrated intensity of pUb(Ser65) in **C.** Data was normalised to the SCR control (n=3). Mean ± SD; one-way ANOVA with Dunnett's correction.(C and D: work done by Emily Annuario).

2.2.3 KAT8 and KANSL1 mitochondrial localisation could not be confirmed

To be able to better study the role of KAT8 and KANSL1 on mitophagy, I first of all attempted to confirm their suggested mitochondrial localisation by immunofluorescence, as published by Chatterjee et al. All antibodies commercially available at the time against KANSL1 and KAT8 were purchased for testing in POE SHSY5Y cells, after knockdown of the genes (Fig 16A). None of the tested antibodies gave a specific cytoplasmic, or in some cases nuclear, signal (Fig 16A,B). In parallel, the same antibodies were tested in the lab by Dr Marc Soutar by knocking down KANSL1 in POE SHSY5Y cells and Western blotting for the protein in both whole lysates and mitochondrial enriched fractions. In both cases, several bands of the incorrect predicted molecular weight were detected, with no reduction of any band in the knockdown samples. To test the antibodies in the presence of higher amounts of the target proteins, I attempted to overexpress KANSL1, with and without a tag to facilitate detection. Cells were successfully transfected with a TOM70(1-70)-GFP control to tag the mitochondria, but no KANSL1 positive cells could be detected (Fig 16D). This issue in detecting overexpressed KAT8 and KANSL1 has been

previously reported in the literature (Cai *et al.*, 2010) and the in house developed antibody used by the Akhtar lab (Chatterjee *et al.*, 2016) was not available to us to test. Therefore, the partial mitochondrial localisation of KAT8 and KANSL1 remains to confirmed.

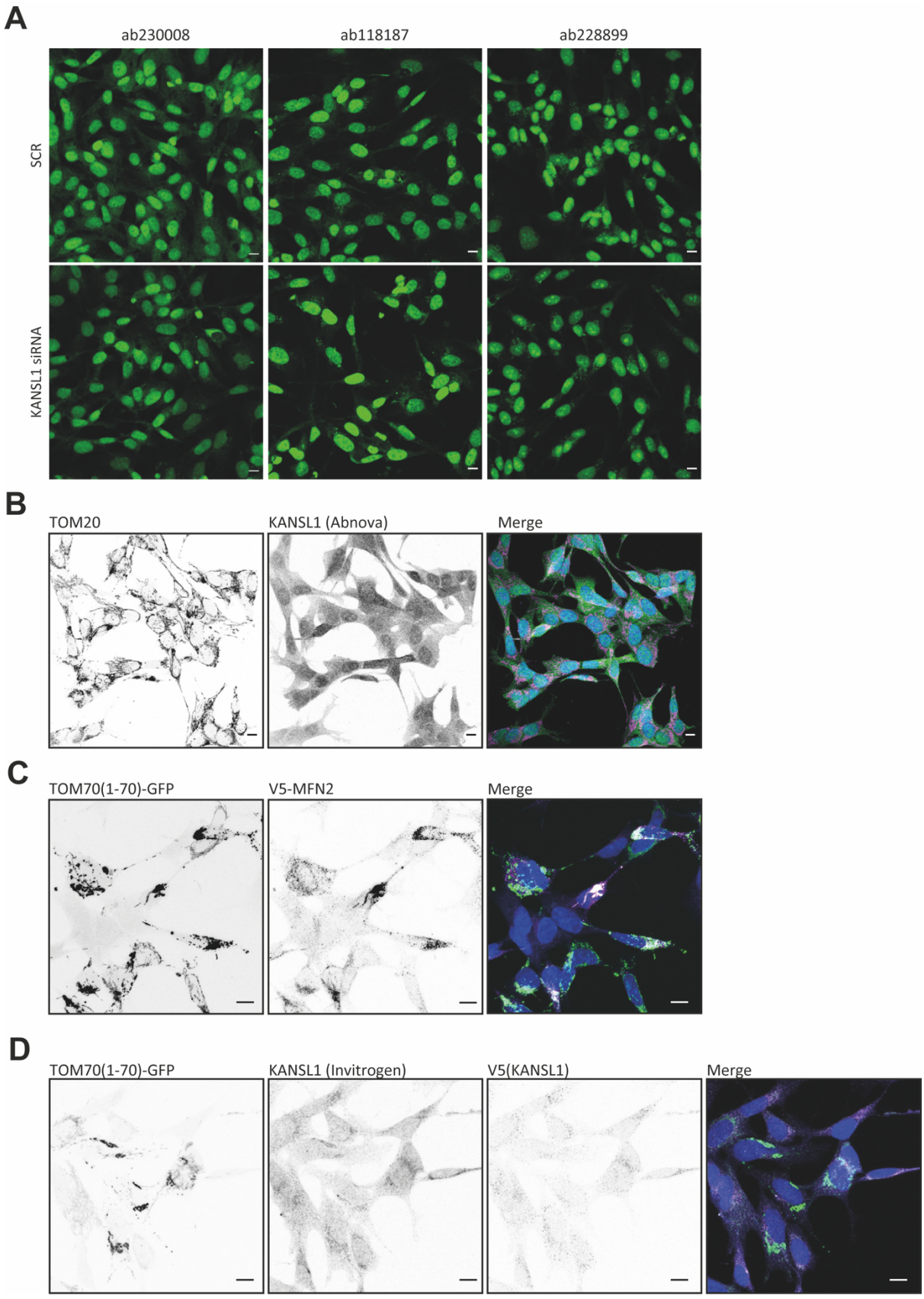

Figure 16. KANSL1 mitochondrial localisation could not be confirmed.

A. POE SHSY5Y cells were transfected with KANSL1 siRNA or SCR control for 72 h before being fixed, stained for KANSL1 with three available Abcam antibodies and imaged on the LSM780 confocal. All three stained the nucleus but knockdown did not reduce the intensity of the fluorescence. **B.** POE SHSY5Y cells were fixed, stained for KANSL1 with the Abnova antibody or TOM20 and imaged on the LSM780 confocal. KANSL1 signal appeared diffuse in the whole cell and not mitochondrial. **C.** To confirm whether the V5 tag antibody worked, and to test the overexpression protocol, POE SHSY5Y cells were transfected with TOM70(1-70)-GFP and V5-MFN2, before fixing, staining for V5 and imaging on the LSM780 confocal. **D.** POE SHSY5Y cells were transfected with TOM70(1-70)-GFP and V5-KANSL1, before fixing, staining for V5 and KANSL1 with the Invitrogen antibody, and imaging on the LSM700 confocal. KANSL1 stain appeared again diffuse and no V5-positive cells were detectable, although GFP-positive cells were present. Scale bars = 10 µm.

2.2.4 KAT8 and KANSL1-deficient cells show a lower mitochondrial membrane potential

Disease-causing mutations and deficiencies in PINK1 cause loss of mitochondrial membrane potential (Wood-Kaczmar *et al.*, 2008; Gandhi *et al.*, 2009; Morais *et al.*, 2009), which is considered one of the signs of mitochondrial dysfunction (See Introduction). In reporting the localisation of KAT8 and KANSL1 at the mitochondria, Chatterjee and colleagues found that knockdown of KAT8 and KANSL1 in HeLa cells reduced mitochondrial respiration and the mitochondrial membrane potential (Chatterjee *et al.*, 2016). Given that mitochondrial depolarisation is one of the triggers of mitophagy, to better understand whether it can impact PINK1 activation, I investigated whether depletion of KAT8 and KANSL1 reduced mitochondrial membrane potential in the POE SHSY5Y cells as well. POE SHSY5Y cells were reverse transfected with siRNA against KAT8 and KANSL1, as well as PINK1, SCR and non transfected controls for 72 h, before loading the cells with Hoechst 33342 and the cationic dye TMRM. TMRM is a cell permeable, red

fluorescent dye that is uptaken by functional, polarised mitochondria and can therefore be used to quantify the mitochondrial membrane potential. Cells were live imaged on the Opera Phenix at 37°C, 5% CO_2 in HBSS and the integrated TMRM intensity was analysed on the automated platform Columbus. As previously shown, knockdown of PINK1 significantly reduced the basal mitochondrial membrane potential in POE SYSH5Y cells. Knockdown of KAT8 and KANSL1 also resulted in a lower membrane potential (Fig 17), confirming the data generated in HeLa cells by Chatterjee and colleagues.

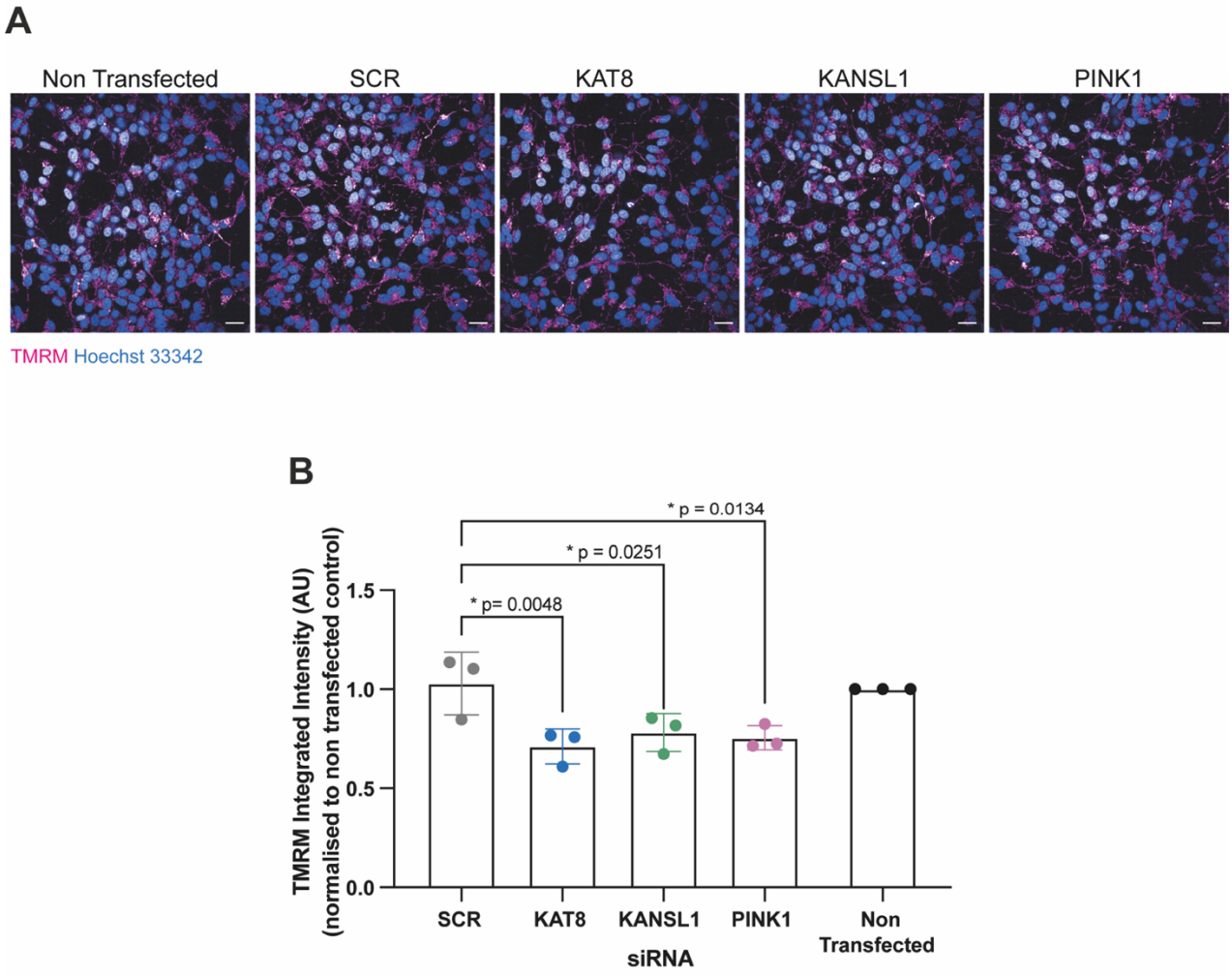

Figure 17. Knockdown of KAT8 and KANSL1 leads to a reduction in basal mitochondrial membrane potential.

A. Representative images of TMRM (magenta) and Hoechst 33342 (blue) following knockdown of SCR, PINK1, KAT8 and KANSL1 and non transfected POE SHSY5Y cells.

Cells were live imaged on the Opera Phenix and the basal TMRM integrated intensity was analysed on Columbus. Scale bar = 20 μm. **B.** Quantification of TMRM integrated intensity levels in **A**. Data was normalised to the non transfected control (n=3). Mean ± SD; one-way ANOVA with Dunnett's correction.

2.2.5 KAT8 and KANSL1 KD affect the early stages of PINK1-dependent mitophagy

To further investigate whether the decrease of pUb(Ser65) levels after knockdown of KANSL1 and KAT8 and treatment to induce mitophagy with O/A for 3 h was due to a delay in the process, I firstly repeated the knockdown conditions over a 7-hour time course of 1 μM O/A treatment, before measuring pUb(Ser65) levels by immunofluorescence on the Opera Phenix. Both knockdowns of KAT8 and KANSL1 reduced pUb(Ser65) levels throughout the time course, with KANSL1 knockdown having a stronger effect, almost to the levels of the PINK1 control knockdown (Fig 18A, B), without affecting cell viability (as assessed by the number of nuclei – Fig 18A inset and C).

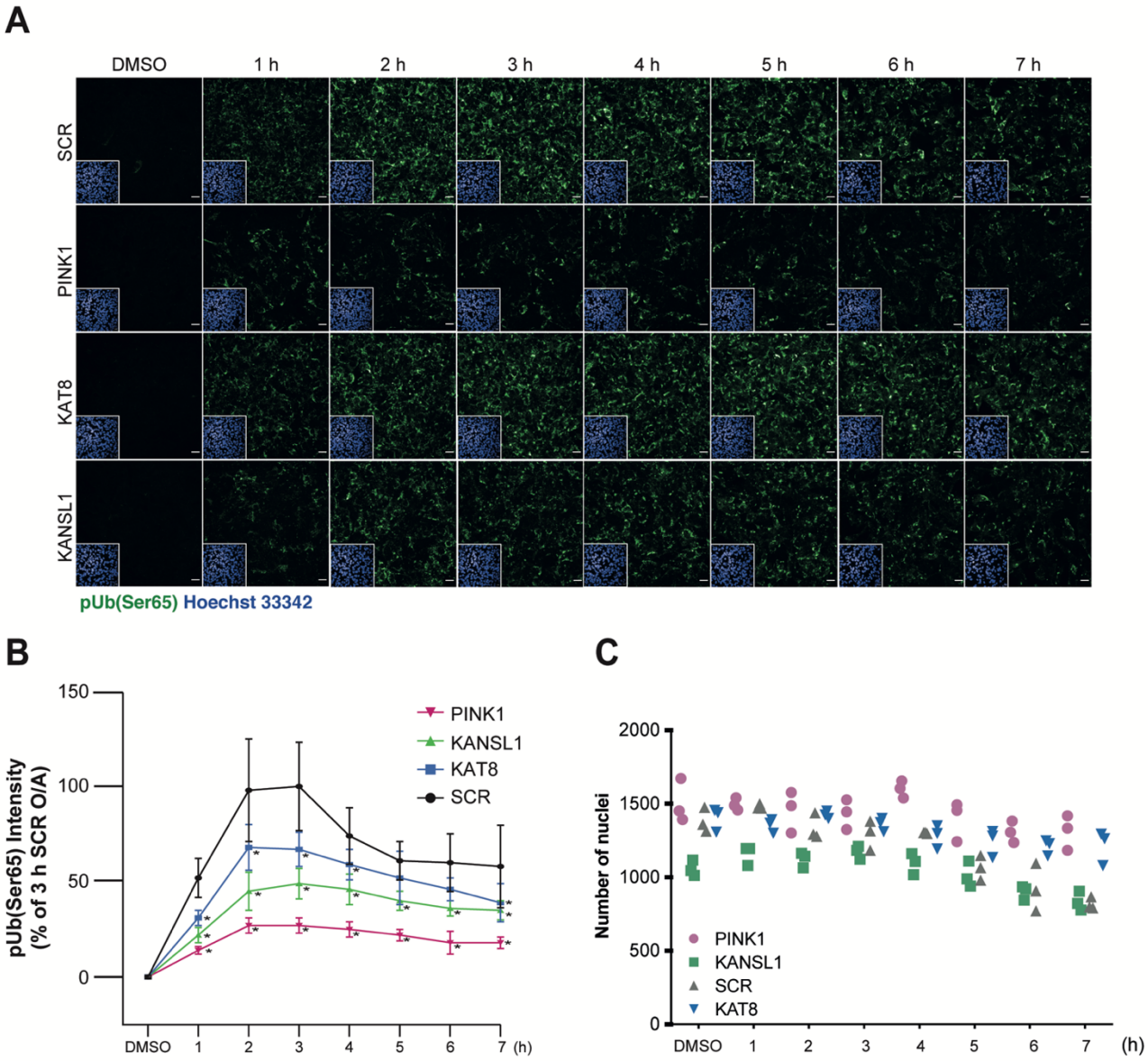

Figure 18. KANSL1 KD decreases pUb(Ser65) signalling over time, more efficiently than KAT8 KD.

A. Representative images of pUb(Ser65) following treatment of SCR, PINK1, KAT8 and KANSL1 KD POE SHSY5Y cells with 1 μM O/A for 0-7 h and imaging on the Opera Phenix. Inset shows Hoechst 33342 stain for the same field of view. Scale bar = 20 μm. **B.** Quantification of pUb(Ser65) integrated intensity levels in **A**. Data was normalised to 3 h SCR control (n=6). **C.** Quantification of the number of nuclei in **A**. Mean ± SD; two-way ANOVA with Dunnett's correction.

To exclude the possibility that the effect of the knockdown of KAT8 and KANSL1 on pUb(Ser65) levels could be due to the overexpression of Parkin in the

SHSY5Ys, the knockdowns were repeated in non-Parkin overexpressing SHSY5Y cells. Cells were reverse transfected with siRNA against KAT8 and KANSL1, as well as the PINK1 and SCR controls, for 72 h before 3 h treatment with 1 μM O/A. Again, knockdown of KAT8 and KANSL1 significantly reduced pUb(Ser65) levels (Fig 19A, B). These data were also confirmed by WB and in the human astrocytoma H4 cell line by Drs Marc Soutar and Ben O'Callaghan in the lab.

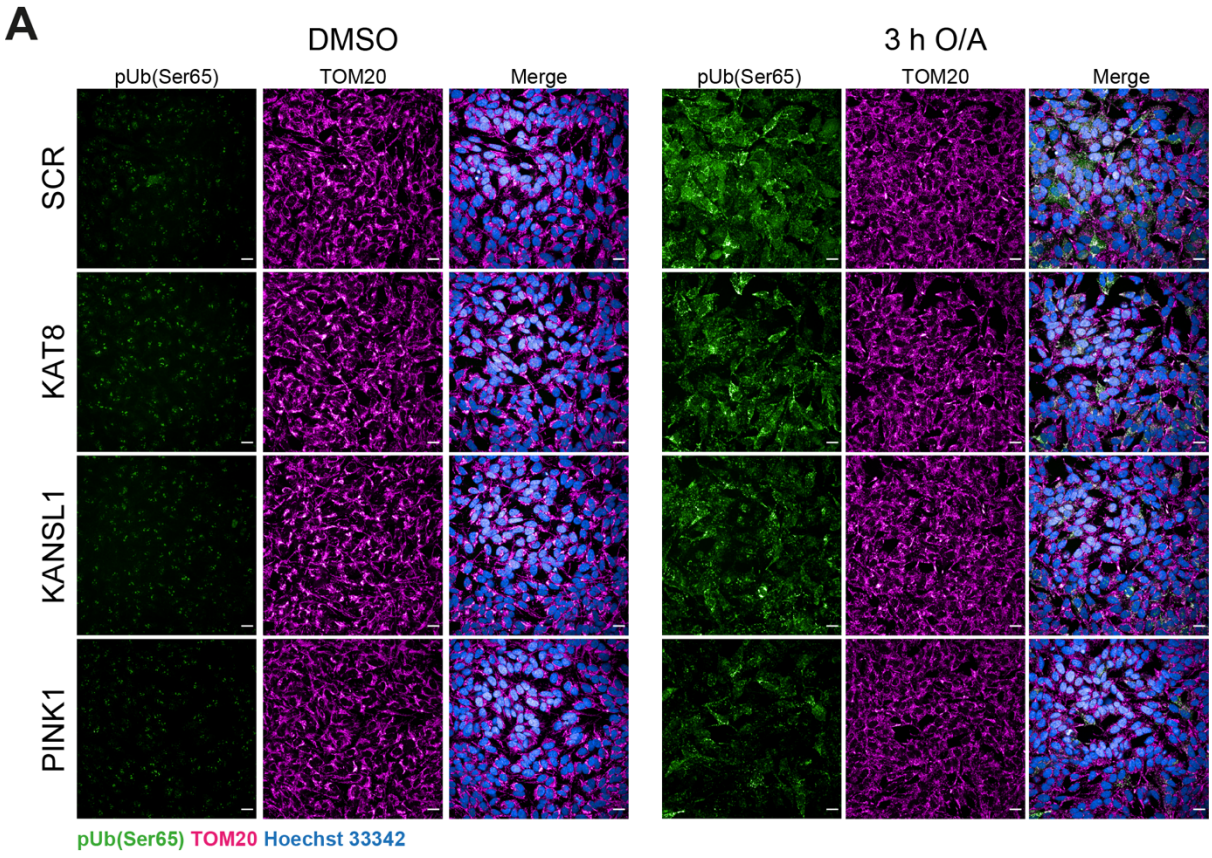

Figure 19. KAT8 and KANSL1 KD decrease pUb(Ser65) levels in non Parkin overexpressing SHSY5Y cells as well.

A. Representative images of pUb(Ser65) (green) and TOM20 (magenta), and merged image with the Hoechst 33342 stain for the nuclei (blue), following treatment of SCR, PINK1, KAT8 and KANSL1 KD in SHSY5Y cells with 1 μM O/A for 3 h and imaging on the Opera Phenix. Scale bar = 20 μm. **B.** Quantification of pUb(Ser65) integrated intensity in **A** (n=6). Mean ± SD; two-way ANOVA with Dunnett's correction.

In the early stages of PINK1-dependent mitophagy, PINK1 is also responsible for the phosphorylation at Ser65 and recruitment to the mitochondria of Parkin (See Introduction and Matsuda *et al.*, 2010; Narendra *et al.*, 2010; Vives-Bauza *et al.*, 2010; Kondapalli *et al.*, 2012; Shiba-Fukushima *et al.*, 2012). To determine whether the effect of KAT8 and KANSL1 was limited to the phosphorylation of ubiquitin or whether it also affected relocation and phosphorylation of Parkin, I used the high content siRNA setup to measure by immunofluorescence the translocation of Parkin to the mitochondria (Fig 20A,B) and its phosphorylation at Serine 65 (pParkin(Ser65)) (Fig 20C,D) in POE SHSY5Y cells. Both the phosphorylation and the recruitment of Parkin were significantly decreased upon knockdown of KAT8 and KANSL1, with the latter having again a stronger effect, in line with the previous data (Fig 18).

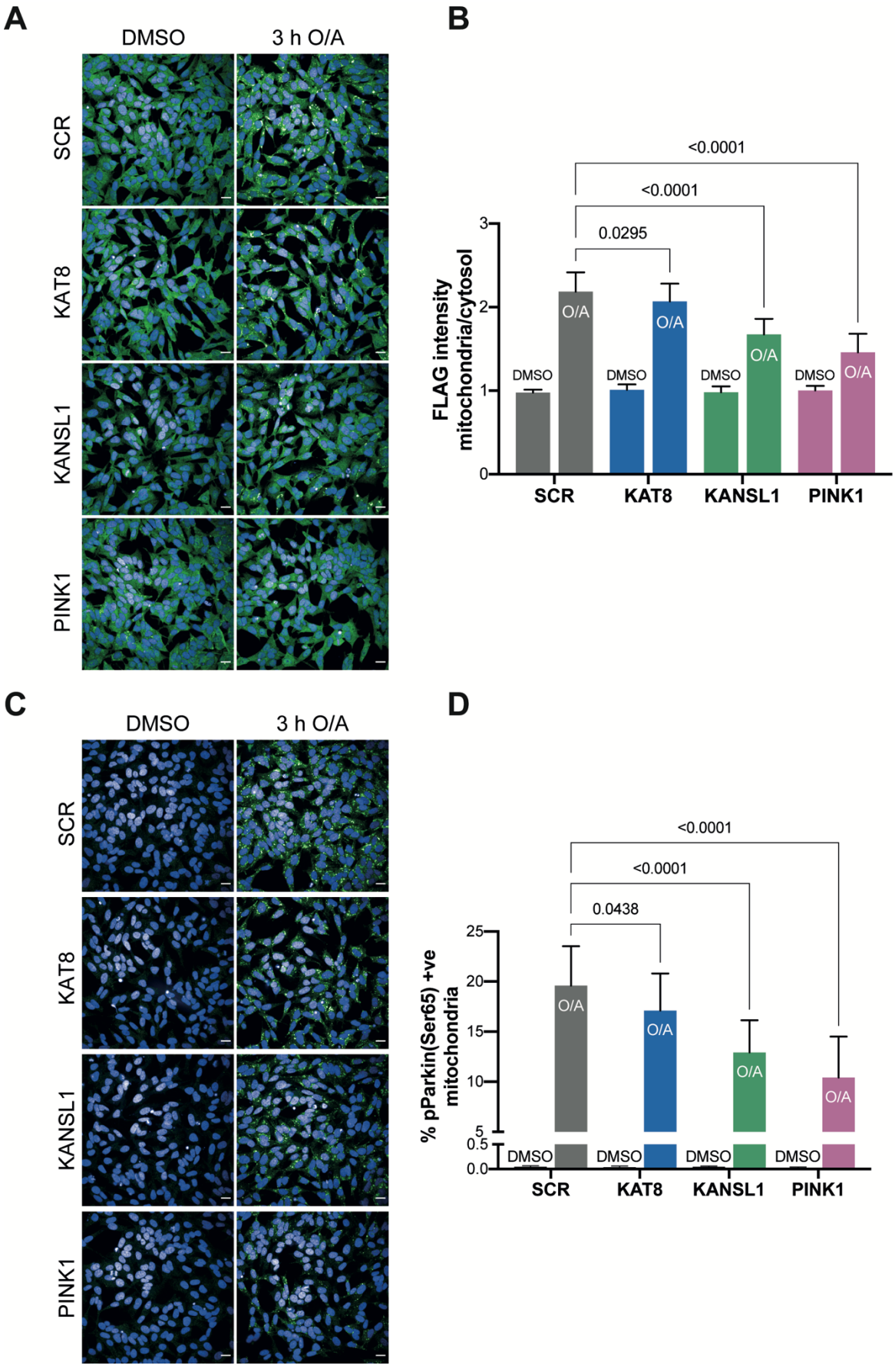
A
DMSO
3 h O/A
SCR
KAT8
KANSL1
PINK1
B
FLAG intensity mitochondria/cytosol
<0.0001
<0.0001
0.0295
DMSO
O/A
SCR
KAT8
KANSL1
PINK1
C
DMSO
3 h O/A
SCR
KAT8
KANSL1
PINK1
D
% pParkin(Ser65) +ve mitochondria
<0.0001
<0.0001
0.0438
DMSO
O/A
SCR
KAT8
KANSL1
PINK1

Figure 20. KAT8 and KANSL1 KD decrease pParkin(Ser65) levels and recruitment of FLAG-Parkin to the mitochondria.

A. Representative images of FLAG (Parkin) (green) and Hoechst 33342 (blue) following treatment of SCR, PINK1, KAT8 and KANSL1 KD POE SHSY5Y cells with 1 μM O/A for 3 h and imaging on the Opera Phenix. Scale bar = 20 μm. **B.** Quantification of the translocation of FLAG-Parkin to the mitochondria (which were labelled with the IMM marker ATPβ), measured as a ratio of the mitochondrial and cytosolic intensities of FLAG in **A** (n=5). **C.** Representative images of pParkin(Ser65) (green) and Hoechst 33342 (blue) following treatment of SCR, PINK1, KAT8 and KANSL1 KD POE SHSY5Y cells with 1 μM O/A for 3 h and imaging on the Opera Phenix. Scale bar = 20 μm. **D.** Quantification of the percentage of mitochondria positive for pParkin(Ser65) in **C** (n=5). Mean ± SD; two-way ANOVA with Dunnett's correction Mean ± SD; two-way ANOVA with Dunnett's correction.

2.2.6 KAT8 and KANSL1 KD decrease mitochondrial clearance

While knockdown of KAT8 and KANSL1 has a strong effect on the levels of pUb(Ser65), pParkin(Ser65) and Parkin recruitment, these are early events in the activation of PINK1-dependent mitophagy (See Introduction). Initial data from the GWAS screen did not find differences in the decrease in TOM20 levels between KAT8 KD and the controls. This could be due to fact that TOM20 is an OMM protein and can be degraded by other pathways than the degradation of the whole organelle (Chan *et al.*, 2011; Yoshii *et al.*, 2011). In order to assess whether the reduced levels of early mitophagy markers (pUb(Ser65), Parkin recruitment and pParkin(Ser65)) result in a decrease of downstream clearance of damaged mitochondria, I next knocked down KAT8, KANSL1 and PINK1, together with the SCR control, in POE SHSY5Y cells and treated the cells with O/A for longer (3, 6 and 9h). Cells were then stained for the mitochondrial peptidase PMPCB, a matrix marker, before analysing

the number of mitochondria spots as a measure of the amount of organelles in the cell, an automated way of scoring the cells for the presence or not of mitochondria after inducing mitophagy (Narendra *et al.*, 2008; Geisler *et al.*, 2010; Narendra, Jin, *et al.*, 2010). Consistently with the pUb(Ser65) time course result (Fig 18), KANSL1 knockdown significantly slowed down mitochondrial clearance compared to the SCR control (Fig 21).

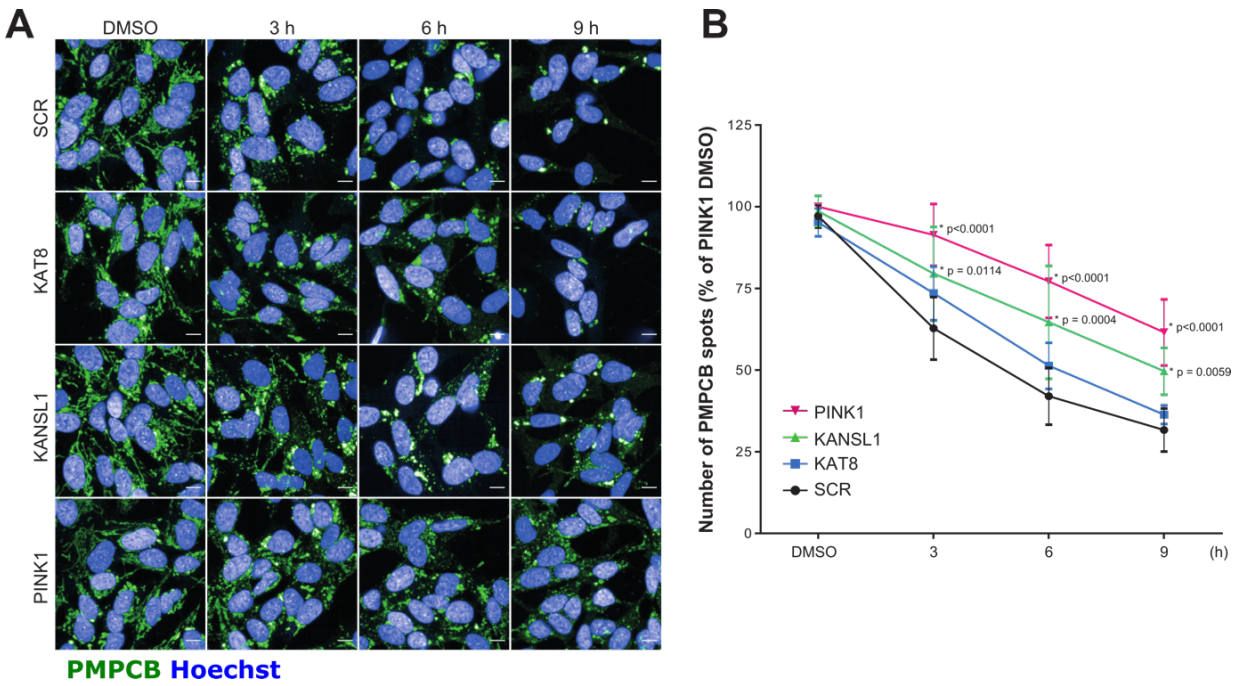

Figure 21. KANSL1 KD decreases downstream mitochondrial clearance.
A. Representative images of PMPCB (green) and Hoechst 33342 (blue) following treatment of SCR, PINK1, KAT8 and KANSL1 KD POE SHSY5Y cells with 1 μM O/A for 3,6,9 h and imaging on the Opera Phenix. Scale bar = 10 μm. **B.** Quantification of the number of PMPCB spots, as a measure of mitochondrial content, in **A.** Data was normalised to the PINK1 DMSO control (n=5). Mean ± SD; two-way ANOVA with Dunnett's correction.

Measuring mitochondrial clearance by measuring the number of spots, however, might present some issues. It requires fixing the cells, while mitophagy is a dynamic process, and it relies on choosing a good mitochondrial marker which is not

degraded by other means. Therefore, I examined the role of KAT8 and KANSL1 in modulating mitophagy in live cells with an alternative method. Knockdown of KAT8 and KANSL1 was repeated in POE SHSY5Y cells stably expressing mt-Keima (a kind gift from Christin Luft and Robin Ketteler, UCL). Mt-Keima is a mitochondrial matrix-targeted dual fluorescence protein whose excitation shifts from a green to a red wavelength in an acidic environment (such as lysosomes), allowing to measure mitophagy as a ratio of the area of red (lysosomal mitochondria) to red plus green (total mitochondria) signals (Katayama *et al.*, 2011; Sun *et al.*, 2015; Klionsky *et al.*, 2021). Cells were reverse transfected for 72 h, before adding Hoechst 33342 and 1 μM O/A (or DMSO control) and live imaging every 2 h overnight on the Opera Phenix (Soutar *et al.*, 2019)(Fig 22A). Images were analysed on Columbus, to identify the cytosolic and the lysosomal mitochondria, until 8 hours, when significant cell death is observed (Fig22C). The mitophagy index, that is the ratio of the areas of lysosomal and total signals, increased over time as the mitochondria were degraded in the O/A treated wells, while no change was present in the DMSO wells (Fig 22B). The mitophagy index increased similarly regardless of the treatments, as the uncouplers valinomycin and CCCP showed no difference compared to O/A (Fig 22D). Knockdown of KAT8 and KANSL1, as well as of the PINK1 positive control, significantly reduced the rate of mitophagy compared to the SCR control, confirming a role for KAT8 and KANSL1 in regulating mitophagy (Fig 22B).

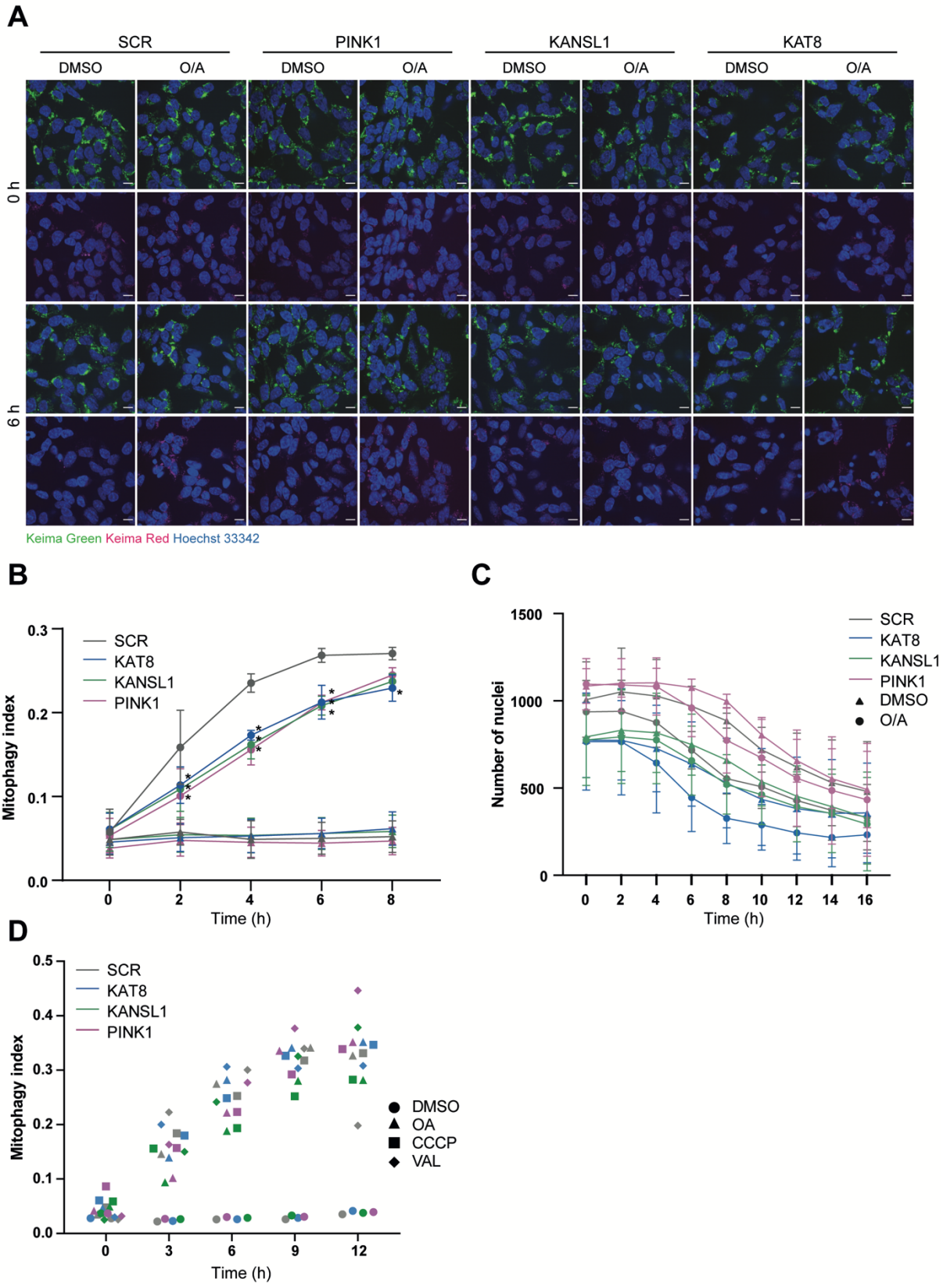

Figure 22. KAT8 and KANSL1 reduce mitochondrial clearance, as measured using the mt-Keima assay.

A. Representative images of the mt-Keima signal at 0 h and 6 h, showing the shift in fluorescence as mitochondria fuse with the acidic lysosomes (magenta signal). KAT8, KANSL1, PINK1 and the SCR control were knocked down in stable mt-Keima POE SHSY5Y cells for 72 h, before adding Hoechst 33342, treating with 1 µM O/A or DMSO control and imaging overnight on the Opera Phenix . Scale bar = 25 µm **B**. Quantification of the mitophagy index, calculated as the ratio of the area of red mitochondria over total mitochondria (n=3).Mean ± SD; two-way ANOVA with Dunnett's correction. **C.** Quantification of the number of nuclei shows significant cell death after 8 h. **D.** Quantification of the mitophagy index of one optimisation plate. KAT8, KANSL1, PINK1 and the SCR control were knocked down in stable mt-Keima POE SHSY5Y cells for 72 h, before adding Hoechst 33342, treating with 1 µM O/A, 10 µM CCCP, or 0.1 µM valinomycin (Val) or DMSO control and imaging overnight on the Opera Phenix and imaging overnight on the Opera Phenix. These treatments equally induced mitophagy, so O/A was chosen for all subsequent experiments.

2.2.7 *KANSL1* is the only gene on the *MAPT* locus able to reduce pUb(Ser65) levels

KANSL1 is located on chromosome 17q21, near the *MAPT* gene. Mutations in this locus cause a variety of neurodegenerative diseases termed tauopathies, pathologically characterised by the presence of tau aggregates. These diseases include Alzheimer's disease (AD), progressive supranuclear palsy (PSP), corticobasal degeneration (CBD) and frontotemporal dementia with parkinsonism linked to chromosome 17 (FTDP-17). The *MAPT* locus is one of the most complex in the human genome. It occurs in 2 haplotypes in linkage disequilibrium, the more common H1 (direct orientation) and the inverted H2 haplotype present in around 20% of Europeans (Stefansson *et al.*, 2005). The H1 haplotype is strongly associated with increased risk of PSP and CBD (Pittman, Fung and de Silva, 2006) and association studies have also linked it to increased risk of PD (Simón-Sánchez *et al.*, 2009). Several studies have reported the presence of tau aggregates in brains

of PD patients and there is evidence to suggest tau can be found in Lewy bodies, therefore it has been assumed that the risk of PD at the 17q21 locus is driven by *MAPT*, but the evidence remains weak (Wray and Lewis, 2010). In order to exclude that the effect we detect on mitophagy is due to another gene on the *MAPT* locus, we used our high content siRNA assay to screen all 32 Open Reading Frames (ORFs) on the 17q21 locus (Table 12). As per the original GWAS screen, genes were screened in duplicate on a plate, across 3 plates per run. Once more, the only hits were KANSL1 and the PINK1 positive control within the plate, suggesting that the decrease in pUb(Ser65) levels is specific to KANSL1 (Fig 23).

17q21 ORFs	
ACBD4	*HEXIM1*
ADAM11	*HIGD1B*
ARHGAP27	*KANSL1*
ARL17A	*KIF18B*
ARL17B	*LRRC37A*
C1QL1	*LRRC37A2*
CCDC103	*MAP3K14*
CDC27	*MAPT*
CRHR1	*MYL4*
DBF4B	*NMT1*
DCAKD	*NSF*
EFTUD2	*PLEKHM1*
FMNL1	*RPRML*
GFAP	*SPPL2C*
GJC1	*STH*
GOSR2	*WNT3*

Table 12. List of the 32 ORFs on chromosome 17q21 screened.

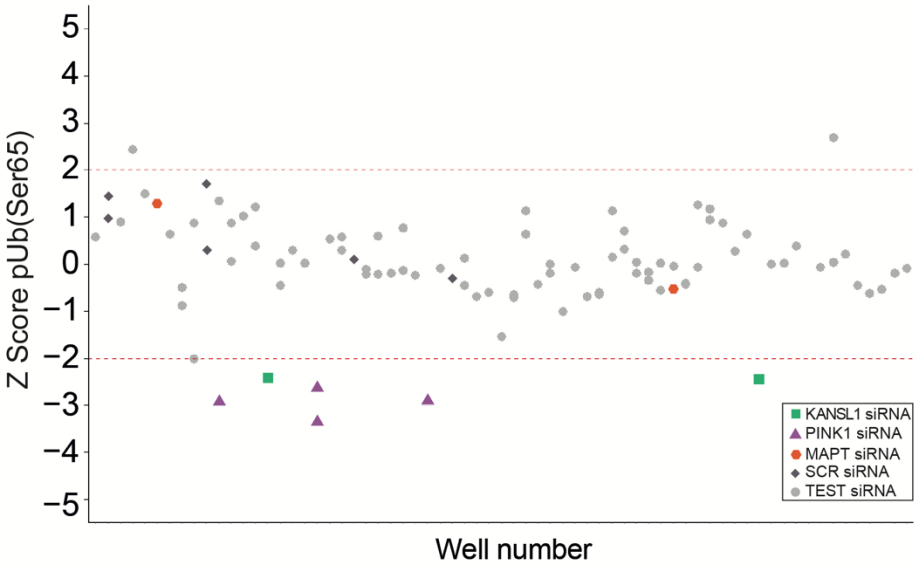

Figure 23. Of all ORFs on the 17q21 locus, only KANSL1 KD significantly reduces pUb(Ser65) levels.

Z-score of pUb(Ser65) intensity of one representative high content mitophagy screen plate of the 32 ORFs on the 17q21 locus (n=2). KANSL1 and PINK1 KD significantly reduce pUb(Ser65) levels by more than 2 SD (Z-score < -2).

2.2.8 KAT8 and KANSL1 knockdown reduce *PINK1* transcription

Having shown a role for KAT8 and KANSL1 in affecting mitophagy initiation and downstream clearance of damaged mitochondria, we then focussed on investigating by which mechanism they could regulate PINK1-dependent mitophagy. KAT8, together with the NSL complex, is mainly responsible for transcriptional regulation via the acetylation of lysine 16 on histone 4. In particular, this epigenetic modification has been linked to the expression of autophagy related genes and autophagy, as starvation or rapamycin treatment decreases H4K16Ac, with effects on cell survival (Füllgrabe *et al.*, 2013), although a role in the regulation of mitophagy genes has not been specifically investigated. Given the effects of a reduction of

KAT8 and KANSL1 on pUb(Ser65), pParkin(Ser65) and Parkin recruitment levels, all of which are PINK1 activity dependent, we examined whether these results were due to the downregulation of *PINK1* expression. POE SHSY5Y cells were transfected for 72 h with siRNA against KAT8 and KANSL1, as well as SCR and PINK1 controls, before the RNA was extracted and retrotranscribed for qPCR. Knockdown of PINK1, KAT8 and KANSL1 were confirmed by a reduction in their mRNA levels (Fig 24B,C,D). Knockdown of PINK1 and KAT8 was further confirmed by WB (Fig 24E), while it was not possible to use this technique to confirm the knockdown of KANSL1, due to the poor quality of the available antibodies (Fig 16). Knockdown of KANSL1 also decreased *PINK1* transcription (Fig 24B). These data were also confirmed in non Parkin overexpressing SHSY5Y and the astroglioma cell line H4. Overall, these data suggests that the NSL complex and acetylation of H4K16 could also be regulating the expression of mitophagy related genes.

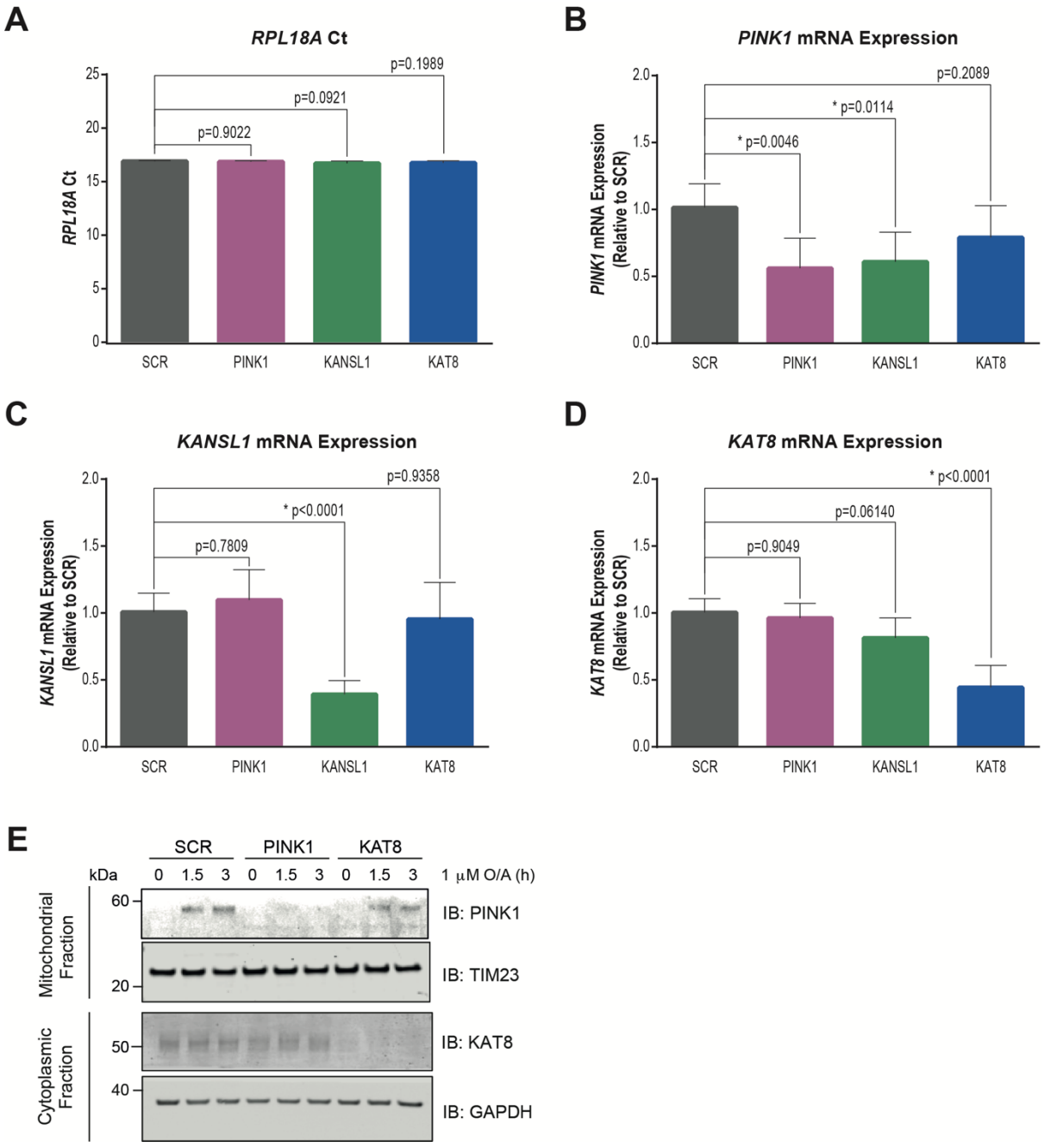

Figure 24. KANSL1 knockdown reduces *PINK1* mRNA levels in POE SHSY5Y cells.

A. Ct values for *RPL18A* were unaffected by siRNA KD. n=6, one-way ANOVA with Dunnett's correction. **B.** Relative *PINK1* mRNA expression levels in SCR, PINK1, KANSL1 and KAT8 siRNA KD POE SHSY5Ys, as measured through RT-qPCR (n=6, one-way ANOVA with Dunnett's correction). **C.** Relative *KANSL1* mRNA expression levels in SCR, PINK1, KANSL1 and KAT8 siRNA KD POE SHSY5Ys,as measured through RT-qPCR (n=6, one-way ANOVA with Dunnett's correction). **D.** Relative *KAT8* mRNA expression levels in

SCR, PINK1, KANSL1 and KAT8 siRNA KD POE SHSY5Ys, as measured through RT-qPCR (n=6, one-way ANOVA with Dunnett's correction). Mean ± SD, work done by Dr Ben O'Callaghan. **E.** Representative WB of mitochondrial and cytoplasmic fractions of SCR, PINK1 and KAT8 siRNA KD POE SHSY5Ys treated with 1 μM O/A for 1.5 or 3 h or DMSO control (n=3, work done by Dr Marc Soutar).

2.3 Discussion

The high content mitophagy siRNA screen was developed to investigate whether the candidate PD risk genes nominated by the PD GWAS analyses could affect mitophagy, a key pathway implicated in PD pathogenesis by the Mendelian genes *PINK1* and *PRKN*. The screen of a prioritised list of GWAS gene candidates identified *KAT8*, a lysine acetyltransferase, as a potential hit modulator of mitophagy. In this Chapter, I described how KAT8 and KANSL1, a regulator of KAT8 and part of the same NSL complex, affected both the early stages of mitophagy initiation (phosphorylation of ubiquitin, recruitment and phosphorylation of Parkin) and the subsequent mitochondrial clearance. Knockdown of KAT8 and KANSL1 reduced the mitochondrial membrane potential and knockdown of KANSL1 reduced *PINK1* mRNA levels.

KAT8 is mainly responsible for the acetylation of H4K16 and is therefore an important regulator of gene expression, since acetylation of histones is linked to transcriptionally active chromatin. Of the 22 proteins confirmed to have acetyltransferase activity, KAT8 is the only KAT reported to be a PD GWAS risk gene and the only one whose knockdown affected mitophagy, a relevant pathway for PD. Like several other KATs (Son *et al.*, 2021), KAT8 has been linked to the regulation of autophagy, although contrasting effects have been reported (Füllgrabe *et al.*, 2013; Hale *et al.*, 2016). In the former, starvation or treatment with rapamycin decreased levels of KAT8 and H4K16, modulating expression of autophagy-related genes, while in the latter knockdown of KAT8 increased autophagosome formation under normal nutritive conditions. While further studies will be needed to understand how KAT8 modulates autophagy, in neither paper the authors investigated the

effects on mitophagy. Given the transcriptional role of KAT8, we hypothesised that PINK1 and/or Parkin could also be target of KAT8-mediated gene expression regulation. In our qPCR data, knockdown of KANSL1 reduced *PINK1* mRNA levels, which could explain the reduction in PINK1-dependent mitophagy detected in the screen and confirmed in all subsequent experiments. Importantly, these data, as well as all the data presented in this Chapter, were also generated using siRNA pools to knockdown PINK1, KAT8 and KANSL1. As for the screen data in Chapter 1, deconvolution of the single siRNA and validation of their effect individually will be essential to allow proper interpretation of the results.

However, whether the reduction in *PINK1* mRNA explains the whole phenotype remains to be confirmed. Chatterjee and colleagues proposed that KAT8 might have other targets within the mitochondria, apart from mtDNA (Chatterjee *et al.*, 2016), and a relevant number of mitochondrial proteins are acetylated, although the enzymes responsible are unknown (Baeza, Smallegan and Denu, 2016). KAT8 could modulate PINK1 levels at the mitochondria by acetylating mitochondrial import machinery, or by directly acetylating PINK1 or ubiquitin itself (Swatek and Komander, 2016). Mass spectrometry analysis of acetylation levels at the mitochondria, after induction of mitophagy and after depleting KAT8 and KANSL1, will be useful to dissect the contribution of acetylation to the regulation of mitophagy (See also Discussion Chapter).

While KAT8 has been reported to belong to two different complexes, the MSL complex and the NSL complex, which confer the enzyme different target specificity (Cai *et al.*, 2010), the latter was of particular interest due to the work by Chatterjee

and colleagues identifying KAT8 and several NSL subunits at the mitochondria (Chatterjee *et al.*, 2016). Interestingly, knockdown of those 4 subunits, KANSL1, KANSL2, KANSL3 and MCRS1 that were identified in the mitochondria, were also able to significantly decrease pUb(Ser65) levels. Of these NSL subunits, KANSL1 (KAT8 Regulatory NSL Complex Subunit 1) is of particular interest. KANSL1 has been mainly studied in the context of the neurodevelopmental Koolen-de Vries syndrome, which is caused by haploinsufficiency of KANSL1 due to point mutations or microdeletions in this gene (Koolen *et al.*, 2012; Zollino *et al.*, 2012). Children with Koolen-de Vries present with mild to moderate intellectual disability, hypotonia, characteristic facial features and a friendly disposition, while little information is available regarding the effects in adult patients. However, KANSL1 was also identified as a possible PD GWAS risk gene in 2017 (Chang *et al.*, 2017) and more recently coding variants in KANSL1 were linked to late onset PD (Soto-Beasley *et al.*, 2020). Knockdown of KANSL1 strongly decreased mitophagy upon O/A treatment, to levels almost comparable to knockdown of PINK1 and stronger than the effect of the reduction in KAT8 levels. This stronger effect could be due to the role of KANSL1 as a scaffold of the NSL complex and activator of KAT8 (Dias *et al.*, 2014; Sheikh, Guhathakurta and Akhtar, 2019), so that lower levels of KANSL1 destabilise the whole complex and reduce the acetyltransferase activity of KAT8, more than the knockdown of KAT8 itself. Of note, while the work in this thesis focussed only on KANSL1 as a candidate regulator of mitophagy, as it has been proposed to be a PD GWAS gene (Chang *et al.*, 2017), knockdown of KANSL2, KANSL3 and MCRS1 had a similar effect on reducing the levels of pUb(Ser65) after the induction of mitophagy (Fig 15). Therefore, future work to dissect the role of the

NSL complex in regulating PINK1-dependent mitophagy should also include the analysis of these three subunits.

KANSL1 is located on the 17q21 locus, which is known in neurodegeneration as the *MAPT* locus. Given the weak evidence for tau pathology in PD, it is relevant that only depletion of KANSL1 of all ORFs in the locus decreases pUb (Ser65) levels. While this does not exclude a possible role of any of the ORFs in PD, it strengthens the hypothesis for a role of KANSL1 as a sporadic risk gene for PD by acting on mitophagy. In particular, while analysis of this region is difficult due to its genetic complexity, several PD variants are located within KANSL1 and correspond to missense mutations in the protein sequence. Furthermore, haploinsufficiency of KANSL1 in iPSC – derived neurons from Koolen – de Vries patients has been recently proposed to cause defective autophagy (Linda *et al.*, 2020), further highlighting the potential of the NSL complex to regulate mitophagy.

Of note, on the NSL subunits, OGT was the only one whose knockdown significantly increased pUb(Ser65) levels after 3 h of O/A treatment. This is in line with data from a whole genome CRISPR screen on regulators of Parkin expression (Potting *et al.*, 2017), where depletion of OGT was linked to higher levels of Parkin, although recent work in hematopoietic stem cells found a reduction in *PINK1* mRNA levels in OGT knockout cells (Murakami *et al.*, 2021). OGT is an enzyme that catalyses the transfer of an O-linked β-N-acetylglucosamine on Serine and Threonine residues. This post translational modification has been linked to PD, as it is one of the PTMs on α-synuclein, and to autophagy (Wani *et al.*, 2017; Levine *et al.*, 2019; Lee *et al.*, 2021), making it a target of interest. Further work will be needed

to understand how OGT affects mitophagy in neurons and whether this could be a pathway to target in Parkinson's disease.

While intriguing that the only NSL subunits to reduce pUb(Ser65) levels were the ones proposed to partially localise at the mitochondria, it was not possible to confirm this, neither by immunofluorescence or by WB, probably due to the poor quality of the available commercial antibodies. Detection of KAT8 and KANSL1 was also unsuccessful after overexpression of the genes in POE SHSY5Y cells, even when both proteins were tagged with the V5 tag. This might be due to tight regulation of KAT8 and KANSL1 levels within the cell, which does not allow high levels of the proteins. Furthermore, KANSL1 is predicted to be a disordered protein, which might lead to hidden epitopes or tags when attempting to detect it using antibodies. This difficulty in detecting overexpressed FLAG - tagged KAT8 and KANSL1 in HEK293 and HeLa cells has been previously reported by Cai and colleagues (Cai *et al.*, 2010) and the only antibodies reported in the literature to be effective in IF were developed in house by the Akhtar lab and not made available to us. The issues with overexpression also meant I was not able to perform rescue experiments in the POE SHSY5Y cells after knockdown of either KAT8 or KANSL1, as well as modelling the effect of the PD risk SNPs mutations in KANSL1. Future work should be aimed at generating better tools to detect KANSL1 and KAT8, potentially using the new generations of smaller protein tags and fluorescent systems such as nanobodies. Rescue experiments should still also be carried out, potentially in knockout cell lines generated by CRISPR-Cas9, to ensure lower or no levels of endogenous protein remains, or using alternative methods such as transfecting mRNA instead of a cDNA plasmid to express the protein of interest. In particular, it would be of interest to

overexpress the 4 SNPs that cause missense mutations in KANSL1, to determine whether the PD-associated variants have a stronger effect on mitophagy and providing further evidence for the role of mitophagy in PD.

In conclusion, we have identified two novel regulators of PINK1-dependent mitophagy, KAT8 and KANSL1, which interact and are both associated with increased risk of sporadic PD, providing further evidence for a pathogenic role of mitochondrial quality control in the disease. More importantly, for the first time it provides evidence that mitophagy may also be relevant in the most common, idiopathic forms of the disease. Recent AD GWAS analysis have identified both *KAT8* and *KANSL1* as possible risk genes, suggesting they might play a broader role in neurodegeneration (Jun *et al.*, 2016; Marioni *et al.*, 2018; Jansen *et al.*, 2019). The NSL complex seems to act on PINK1 – dependent mitophagy by regulating the expression of PINK1, although other molecular mechanisms, such as acetylation of members of the mitophagy pathway cannot be excluded. However, these data were generated in an immortalised cell line overexpressing Parkin, which is a useful way of validating the screen data and investigating the mechanism but is not a disease relevant cell model. In the next chapter, I will describe the optimisation of iPSC-derived neuronal models to investigate mitophagy and evaluate the role of KAT8 and KANSL1 in neuronal mitochondrial quality control using CRISPRi.

Chapter 3

Development of iPSC-derived neurons and iNeurons as a model to study mitophagy

3.1 Introduction

3.1.1 Mitochondrial quality control in immortalised cell lines *versus* neurons

Mitochondrial quality control pathways have been mostly investigated in immortalised cell lines, which have been essential to understand the mechanisms of the proteins involved. However, given the genetic evidence of their role in the pathogenesis of neurodegenerative diseases, it is necessary to study mitochondrial dysfunction and clearance in more disease relevant cell models, such as neurons.

Neurons are postmitotic, morphologically complex cells, with high energy and calcium buffering requirements, unlike immortalised cell lines. Neurons mostly rely on oxidative phosphorylation to produce ATP, and are therefore less able to withstand stresses that involve mitochondria, compared to cell lines that are mostly dependent on glycolysis for their energetic needs (Hall *et al.*, 2012; Mot *et al.*, 2016). Finally, the mammalian cell lines used so far to study mitophagy, such as HeLa cells (Human Protein Atlas, https://www.proteinatlas.org), not always express endogenous levels of the proteins of interest (e.g. Parkin), and require their overexpression, which might lead to off target effects. Therefore, it is important to investigate the mechanisms of neuronal mitophagy in physiological conditions, to be able to develop effective therapies for PD patients with mitochondrial dysfunction.

3.1.2 PINK1-dependent mitophagy in neurons *in vivo*

Studies of mitophagy in immortalised cell lines have underlined the importance of PINK1 and Parkin in mitochondrial quality control upon mitochondrial stresses. However, the rodent models of the genetic forms of PD struggled to recapitulate the key features of the disease (Dawson, Ko and Dawson, 2010), raising questions on whether this pathway was relevant *in vivo*. In particular, PINK1 and Parkin knockout mice models don't show degeneration of dopaminergic neurons in the substantia nigra or a motor phenotype, unless further crossed with mice models of mitochondrial dysfunction due to the accumulation of mutations in the mtDNA (Paul and Pickrell, 2021) or aged for more than 2 years (Noda *et al.*, 2020). Rat knockout models of PINK1, but not of Parkin, have been reported to show some degeneration of dopaminergic neurons and motor dysfunction but don't reproduce all disease phenotypes either (Creed and Goldberg, 2018). Our first understanding of the role of PINK1 and Parkin came from studies in *Drosophila*, as PINK1 and Parkin knockout or mutant flies show PD-like phenotypes, including muscle degeneration, reduced lifespan and degeneration of the dopaminergic neurons, and mitochondrial dysfunction (Clark *et al.*, 2006; Park *et al.*, 2006; Yang *et al.*, 2006).

The recent development of mitophagy reporter animal models, such as the mitoQC (McWilliams *et al.*, 2016) and the mtKeima (Sun *et al.*, 2015) mice, and the mitoQC and mtKeima flies (Cornelissen *et al.*, 2018; Lee *et al.*, 2018), have allowed detection of mitophagy in neurons and in other tissues *in vivo*. However, these models have yielded contrasting results when used to investigate the role of PINK1 and Parkin *in vivo*. In particular, while the mitoQC mice and flies showed that PINK1 is dispensable for basal mitophagy (Lee *et al.*, 2018; McWilliams *et al.*, 2018), the

mtKeima flies and mice exhibited impaired mitophagy when PINK1 or Parkin were knocked out (Cornelissen *et al.*, 2018; Kim *et al.*, 2019; Liu *et al.*, 2021). These findings could be due to the different design of the reporters (See Introduction), as the mitoQC construct is targeted to the outer mitochondrial membrane and can undergo degradation independently of mitophagy of the whole organelle, making it a less sensitive reporter of mitophagy *in vivo* (Katayama *et al.*, 2020; Liu *et al.*, 2021). Therefore, studies with novel reporters, such as the mitoSRAI (Katayama *et al.*, 2020) or evolutions of the mitoQC reporter where it is targeted to the matrix (Ordureau *et al.*, 2020), will be necessary to understand whether PINK1-dependent mitophagy plays a role *in vivo*.

As well as the fluorescent reporters, other studies have focused on the detection of pUb(Ser65) levels as a measure of PINK1-dependent mitophagy. Mice models with mitochondrial dysfunction, like the Mutator mice that accumulate mutations in the mtDNA, have higher levels of pUb(Ser65) in the brain, suggesting activation of PINK1-dependent mitophagy (Pickrell *et al.*, 2015). PINK1-dependent pUb(Ser65) signal can be detected in *Drosophila* brains (Shiba-Fukushima *et al.*, 2017; Usher *et al.*, 2021) and in mice brains (Watzlawik *et al.*, 2020), and increases with age and PD and AD disease status in human post mortem brain (Fiesel *et al.*, 2015; Hou *et al.*, 2018; Watzlawik *et al.*, 2020). Furthermore, using a sensitive sandwich ELISA method, pUb(Ser65) was detected in plasma from blood of healthy controls and reduced in PD patients with a PINK1 mutation, suggesting its potential use as a biomarker of activated mitophagy or reduced clearance (Watzlawik *et al.*, 2020).

3.1.3 Mitophagy in primary and iPSC – derived neurons

Initial studies to understand the mechanism of mitophagy in neurons, how it is activated and where it occurs, were carried out in primary rat and mouse cortical or hippocampal neurons. These studies primarily looked at the translocation of over-expressed Parkin from the cytosol to the mitochondria, or the co-localisation of mitochondria and LC3 as a marker of mitophagy, but yielded contrasting results. While some groups reported slow, PINK1-dependent Parkin recruitment after depolarisation of the mitochondria in neurons overexpressing Parkin (Vives-Bauza *et al.*, 2010; Cai *et al.*, 2012; Joselin *et al.*, 2012; Ashrafi *et al.*, 2014), other groups were unable to replicate it with endogenous levels of Parkin (van Laar *et al.*, 2011). This was suggested to be due mainly to differences in culture conditions, such as the presence or not of antioxidants (Joselin *et al.*, 2012) or apoptosis inhibitors (Cai *et al.*, 2012) in the media, as well as being linked to whether cells were forced to rely on oxidative phosphorylation as a source of energy (van Laar *et al.*, 2011). Subsequent studies used more specific indicators of mitophagy, such as the mtKeima reporter (Bingol *et al.*, 2014) or pUb(Ser65) staining (Fiesel *et al.*, 2015; López-Doménech *et al.*, 2021), detecting PINK1-dependent mitophagy in primary rat and mouse neurons.

In order to further assess mitophagy in cells with endogenous levels of Parkin and on patient genetic backgrounds, iPSC-derived neurons were used as a disease-relevant model, but whether mitophagy could be active in neurons remained controversial. While an initial study reported PINK1-dependent Parkin recruitment and reduced mtDNA copy number in iPSC-derived DA neurons (Seibler *et al.*, 2011), another study using degradation of mitochondrial proteins as a marker of mitophagy could not detect it (Rakovic *et al.*, 2013). Since then, several studies have reported

regulation and impairment of mitophagy in this system. Mitophagy has been detected in iPSC-derived DA and cortical neurons in several ways: by measuring the co-localisation of mitochondrial markers and LC3 or lysosomal dyes (Hsieh *et al.*, 2016; Martín-Maestro *et al.*, 2017; Oh *et al.*, 2017; Berenguer-Escuder *et al.*, 2020; Schwartzentruber *et al.*, 2020; Stathakos *et al.*, 2020); by measuring the degradation of mitochondrial proteins or accumulation of PINK1 or Parkin by WB (Hsieh *et al.*, 2016; Oh *et al.*, 2017; Soutar *et al.*, 2018); by measuring pUb(Ser65) levels by WB and ICC (Oh *et al.*, 2017; Shiba-Fukushima *et al.*, 2017; Tsefou *et al.*, 2021); by using mitophagy reporters, such as mtKeima (Hsieh *et al.*, 2016; Oh *et al.*, 2017; Suzuki *et al.*, 2017; Shaltouki *et al.*, 2018).

iPSC-derived neurons are an important cell model to study neurodegeneration, as the generation of cell types relevant in the disease with different genetic backgrounds from patients enables research into the early pathogenic mechanisms. However, like any other model, they still have some limitations. Culturing iPSC-derived neurons is labour intensive, long, costly and often highly variable between inductions of the same line and between different iPSC lines. Furthermore, as the reprogramming of somatic cells to iPSCs erases their epigenetic signature, iPSC-derived neurons are more similar to foetal neurons and often do not recapitulate the phenotypes of diseases of ageing, such as neurodegeneration, unless they are kept in culture for months, or years (Sposito *et al.*, 2015).

In order to model ageing in neurons, several groups have developed techniques to directly reprogramme somatic cells from patients to neurons, by

overexpressing transcription factors that are key for determining and maintaining neuronal fate (Vierbuchen *et al.*, 2010; Pang *et al.*, 2011). These induced neurons, or iNeurons, maintain the epigenetic signature of the somatic cells of origin and are therefore considered to be better models of aged neurons (Mertens *et al.*, 2015). However, the direct reprogramming of somatic cells is not efficient, and yields a low percentage of neurons. To overcome this issue, Zhang and colleagues applied the same principle of overexpressing neuronal transcription factors, such as Neurogenin 2 (Ngn2), to iPSCs (Zhang *et al.*, 2013). This allowed a higher yield of excitatory neurons and more efficient reprogramming, starting from a population of cells capable of unlimited self-renewal and therefore suited for bigger scale studies. Since their initial development, iNeurons have been increasingly used to model neurodegeneration, including to study mitophagy in a neuronal system. For example, iNeurons from patient fibroblasts were used to confirm pUb(Ser65) as a physiological marker of mitochondrial stress (Fiesel *et al.*, 2015) and iNeurons from embryonic stem cells were employed to study the dynamics and targets of Parkin ubiquitylation in a system with endogenous Parkin levels, as well as the role of pUb(Ser65) in neurons (Ordureau *et al.*, 2018, 2020).

In this chapter, I will describe the optimisation of iPSC-derived cortical neurons and iNeurons as a model to study mitophagy, and the role of KAT8 and KANSL1, in a more physiological system.

3.2 Results

3.2.1 Detection of pUb(Ser65) levels in iPSC-derived cortical neurons with PINK1 mutations

To be able to study PINK1-dependent mitophagy in disease-relevant cell lines, it was first of all necessary to optimise the neuronal cell culture and experimental conditions. In particular, given the initial controversy on the relevance and presence of mitophagy in neuronal cells, including in iPSC-derived neurons (see Chapter Introduction), I initially aimed to determine whether it was possible to detect mitophagy using the iPSC models available in the lab. As a continuation of the work carried out in the SHSY5Y cells, I firstly opted for the detection of pUb(Ser65) as a marker of PINK1-dependent mitophagy in iPSC-derived cortical neurons. As the phosphorylation of ubiquitin on Serine 65 is dependent on PINK1, I selected two iPSCs lines from a family carrying a novel PINK1 mutation (p.W90LfsX12) as positive controls for the optimisation of the experimental set up. The chosen lines, which were reprogrammed by the lab of my secondary supervisor Prof Sonia Gandhi, were one heterozygous (from the mother, unaffected) and one homozygous (from the daughter; also carrying a previously reported Parkin p.R275W het mutation, with early onset PD) for the mutation, which is predicted to cause a frameshift and introduction of a stop codon in exon 1 (Fig 25). Given that the mutation in PINK1 was predicted to cause degradation of the mutated PINK1 transcript, these two lines would allow to model the effect of a complete absence of PINK1 on a patient genetic background (Hom line), as well as the effect of a reduced PINK1 dosage on a healthy genetic background (Het line).

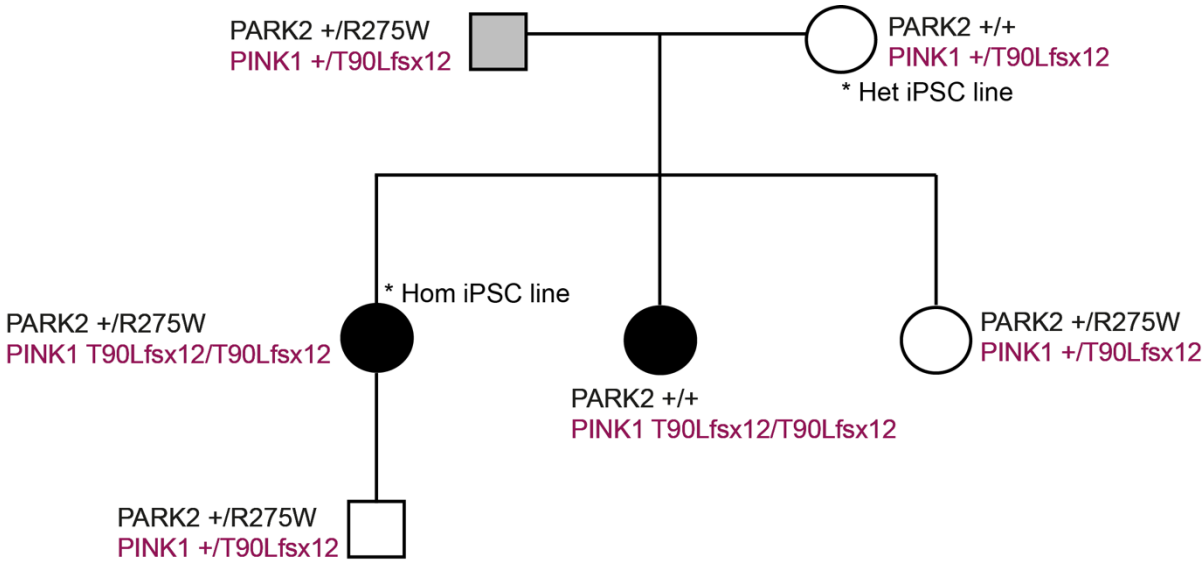

Figure 25. Family tree of the PD family with PINK1 and Parkin mutations. Parkin (PARK2) p.R275W and PINK1 p.W90LfsX12 mutations, the + sign indicates the wildtype allele. In the family tree, squares indicate males and circles females. The two black circles indicate the affected individuals. The grey colour indicates a possibly affected individual, where not enough information is available for diagnosis. The white colour indicates healthy individuals.

First of all, I optimised an experimental set up for the detection of pUb(Ser65) in iPSC-derived cortical neurons using immunofluorescence and high content imaging on the Opera Phenix. Imaging offers several advantages over techniques such as Western blotting, which were previously used to detect the degradation of mitochondria in such neurons (Soutar *et al.*, 2018). In particular, it allows to perform single cell analysis of exclusively the cells of interest, identified with a suitable neuronal or glial marker, and this way also measure the composition of the culture as a result of different inductions. Furthermore, imaging on a high content system enables miniaturisation of the setup, meaning each experiment would require fewer cells and reagents.

The iPSCs were differentiated into cortical neurons using dual SMAD inhibition, as per the Shi *et al.* protocol (Shi, Kirwan and Livesey, 2012). Cells were plated in the inner 60 wells of several 96 well plates at day 50 post differentiation and cultured in maintenance media until at least day 80. From day 80 onwards, plates were treated with 1 μM O/A for either 3 h or 6 h before fixing and staining for pUb(Ser65) and TOM20. Plates were imaged on the Opera Phenix and analysed on Columbus for quantification of pUb(Ser65) levels in whole cell (defined on the TOM20 signal – Fig 26A, B). In a blind experiment, I was able to detect a clear dose dependent effect of pUb(Ser65) levels, with the heterozygous line showing half the levels of pUb(Ser65) compared to the control line and the homozygous line showing very low levels of pUb(Ser65) (Fig 26C). This was replicated at different ages with similar results. In order to confirm these results with an alternative method, I treated neurons at day 130 after the start of differentiation with 1 μM O/A (Soutar *et al.*, 2018) for either 48, 72 or 96 hours before collection of whole cell lysates and blotting for PINK1. As expected, neurons from the homozygous lines did not show accumulation of PINK1 (Fig 26D). However, the treatment did cause cell death and it was not possible to collect protein from the heterozygous line, therefore this experiment would need to be repeated at a much higher cell density, to also allow quantification of the mitochondrial markers.

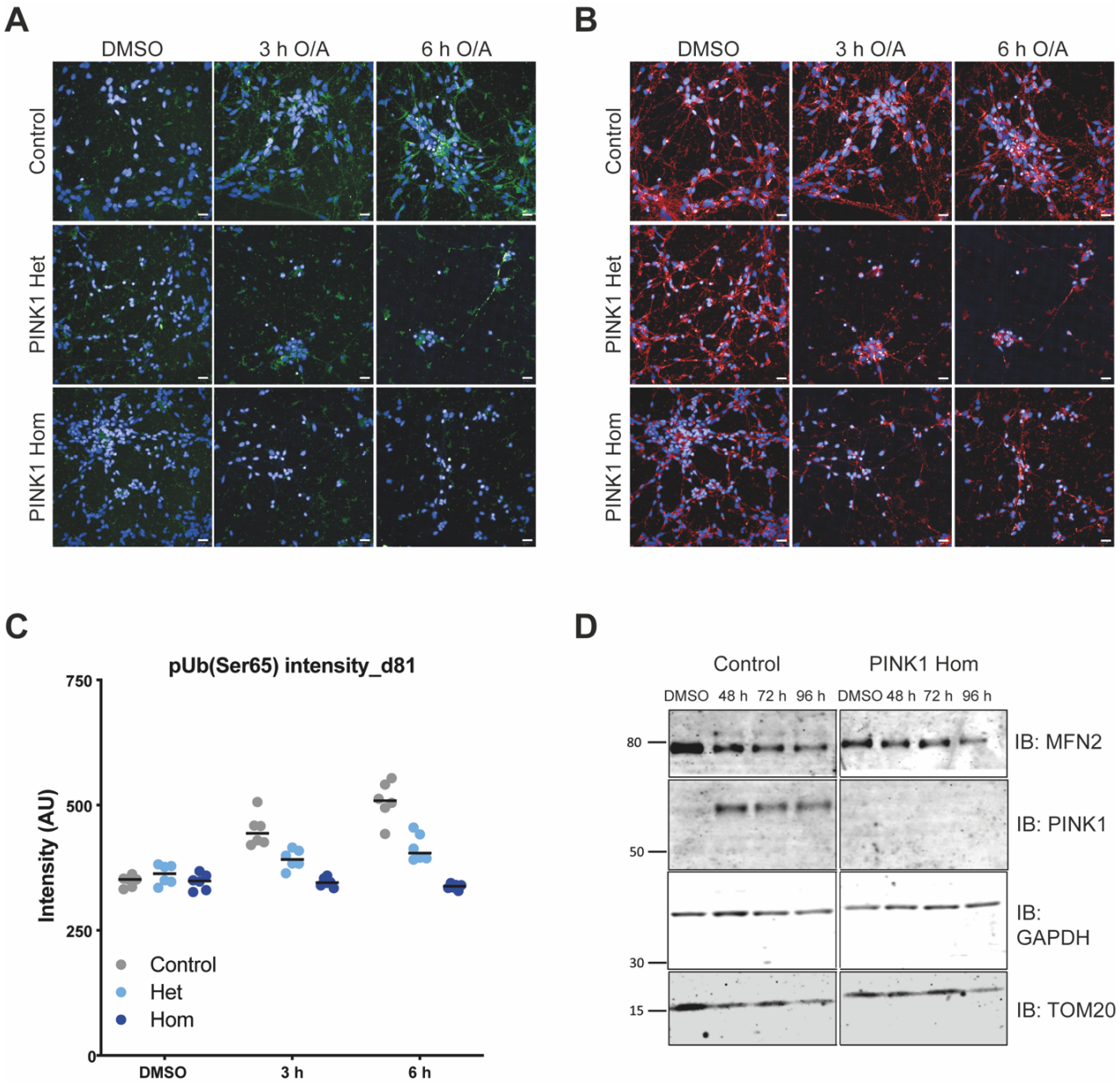

Figure 26. Detection of pUb(Ser65) and PINK1 in iPSC-derived cortical neurons

A, B. Day 81 iPSC-derived cortical neurons from control and from PINK1 W90L HET and HOM lines were treated with 1 µM O/A for 3 or 6 h prior to staining for pUb(Ser65) (**A**) and TOM20 (**B**), and imaging on the Opera Phenix. Scale bar = 20 µm. **C.** Quantification of pUb(Ser65) intensity in **A** at day 81 after the start of differentiation. **D.** WB of whole cell lysates of iPSC-derived cortical neurons at day 130 post differentiation treated with 1 µM O/A for 48, 72 or 96 h.

To confirm the pUb(Ser65) phenotype in another neuronal cell line, midbrain dopaminergic (mDA) neurons were differentiated from the 2 PINK1 pW90L lines and treated with O/A (work done by Gurvir Virdi and James Evans), before harvesting protein for WB analysis. PINK1 protein levels were again halved in the heterozygous line compared to control and undetectable in the homozygous line (Fig 27A,C). This was also reflected in the levels of pUb(Ser65) (Fig 27B,D). In summary, we were able to detect PINK1 and pUb(Ser65) in different iPSC-derived disease-relevant neuronal lines. Therefore, this experimental set up, using immunofluorescence and WB to measure pUb(Ser65) and PINK1 levels in neuronal cells, was used to study the role of KAT8 and KANSL1 in regulating PINK1-dependent mitophagy in iPSC-derived neurons.

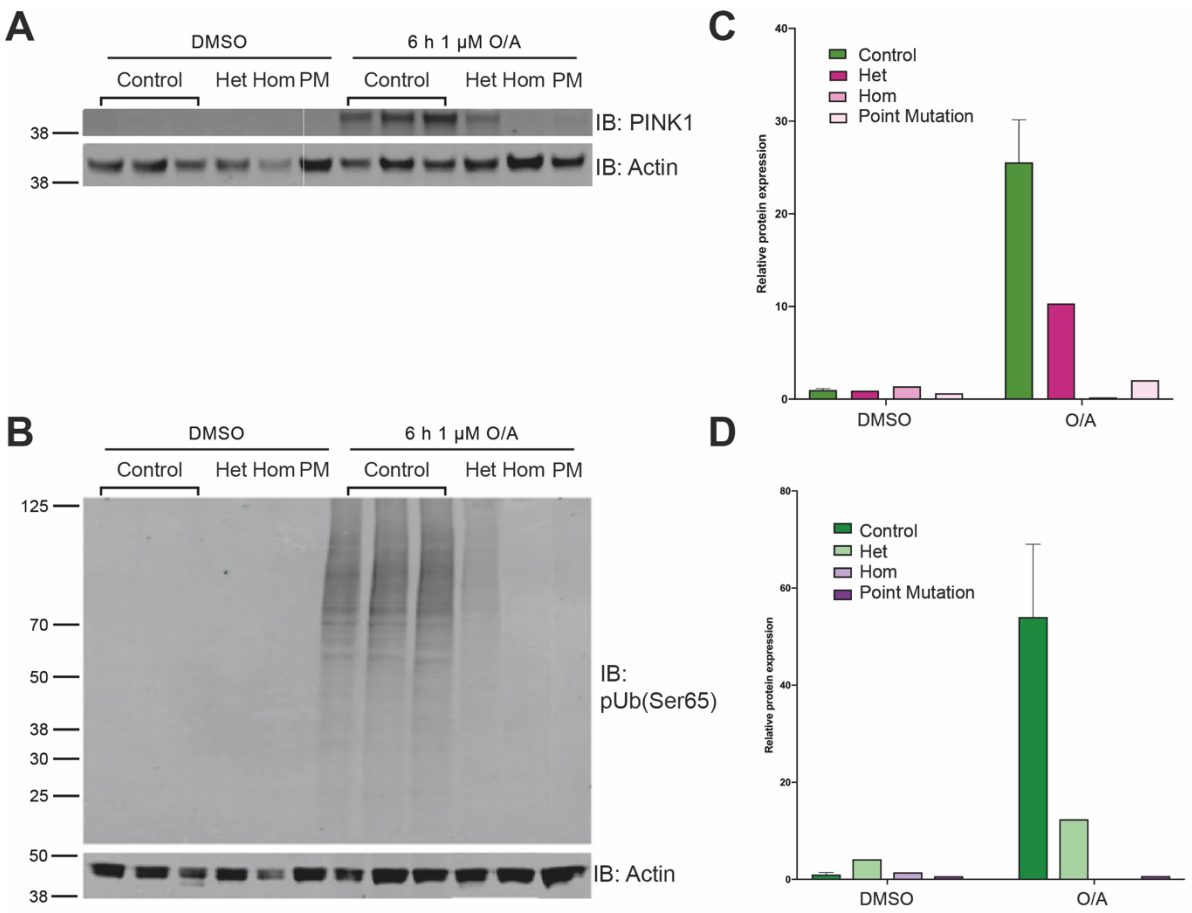

Figure 27. Detection of pUb(Ser65) and PINK1 in iPSC-derived midbrain dopaminergic neurons

A, B. 4 week iPSC-derived midbrain dopaminergic neurons from control and from PINK1 W90L HET and HOM lines were treated with 1 µM O/A for 6 h, prior to collection of whole cell lysates and WB for levels of PINK1 (**A**) and pUb(Ser65) (**B**). PM: Point Mutation - PINK1 line with homozygous p.I368N mutation, unrelated to the PINK1 family in Fig 25. **C** Quantification of the relative protein levels of PINK1 in **A**. **D.** Quantification of the relative protein levels of pUb(Ser65) in **B**. (work done by Gurvir Virdi and James Evans)

3.2.2 iNeurons as a model to investigate mitophagy and the role of KAT8 and KANSL1

In order to investigate KAT8- and KANSL1-dependent modulation of mitophagy in a more physiological system, that is in iPSC-derived neurons, it was first necessary to choose a model in which manipulation of the two genes was possible in a neuronal system. For this purpose, we selected the CRISPRi - i^{3}Neuron model (C. Wang *et al.*, 2017; Tian *et al.*, 2019). This iPSC line harbours a doxycycline-inducible Ngn2 cassette integrated in the safe harbour adeno-associated virus integration site 1 (AAVS1) locus. This allows rapid differentiation of the iPSCs into cortical neurons without the need for lentiviral transfection of the Ngn2 expression cassette, therefore resulting in a less variable neuronal population that doesn't require downstream selection and that is more amenable to wide scale studies. Furthermore, it has a dCas9-KRAB expression cassette under a CAG promoter integrated in the CYLBL safe harbour locus. The KRAB domain is a transcriptional repressor, and fusion to a catalytically inactive Cas9 protein (dCas9) allows precise targeting of the machinery to genes of interest using single guide RNAs (sgRNAs), leading to efficient knockdown of the genes via CRISPRi (Gilbert *et al.*, 2013, 2014). The possibility of knocking down KAT8 and KANSL1 in neurons was preferable to the generation of a knockout model of the genes, as not only it allows to model a loss of function mutation in the same way as the siRNA high content screen does, but also because both KAT8 and KANSL1 have been proposed to be essential for development (Thomas *et al.*, 2008; Koolen *et al.*, 2012; Zollino *et al.*, 2012). Therefore, full depletion of either gene might not result in neuronal differentiation and cell survival.

Setting up the CRISPRi - i^{3}Neuron model required the optimisation of three key aspects. First of all, iNeurons resulting from the direct differentiation of the iPSCs were extensively characterised, with particular focus on optimising the protocol to obtain homogenous mature, functional neurons. Secondly, I optimised a series of assays to detect mitophagy in the iNeurons, using a combination of immunofluorescence and WB. Finally, the parameters for CRISPRi knockdown of KAT8 and KANSL1, as well as PINK1 as a control, were selected.

3.2.3 The i^{3}Neurons can be differentiated into cortical neurons

To confirm the differentiation of the iPSCs into cortical neurons, I treated the cells for 72 h with doxycycline to induce expression of Ngn2, before final plating the iNeurons in 96-well plates and maintaining them in culture, until fixing and staining for neuronal markers (Fernandopulle *et al.*, 2018) (Fig 28A). As expected, at week 2 *in vitro*, the iNeurons stained positively for the neuronal markers NeuN, MAP2 and β3 Tubulin (Fig 28B). At this age, the iNeurons still stained positive for the neural stem cell marker Nestin (Fig 28B). Staining for these markers was confirmed by qPCR (Fig 28C). As expected, iNeurons at this age did not expressed markers of pluripotency, such as Oct4 and NANOG, but expressed precursor markers such as Nestin and early neuronal markers MAP2 and β3 Tubulin (*Tuj1*).

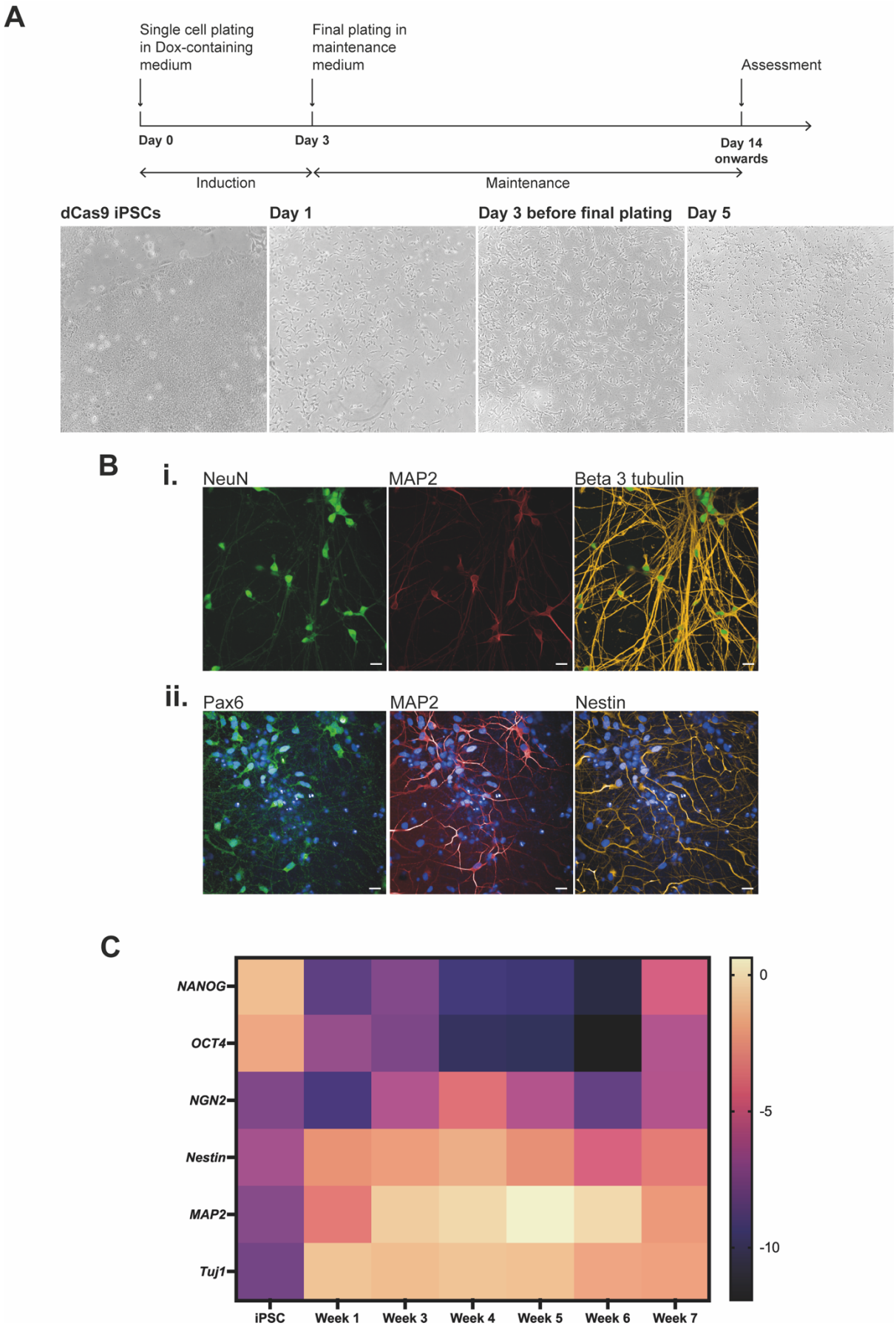
A
Single cell plating in Dox-containing medium
Final plating in maintenance medium
Assessment
Day 0
Day 3
Day 14 onwards
Induction
Maintenance
dCas9 iPSCs
Day 1
Day 3 before final plating
Day 5
B
i.
NeuN
MAP2
Beta 3 tubulin
ii.
Pax6
MAP2
Nestin
C
NANOG
OCT4
NGN2
Nestin
MAP2
Tuj1
iPSC
Week 1
Week 3
Week 4
Week 5
Week 6
Week 7
0
-5
-10

Figure 28. The i^{3}Neurons can be differentiated into cortical neurons.
A. Protocol for the differentiation of the i^{3}Neurons and representative brightfield images of the cells at different timepoints of differentiation **B.** Day 10 **(i)** and Day 14 **(ii)** i^{3}Neurons were fixed and stained for neuronal markers NeuN, MAP2 and Beta 3 Tubulin **(i)**, and precursor markers Pax6 and Nestin **(ii)**, before imaging on the Opera Phenix. Scale bar = 20 μm. **C.** qPCR quantification of neuronal development genes in the i^{3}Neurons at different ages, shown as -ΔCt of the gene of interest minus the *RPL18A* housekeeping gene (C. Wang *et al.*, 2017). More negative values (darker shade) indicate lower levels of expression of the indicated gene (n=2).

In order to confirm that the direct differentiation protocol could give rise to functional, electrically active neurons, I performed calcium imaging. The iNeurons were maintained post differentiation in two different types of maintenance medium, reported to have different effects on the maturation of the cultures. The traditional N2B27 medium used for maintenance of cortical neurons (Shi, Kirwan and Livesey, 2012) was compared to the Brainphys maintenance medium, which has been suggested to promote neuronal activity (Bardy *et al.*, 2015). To measure intracellular calcium levels, iNeurons were loaded with the ratiometric fluorescent calcium indicator Fura-2 AM in HBSS for 30 minutes before imaging. Interestingly, the iNeurons cultured in Brainphys media responded to stimulation with 5 μM glutamate (Fig 29A), while the iNeurons maintained in N2B27 failed to respond (Fig29B), suggesting a possible difference in maturity of the cultures. While these data are very interesting, they are still preliminary and will need replicating.

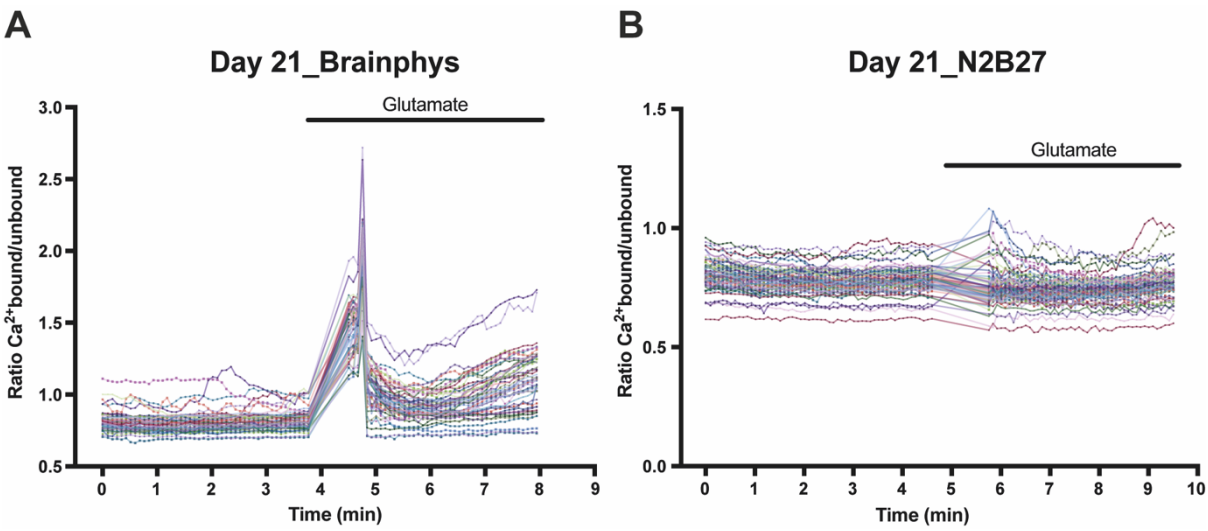

Figure 29. The i^{3}Neurons cultured in Brainphys, but not in N2B27, respond to glutamate stimulation.

Day 21 i^{3}Neurons cultured in N2B27 (**A**) or Brainphys (**B**) were loaded with the calcium indicator dye Fura-2 AM before imaging. The neurons were stimulated by adding 5 μM glutamate (n=1).

3.2.4 Mitophagy can be detected in the i^{3}Neurons

Following on from the optimisation of the detection pUb(Ser65) signalling in the PINK1 iPSC-derived cortical neurons, I investigated whether mitophagy could be detected in the i^{3}Neurons, as they differentiate and mature as well as in the different types of media. To this purpose, iNeurons were final plated in 96 well plates and maintained in culture in N2B27 medium until day 14 or further, before a time course of treatment with 1 μM O/A. Cells were then stained for pUb(Ser65) and neuronal markers, before imaging on the Opera Phenix (Fig 30A). As expected, the levels of pUb(Ser65) intensity within the iNeurons increased over time upon O/A-induced mitochondrial depolarisation (Fig 30B).

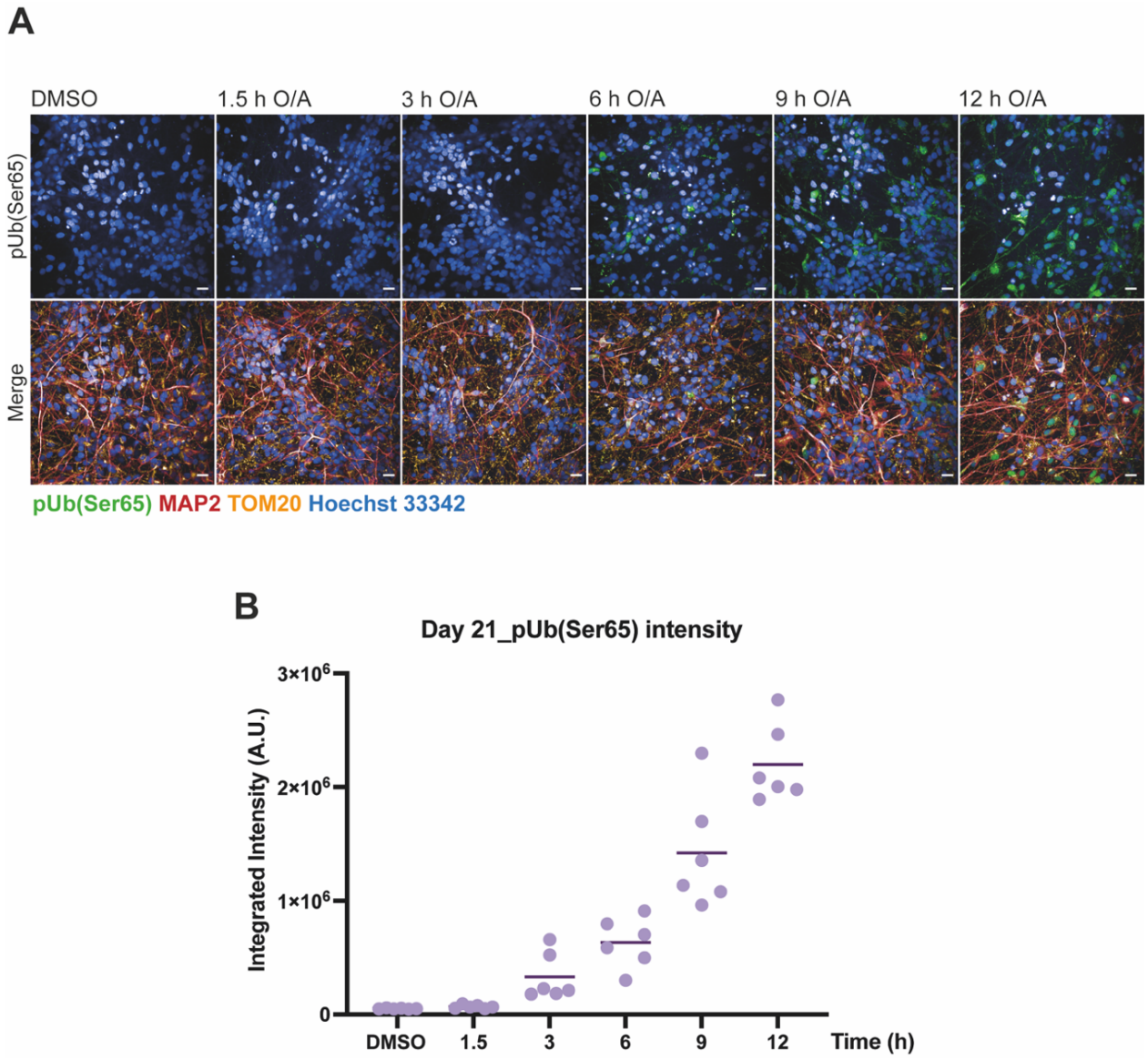

Figure 30. i^{3}Neurons cultured in N2B27 can activate PINK1-dependent mitophagy in response to O/A treatment.

A. Day 21 i^{3}Neurons were treated with 1 μM O/A for 1.5, 3, 6, 9 and 12 h or DMSO control, prior to being fixed and stained for pUb(Ser65), TOM20, Hoechst 33342 and neuronal marker MAP2. Cells were imaged on the Opera Phenix. Scale bar = 20 μm. **B.** Quantification of pUb(Ser65) intensity levels in **A**, within MAP2 positive cells only. Each dot represents one well in the 96-well plate, the line represents the mean (n=1).

To confirm the induction of mitophagy using an alternative method, iNeurons were grown in either Brainphys or N2B27 medium until day 14 or further, before collection of whole cell lysates and immunoblotting. pUb(Ser65) and accumulation of PINK1 was detected in iNeurons kept in culture up to day 30 in N2B27 maintenance medium (Fig 31A,B). Interestingly, from day 40 onwards, the iNeurons were not able to activate PINK1-dependent mitophagy as much as the younger iNeurons (Fig 31B). Similarly, iNeurons maintained in Brainphys showed no accumulation of pUb(Ser65) or PINK1, compared to same age iNeurons maintained in N2B27 (Fig 31C). The lack of PINK1 accumulation was not due to reduced expression of *PINK1* in Brainphys cultured iNeurons, as *PINK1* mRNA was equally detected by qPCR across all ages (Fig 31D). Indeed, PINK1 protein could be detected in Brainphys cultured iNeurons after treatment with the proteasome inhibitor MG132 (Fig 31C). Treatment with MG132 blocks the degradation of the PARL cleaved form of PINK1, which can then be detected by WB (Yamano and Youle, 2013; Wang *et al.*, 2019), indicating that PINK1 is translated in the Brainphys iNeurons but doesn't accumulate on the mitochondria and initiate mitophagy. As previous studies have suggested that mitophagy might be limited and slower in mature neurons (Cai *et al.*, 2012; Puri *et al.*, 2019), the lack of detection of pUb(Ser65) upon treatment with O/A in older iNeurons, as well as neurons maintained in a medium proposed to promote functional activity, could indicate that iNeurons can become mature neurons, impacting their ability to degrade mitochondria.

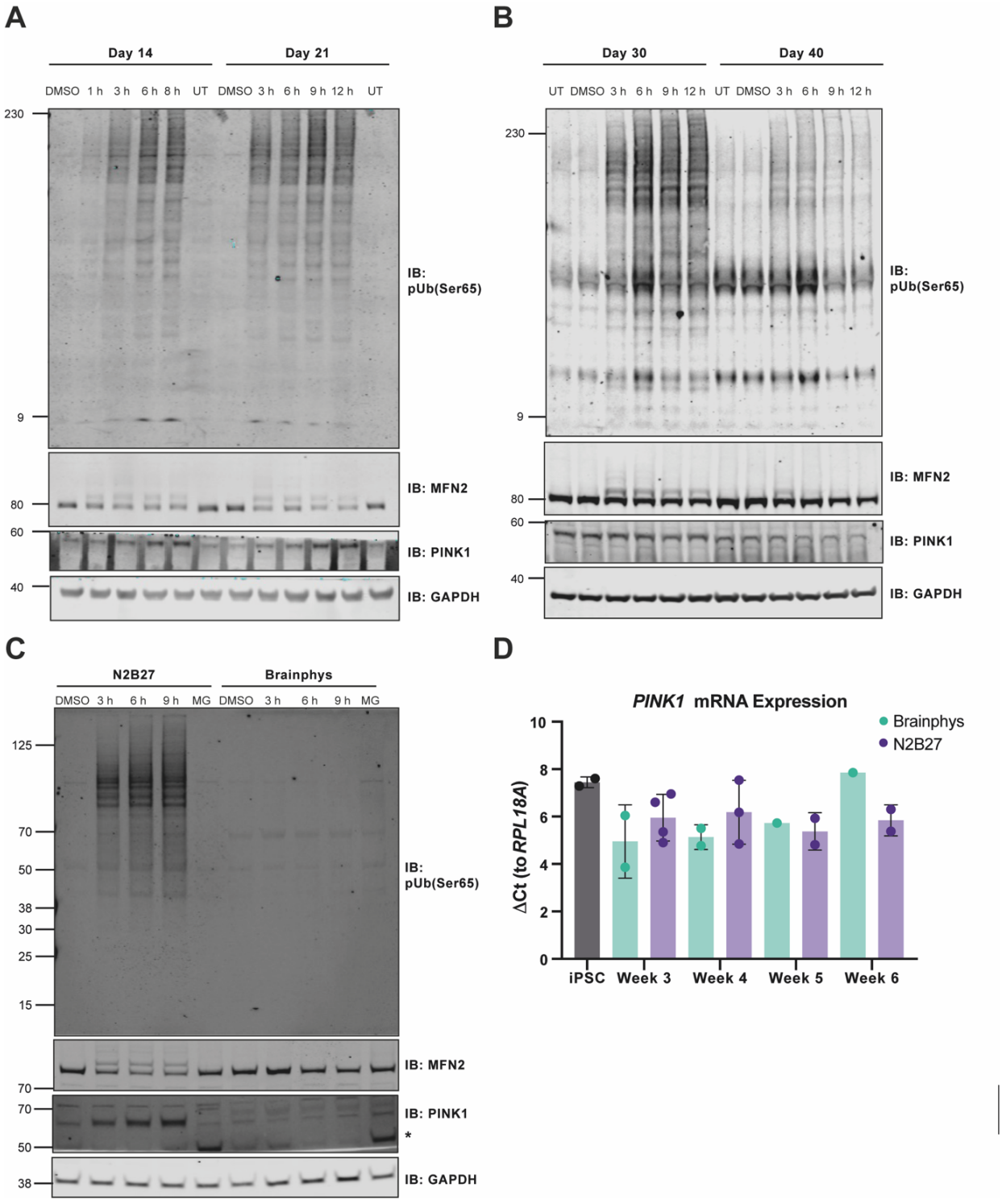

Figure 31. The i^{3}Neurons cultured in N2B27, but not in Brainphys, activate mitophagy in response to O/A treatment.

A. WB of whole cell lysates of day 14 and 21 i^{3}Neurons cultured in N2B27 and treated with 1 μM O/A for 1,3,6 and 8 h and 3,6, 9 and 12 h or DMSO control. UT: untreated. **B.** WB of whole cell lysates of day 30 and 40 i^{3}Neurons cultured in N2B27 and treated with 1 μM O/A

for 3,6, 9 and 12 h or DMSO control. UT: untreated. Blots in A and B were run by Dr Marc Soutar. **C.** WB of whole cell lysates of day 21 i^3Neurons cultured in N2B27 or Brainphys and treated with 1 μM O/A for 3,6 and 9 h, DMSO control or 10 μM MG132 (indicated as MG) for 9 h to block proteasome-mediated degradation. Asterisk indicates PARL-cleaved PINK1. **D.** qPCR quantifying expression of *PINK1* in i^3Neurons at different ages cultured in N2B27 or Brainphys. Data are shown as ΔCt of the gene of interest minus the *RPL18A* housekeeping gene (n=2).

To determine whether the different response of the iNeurons to O/A in the two culture media could be due to the different energetic status of the cells, the Seahorse Mito Stress Test was carried out on day 14 iNeurons in Brainphys or N2B27. The Mito Stress Test measures mitochondrial function by measuring the oxygen consumption rate (OCR) in response to sequential inhibition of the electron transport chain with oligomycin, FCCP, antimycin A/rotenone. After normalising the OCR by the number of nuclei in the well, the iNeurons cultured in Brainphys showed higher OCR parameters, suggesting a more energetic status of the cells, compared to the iNeurons cultured in N2B27 (Fig 32) .

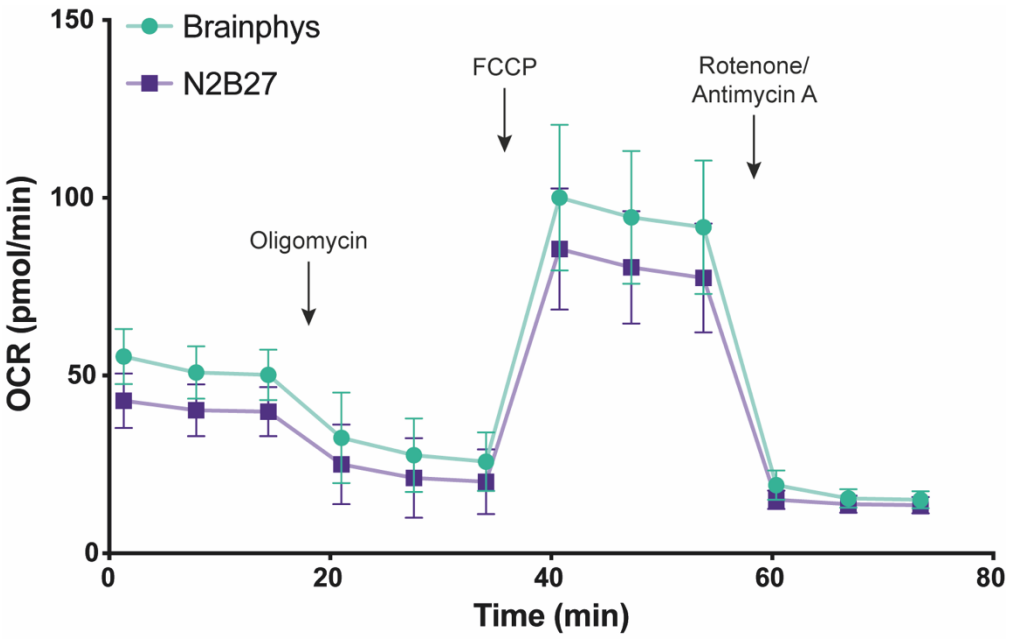

Figure 32. The i^{3}Neurons cultured in Brainphys are more energetic than those cultured in N2B27.

OCR of day 14 iNeurons cultured in Brainphys or N2B27 measured using the Seahorse Mito Stress Test, after sequential addition of oligomycin, FCCP and antimycin A/rotenone (n=1). Measurements were normalised to the number of nuclei, which was obtained by loading the cells with Hoechst 33342 after the final time point and imaging immediately on the Opera Phenix.

3.2.5 Selection of the single guide RNAs to perform CRISPRi in the i^{3}Neurons

To study how perturbation of KAT8 and KANSL1 levels affects mitophagy in the i^{3}Neurons, I then optimised the conditions to achieve efficient knockdown via CRISPRi. This technology requires the transduction of the iPSCs with a lentivirus expressing a sgRNA targeting the gene of interest, before inducing differentiation into iNeurons within 24h of transduction (Tian *et al.*, 2019) (Fig 33A). To select the

optimal sgRNAs against KAT8, KANSL1 and PINK1, the guides with the highest predicted target gene activity were selected for each gene from the hCRISPRi-v2.1 library (Horlbeck *et al.*, 2016). This resulted in first instance in 5 guides selected for KANSL1 and PINK1, and 6 guides for KAT8, the top 3 for each predicted transcription start site (See Materials and Methods). The selected sgRNAs, as well as a non targeting control, were each inserted into a lentiviral vector under a U6 promoter and an mApple fluorescent reporter, before being packaged into lentivirus particles using a second-generation system. To further choose which of these top guides to carry forward for subsequent mitophagy experiments in the iNeurons, I evaluated the knockdown efficiency of each one by measuring the relative expression of *PINK1*, *KAT8* and *KANSL1* (compared to the non targeting control) by qPCR. The dCas9 iPSCs were transduced for 48 h (for PINK1 guides) or 24 h (for KAT8 and KANSL1 guides), with different dilutions of lentivirus (1:2, 1:5 and 1:10). Successful transduction was assessed by presence or absence of mApple signal and wells with estimated comparable levels of transduction efficiency were lysed for RNA extraction and qPCR. Transduction of the KAT8 and KANSL1 sgRNAs caused extensive cell death after 24h, suggesting potential high levels of knockdown, as both genes have been reported to be essential for cell survival (Gupta *et al.*, 2005; Taipale *et al.*, 2005; Radzisheuskaya *et al.*, 2021), therefore they were evaluated at an earlier timepoint compared to the PINK1 guides.

Of the PINK1 guides, sequence 4 (S4) achieved robust knockdown of PINK1, with undetectable levels of PINK1 mRNA, with S3 also causing a 70% reduction in PINK1 levels (Fig 33B). Therefore, both guides were selected for downstream experiments. Good knockdown of KAT8 was detected with 5 of the 6 sgRNAs, with

guides targeting the first transcription start site (P1) achieving 90% knockdown (Fig 33C). Due to the essential role of KAT8 in cell cycle and development, as well as to better model the effects of the PD GWAS SNP, which does not abolish expression of KAT8, I also selected one of the guides (P2 S1) that caused a 50% reduction of KAT8 levels, to potentially improve cell survival and differentiation. Due to the high levels of cell death caused by transduction of the KANSL1 sgRNAs and the consequent low quality of the extracted RNA, it was not possible to confidently evaluate which sgRNA achieved the best knockdown. Therefore, the top 2 guides with predicted highest activity were selected.

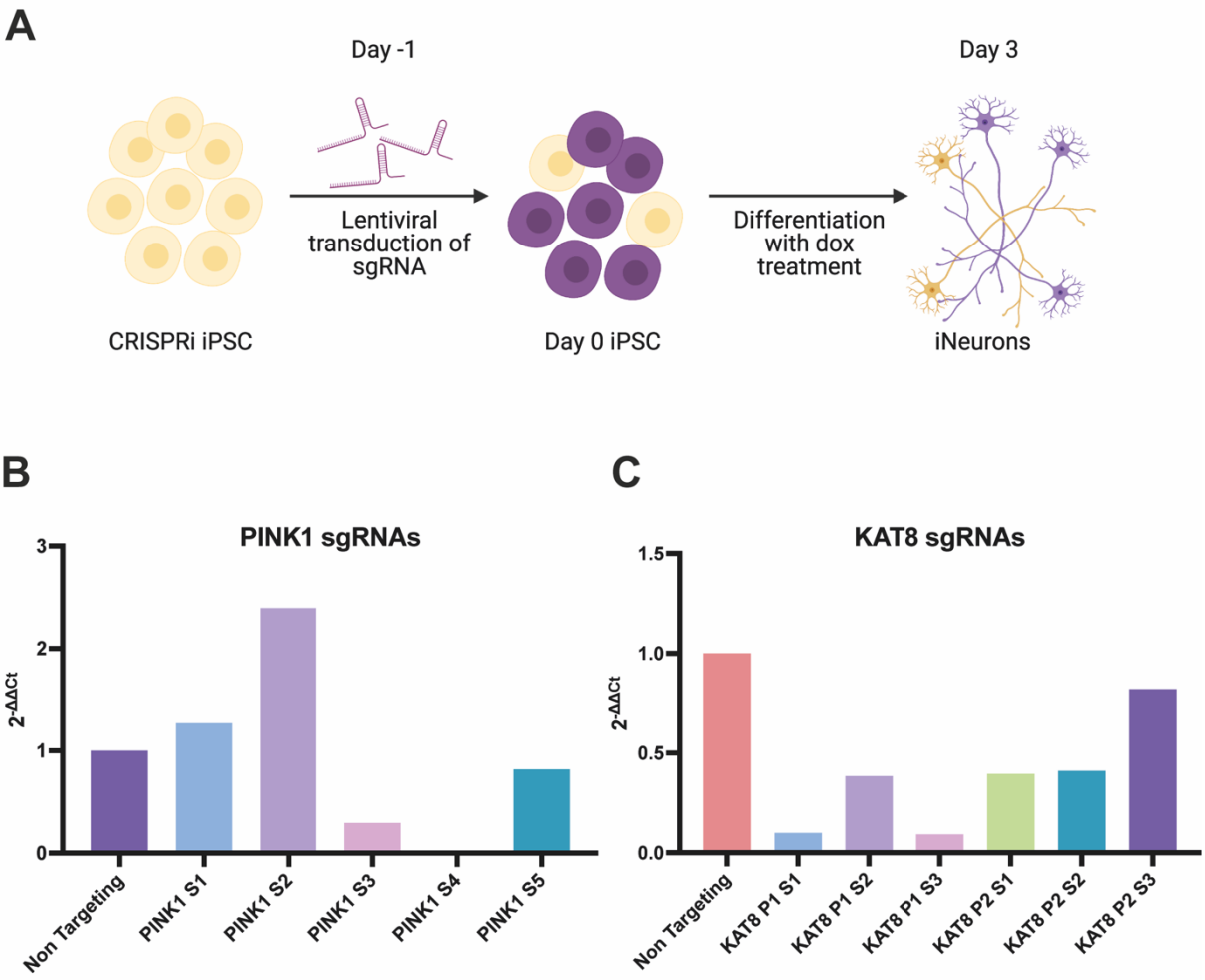

Figure 33. Selection of the sgRNAs to knock down KAT8 and PINK1.
A. Outline of the experimental setup for CRISPRi in the i^{3}Neurons. **B.** Relative *PINK1* mRNA expression levels in the dCas9 iPSCs transduced for 48 h with sgRNAs against *PINK1* and measured by RT-qPCR. Expressions levels were normalised to the *RPL18A* housekeeping gene and the Non targeting sgRNA control (n=1). **C.** Relative *KAT8* mRNA expression levels in the dCas9 iPSCs transduced for 24 h with sgRNAs against *KAT8* and measured by RT-qPCR. Expressions levels were normalised to the *RPL18A* housekeeping gene and the Non targeting sgRNA control (n=1).

3.2.6 Detection of mitophagy in the i^{3}Neurons after CRISPRi-mediated knockdown of KAT8 and KANSL1

To investigate whether knockdown of KAT8 and KANSL1 could affect mitophagy in the i^{3}Neurons, the dCas9 iPSCs were then transduced for 24 h with the selected sgRNAs, before inducing differentiation by fully changing the media to doxycycline - containing induction medium. After 72 h, the iNeurons were final plated and cultured until harvesting at day 14 and day 21 (Fig 34A). At this stage, the iNeurons were cultured in N2B27 maintenance medium, to allow detection of PINK1-dependent mitophagy.

All transduced iPSC successfully differentiated, although transduction of the KANSL1 and in particular of the KAT8 sgRNAs yielded a lower number of neurons. The knockdown efficiency of each gene was evaluated by qPCR at day 3 (i.e. at final plating stage) to confirm successful CRISPRi in the initial stages of development. All 3 genes were successfully knocked down with the top selected sgRNAs, including at

a lower level KANSL1 (Fig 34B), although this result is preliminary and will need repeating.

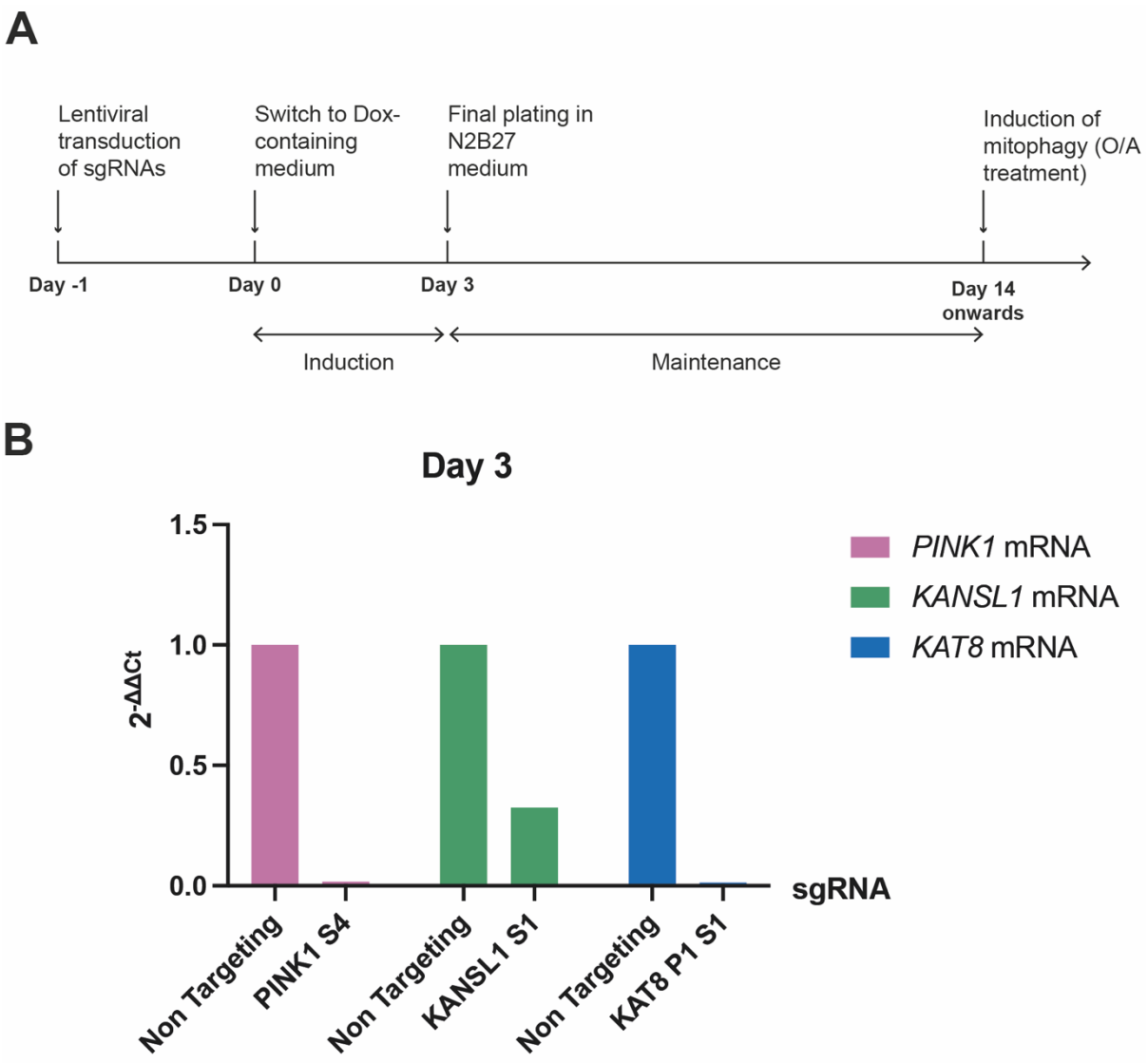

Figure 34. Knockdown of KAT8, KANSL1 and PINK1 in the i^{3}Neurons

A. Timeline of the sgRNA transduction, doxycycline-induced differentiation and mitophagy assessment of the CRISPRi i^{3}Neurons. **B.** Relative *PINK1*, *KANSL1* and *KAT8* mRNA expression levels in day 3 i^{3}Neurons measured by RT-qPCR. Expressions levels were normalised to the *RPL18A* housekeeping gene and the Non targeting sgRNA control (n=1).

At day 21, the iNeurons were checked for mApple fluorescence as a marker of successful transduction and were treated with 1 μM O/A or DMSO control for 9 h

before harvesting for WB and qPCR. The non targeting and PINK1 CRISPRi iNeurons showed a good transduction efficiency, estimated by the number of mApple positive cells. The KANSL1 CRISPRi iNeurons showed a modest level of cell death, with a good number of mApple positive cells, while few surviving cells in wells transduced with the KAT8 sgRNAs were unhealthy looking and mApple negative, possibly due to the lethality of low levels of KAT8. A 90% knockdown of PINK1 was achieved with both selected guides (S4 and S3), as assessed by qPCR (Fig 35A) and WB after a 9 h treatment with 1 μM O/A (Fig 36A,B). This was also reflected in the lack of phosphorylation of ubiquitin or ubiquitylation of MFN2 upon PINK1 knockdown (Fig 36A,C). Both KANSL1 sgRNAs caused a partial reduction of *KANSL1* mRNA levels (Fig 35B). Interestingly, knockdown of KANSL1 with both guides appeared to cause a slight reduction in *PINK1* mRNA levels (Fig 35A), confirmed by the reduction in PINK1 protein levels and pUb(Ser65) levels upon treatment with 1 μM O/A (Fig 36). This reflects the effect on *PINK1* transcription seen in POE SHSY5Y cells after KANSL1 KD (Fig 24B), although it will need to be repeated and confirmed. While transduction of the KAT8 sgRNAs seems to show a reduction in *KAT8* mRNA levels (Fig 35C), due to the poor quality of the neuronal culture (also reflected in the late amplification of the housekeeping gene *RPL18A* - Fig 35D), it was not possible to conclude whether there is an effective reduction in PINK1 and pUb(Ser65) levels. While preliminary and in need of further optimisation, all together, these data show that it is possible to successfully achieve knockdown of PINK1 and KANSL1 in the CRISPRi - i^{3}Neurons and that it can be used to study the role of KAT8 and KANSL1 on mitophagy in a more physiologically relevant cell model.

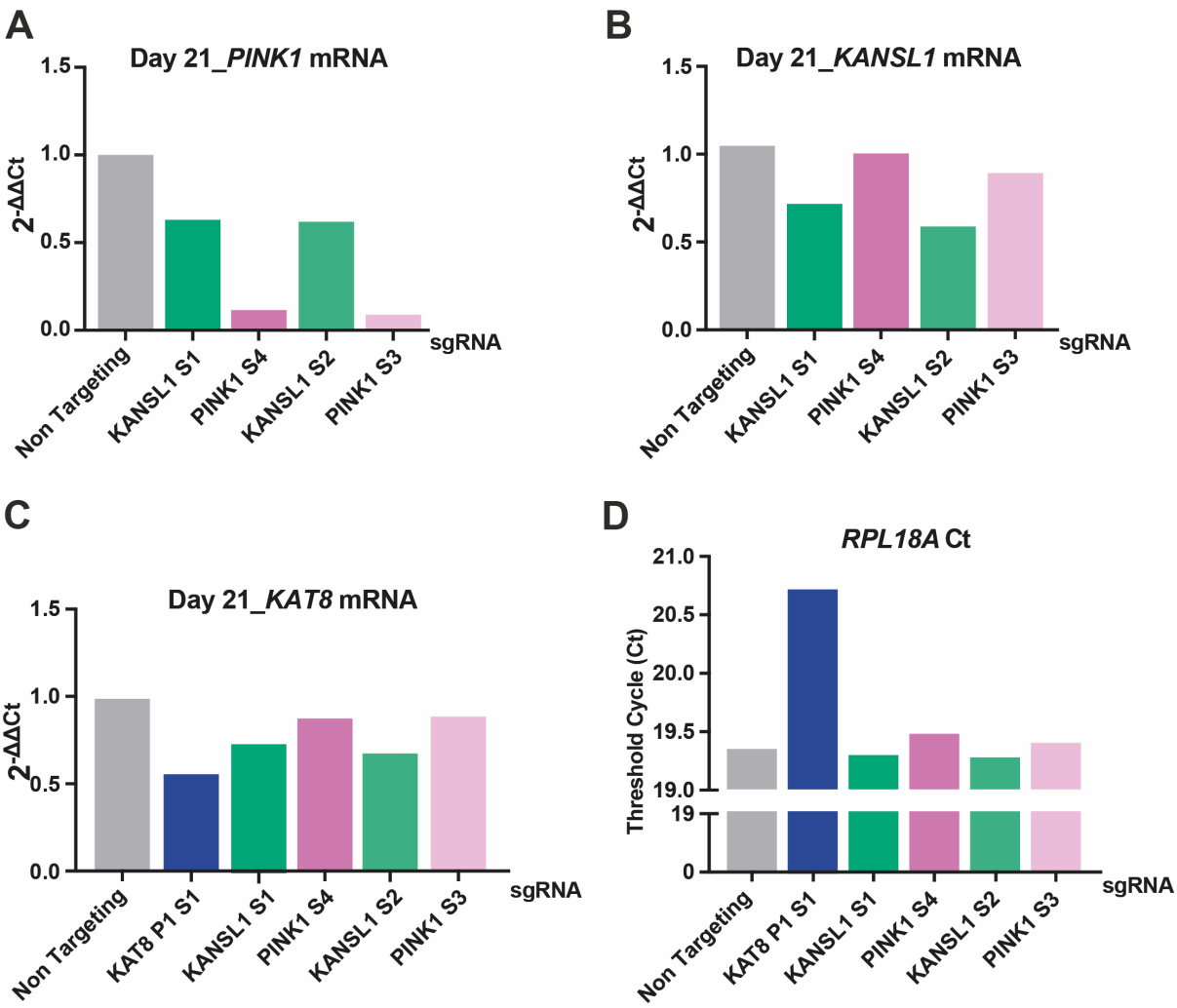

Figure 35. Assessment of CRISPRi knockdown of PINK1 and KANSL1 in day 21 i^{3}Neurons by qPCR.

A. Relative *PINK1* mRNA expression levels in day 21 i^{3}Neurons measured by RT-qPCR. **B.** Relative *KANSL1* mRNA expression levels in day 21 i^{3}Neurons measured by RT-qPCR. **C.** Relative *KAT8* mRNA expression levels in day 21 i^{3}Neurons measured by RT-qPCR. Expressions levels in **A**, **B** and **C** were normalised to the *RPL18A* housekeeping gene and the Non targeting sgRNA control (n=1). **D.** Threshold cycle of the housekeeping gene *RPL18A* in day 21 i^{3}Neurons, used to normalise the data in **A-C.**

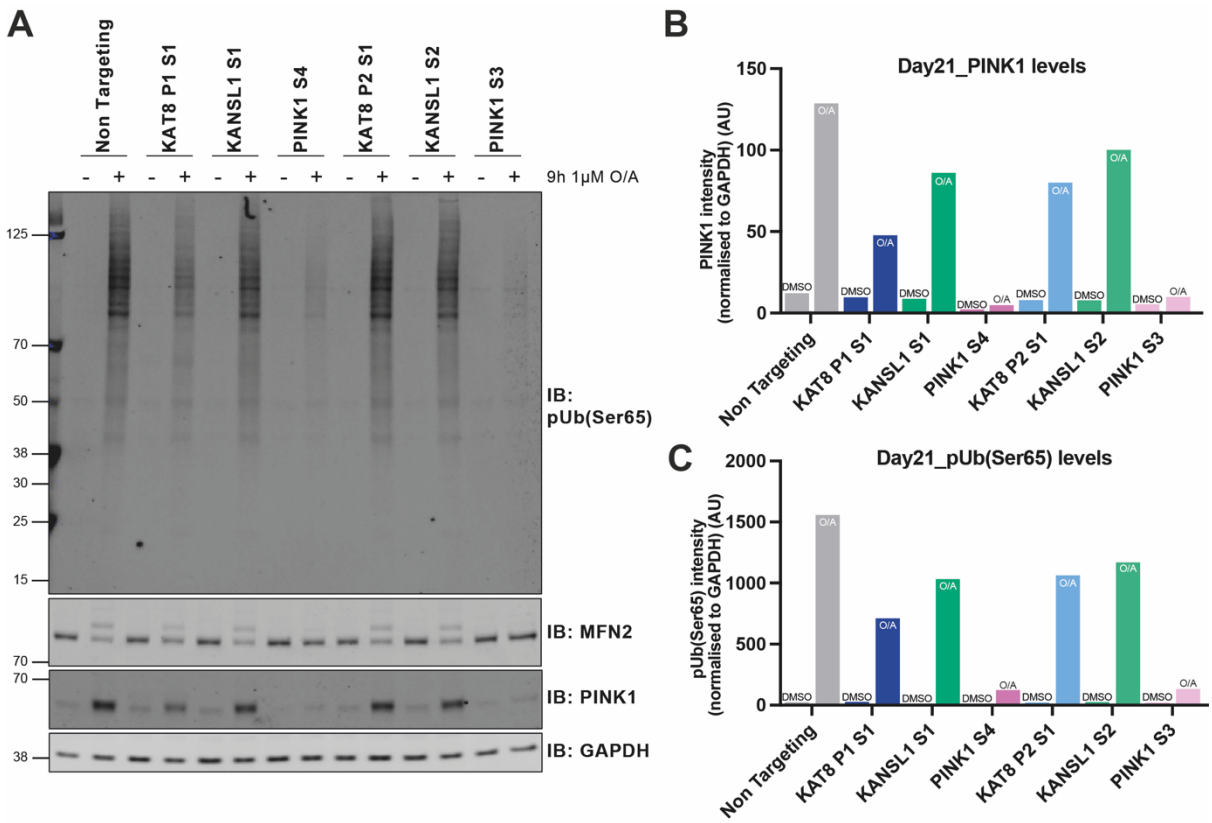

Figure 36. Assessment of mitophagy in day 21 i^{3}Neurons after knockdown of PINK1, KANSL1 and KAT8

A. WB of whole cell lysates of PINK1, KANSL1 and KAT8 CRISPRi i^{3}Neurons at day 21, treated with 1 μM O/A for 9h or DMSO control **B.** Quantification of PINK1 levels in **A** normalised to the GAPDH housekeeping band (n=1). **C.** Quantification of pUb(Ser65) levels in **A** normalised to the GAPDH housekeeping band (n=1).

3.3 Discussion

The failure of many clinical trials for neurodegenerative diseases, including PD, has been partially, but not only, ascribed to targets and mechanisms studied in inadequate cell and animal models (Charvin *et al.*, 2018). Together with better understanding in PD genetics, patient stratification and biomarker development, this has highlighted the need for more physiological disease-relevant models, able to reproduce the hallmarks of the disease, including disease progression. Mitochondrial quality control has been mainly studied in immortalised cell lines, and the role of mitophagy in the brain was originally considered controversial, as it had been hard to detect in neurons. Given the genetic evidence of the importance of mitophagy in the pathogenesis of PD, however, it is essential to understand mitochondrial quality control in a physiological system, with endogenous levels of the proteins involved and similar bioenergetic requirements, and in recent years several studies have described mitochondrial degradation in neuronal cells, both primary and derived from iPSCs.

The development of iPSCs in particular have enabled the modelling of pathogenic mechanisms rising from specific genetic mutations or variants, by generating iPSCs from PD patients and differentiating them in 2D and 3D cortical and dopaminergic neuronal cultures, as well as co-culture systems of neurons and glia. While I was able to discover a role for KAT8 and KANSL1 in PINK1-depenent mitophagy using SHSY5Y cells, it was important to develop and optimise a model to study their effect in neurons. To first set up this system, I again took advantage of the specificity of PINK1-dependent phosphorylation of ubiquitin and used patient

iPSC-derived neurons with PINK1 mutations to validate it as a marker of mitophagy. Treating both cortical and dopaminergic neurons with O/A leads to an increase in pUb(Ser65) levels, suggesting that these neurons are able to induce mitophagy. This signal is PINK1 dependent, as the patient line with the homozygous W90L mutation shows no pUb(Ser65) signal. However, while pUb(Ser65) is a good marker of the initial stages, these experiments do not show whether there is a reduction of mitochondrial content in the neurons. It will be necessary to set up a model using mitophagy reporters in the iPSC-derived neurons. Using single cell longitudinal imaging it would be possible to track the activation of mitophagy and the fate of the mitochondria over time. This could be done in parallel to developing better triggers of mitophagy *in vitro*, in alternative to using toxic compounds to cause extensive mitochondrial depolarisation, such as testing a mild oxidative stress protocol (Puri *et al.*, 2019; Evans and Holzbaur, 2020) or generating mitochondrial ROS (Ashrafi *et al.*, 2014). Finally, while it is important to understand how neuronal mitophagy is regulated, how mitochondrial quality control is activated in glia and the interplay between glial and neuronal mitophagy are also key aspects. Previous research has suggested that astrocytes in particular could play an important role in mitophagy and in PD (Booth, Hirst and Wade-Martins, 2017). Damaged neuronal mitochondria can be degraded in neighbouring astrocytes, in a process called transmitophagy (Davis *et al.*, 2014; Morales *et al.*, 2020), and *viceversa* astrocytes can donate healthy mitochondria to damaged DA neurons (Cheng *et al.*, 2020). Moreover, PINK1 has been proposed to phosphorylate ubiquitin predominantly in astrocytes and not in neurons (Barodia *et al.*, 2019) and other evidence points to changes in the metabolism of PD patient astrocytes (Sonninen *et al.*, 2020). Recently, *LRRC37A* and *LRRC37A2* on the 17q21 locus were found to be associated with protective

haplotypes for PD and highly expressed in astrocytes in the SN, further underlying the importance of the *MAPT* locus and a role for astrocytes in PD pathogenesis (Bowles *et al.*, 2021). Therefore, given the increasing evidence of the importance of astrocytes in PD, mitophagy should also be studied in neuron-astrocyte co-culture systems, where it is possible to also pair iPSC-derived neurons and astrocytes from patients and controls.

To be able to study the effect of KAT8 and KANSL1 on mitophagy in neurons like I did in the SHSY5Y cells, I selected the CRISPRi i^{3}Neuron system. This cell line has several advantages compared to the traditional differentiation methods, which are lengthy and labour intensive. Overexpressing Ngn2 easily produces cortical neurons after only 3 days of differentiation and the resulting iNeurons are partially mature within weeks instead of months. iNeurons obtained from rapid differentiation are also less variable within the same inductions and across different inductions, making them a good model in particular for screening purposes. While some reports suggest that the overexpression of Ngn2 might not lead to as pure a population as previously thought (Lin *et al.*, 2020), in the i^{3}Neuron model I used the Ngn2 cassette is inserted in a safe harbour locus and not randomly inserted via a lentiviral transduction, leading to a reduced variability within the neuronal population. However, using the iNeurons to model a neurodegenerative disease still has potential drawbacks. The rapid differentiation does not retrace normal neuronal development, which could lead to a less mature system in culture, although changes to the protocol, such as co-culturing with primary astrocytes or switching to culture media such as Brainphys, could potentially improve this aspect. Furthermore, the i^{3}Neuron line is not a patient line, meaning it is not possible to model the disease

phenotype linked to a certain genetic background. However, it would be possible to also obtain iNeurons from patient iPSC lines, by transducing the neural transcription factors. Finally, while the CRISPRi i^{3}Neurons were essential to be able to model the reduction of KAT8 and KANSL1 levels in neurons, overexpressing Ngn2 leads to a cortical neuron fate and therefore not the cell type that degenerates in PD and that could be key for PINK1-dependent mitophagy. Overexpression of dopaminergic neurons factors together with the neural factors such as Ngn2 allows to rapidly induce iPSCs or fibroblasts to dopaminergic neurons (Carter, Halmai and Fink, 2020), with such a system recently used to study mitophagy (Schwartzentruber *et al.*, 2020). Combining the induced dopaminergic neurons with CRISPRi to knock down KAT8 and KANSL1 could be a better way of modelling their effect on mitophagy and in PD.

Similarly to the iPSC-derived cortical and dopaminergic neurons, the CRISPRi-i^{3}Neurons were also able to induce mitophagy upon mitochondrial stress, as shown by the accumulation of PINK1 and increase in pUb(Ser65) levels. However, the induction of mitophagy appeared to be dependent on the culture conditions of the cells. While the iNeurons cultured in N2B27 responded to O/A treatment, the cells grown in Brainphys did not. Brainphys is reported to promote neuronal activity (Bardy *et al.*, 2015), which is reflected in the different response to glutamate during calcium imaging (Fig 29). Interestingly, iNeurons cultured in N2B27 for longer (more than 40 days) also did not activate mitophagy as well as the younger iNeurons (Fig 31). This different activation of mitophagy could be an insight in how mitochondrial degradation in regulated in electrically active, older neurons. Neurons with higher energetic requirements and dependence on oxidative

phosphorylation might not activate mitophagy in response to a widespread mitochondrial stress such as that caused by treatment with O/A. Further Seahorse experiments will be required to confirm whether the Brainphys neurons are indeed more energetic than those in N2B27, as well as looking at other parameters of mitochondrial physiology such as the mitochondrial membrane potential. If the degradation of damaged mitochondria is a rare or limited event in mature neurons, then better techniques to detect it are required. Single cell imaging is preferrable to Western blotting, including using the mitophagy reporters such as mt-Keima and mitoSRAI, and longitudinal imaging of single damaged mitochondria would allow to track their fate and understand how mitophagy is regulated, as recently suggested (Kleele *et al.*, 2021; Li *et al.*, 2021). However, it is not possible to exclude that the different induction of mitophagy could be due to the composition of Brainphys compared to N2B27. While both maintenance media contained antioxidants, N2B27 contained 5 times the amount of glucose than Brainphys, which has an effect on mitochondrial bioenergetic and the initiation of mitophagy (van Laar *et al.*, 2011; Lee, Zhang and Liu, 2015). Experiments supplementing Brainphys with additional glucose or switching the cultures before treatment with O/A could shed light on whether the culture conditions affected mitophagy more than the electrical activity or age of the culture.

Finally, modelling the role of KAT8 and KANSL1 in neurons requires further optimisation. While CRISPRi knockdown of a gene not essential for cell survival, such as PINK1, was highly efficient, knockdown of KAT8 caused widespread cell death and it was not possible to study its role in modulating mitophagy. Given the essential role of the NSL complex in cell survival (Thomas *et al.*, 2008;

Radzisheuskaya *et al.*, 2021), modelling KAT8 might require lower levels of knockdown, such as by modulating the sgRNA efficiency by introducing mismatches in the guides (Jost *et al.*, 2020). Indeed, knockdown of KAT8 using siRNA in the high content GWAS screen did not cause an increase in cell death (Chapter 1, Fig 13), probably due to being able to achieve only a 50% knockdown in the screen. While the knockdown efficiency was not tested by qPCR in the screen, this lower level of knockdown of KAT8 (and KANSL1) using siRNA was also detected in an independent experiment (Chapter 2, Fig 24). Therefore, future CRISPRi experiments could also be performed only selecting guides that achieve a 50% reduction in KAT8 levels.

Like for the POE SHSY5Ys, CRISPRi-mediated knockdown of KANSL1 in the iNeurons led to a decrease in *PINK1* mRNA levels, PINK1 accumulation and pUb(Ser65) levels, suggesting a potential role in the regulation of mitophagy in a disease-relevant model as well. While it needs replicating, these data indicate that the CRISPRi i^{3}Neuron can be used to study the role of the NSL complex on mitophagy. Overall, the use of CRISPRi in iNeurons, provided that the right experimental conditions are optimised, is a useful tool to investigate the role of novel genes in regulating mitophagy in a physiological system.

Discussion

PD is the fastest growing neurodegenerative disease, with an increasing burden on society, but there are no disease modifying effective therapies available. The analysis of the Mendelian forms of the disease have identified several pathways that are relevant for disease pathogenesis (Singleton and Hardy, 2019), but these mutations represent only a fraction of PD patients. The field of genetics has focused on discovering the common variants that confer increased risk of developing PD, through large scale GWAS analyses. Thanks to these GWAS studies, some of the pathways highlighted by the Mendelian genetics have been identified to be also relevant for sporadic disease, as common variants in genes such as *SNCA* and *LRRK2* confer elevated risk of developing PD. However, for the majority of GWAS loci identified, the connection between risk loci and causal gene is challenging to establish, given the considerable number of variants in non-coding regions and the impossibility to statistically distinguish SNPs in strong linkage disequilibrium (Gallagher and Chen-Plotkin, 2018). Secondly, it is complex to then dissect the contribution of the causal genes and SNPs to disease pathogenesis. Addressing these challenges is critical for moving beyond genetic insights to developing new disease-modifying strategies for PD.

The enrichment of the Mendelian genes in specific pathways, protein aggregation, autophagy/lysosomal degradation and mitochondrial quality control, has led to the fundamental hypothesis of this project, that is, that sporadic risk factors for PD might also impact one of these key pathways. To determine whether PD GWAS risk genes play a role in mitochondrial quality control, and in particular PINK1-

dependent mitophagy, I developed a high content siRNA screen to functionally assess a selection of prioritised candidates. This screen measured both PINK1-dependent phosphorylation of ubiquitin and the degradation of TOM20, a mitochondrial marker. This approach successfully identified one gene, *KAT8*, whose knockdown significantly reduced pUb(Ser65) levels, demonstrating the potential of functional screening as a way of exploiting genetic data. Functional screening can be particularly important to analyse regions in high linkage disequilibrium, such as the *MAPT* locus.

While the high content screen was successful, it can be improved in several ways. This pilot screen will be followed in the lab by a screen of all ORFs in the 90 PD risk loci identified in the latest PD GWAS (Nalls *et al.*, 2019). Druggable genome or whole genome screens, including regulatory elements such as long non coding RNAs, can potentially identify other pathways that play a role in regulating mitophagy. The use of mitophagy reporters and higher resolution imaging, in parallel with pUb(Ser65) as a marker of PINK1-dependent mitophagy, would allow to identify genes that affect downstream events, as well as PINK1-independent mitophagy which leads to mitochondrial degradation without PINK1 activity. The use of strategies to activate expression, such as CRISPRa, in parallel to siRNA/CRISPRi technologies, could help identify novel, potentially tractable, targets which increase mitophagy. Screening in disease-relevant cell lines, iNeurons or neural precursors, as well as glia, will also allow to evaluate relevant pathways more quickly.

The second part of the project focussed on analysing the role of the hit from the mitophagy screen. KAT8 is a lysine acetyltransferase involved mainly in

regulation of gene expression by acetylating histones. Interestingly, another member of one of two KAT8 complexes, KANSL1 in the NSL complex, is also a candidate PD GWAS risk gene, further strengthening the association between sporadic and Mendelian PD. Knockdown of KANSL1, even more so than KAT8, affects the early stages of mitophagy, that is phosphorylation of ubiquitin and recruitment and phosphorylation of Parkin, and leads to subsequent decreased mitochondrial clearance, as measured by the mt-Keima reporter. This could be due to NSL complex-mediated regulation of PINK1 expression, as knockdown of KANSL1 decreased *PINK1* mRNA levels. It will need to be confirmed whether this epigenetic regulation is common across cell types, or whether other mechanisms are at play. In immortalised cell lines, KAT8, KANSL1 and the NSL complex might be differentially expressed among different lines, so comparisons might be necessary to determine the importance of KAT8 for the regulation of PINK1 expression. Moreover, epigenetic regulation of gene expression, including H4K16Ac, is altered in ageing and ageing-related diseases, and acetylation changes have been linked to changes in metabolisms and mitochondrial health (Benayoun, Pollina and Brunet, 2015; Peleg *et al.*, 2016). Altered H4K16 acetylation has been found in post-mortem brains of AD patients, associated in particular with the loci implicated in AD risk by GWAS studies (Nativio *et al.*, 2018) and *KAT8* itself is an AD putative risk gene (Marioni *et al.*, 2018). Recently, a study of post-mortem brains from patients with idiopathic PD found dysregulated histone acetylation, especially in PD Mendelian and GWAS risk genes, such as *SNCA* and *PRKN* (Toker *et al.*, 2021). In particular, expression of mitochondrial genes was the most altered compared to controls, confirming the relevance of impaired cross talk between nuclear and mitochondrial genes for disease pathogenesis (Fairbrother-Browne *et al.*, 2021). While this paper does not

report changes in KAT8-mediated acetylation of H4K16 or H4K5 and H4K8, they did not look at the SN, which is where the pathology is most concentrated and limited in PD patients with *PINK1* and *PRKN* mutations. All together, this underlies the importance of studying whether *PINK1* expression is regulated by KAT8 and KANSL1 in the appropriate models. Not only physiological expression levels of the proteins of interest will be key, but it might be necessary to analyse the effect in aged cultures or post-mortem brains. While complete knockout of KAT8 or KANSL1 is lethal, and KANSL1 haploinsufficiency causes a neurodevelopmental disease, PD is a disease of ageing. Minor impairments in KAT8 and KANSL1 activity, due to the GWAS variants that only confer a low increase in disease risk, could become relevant after decades, in conjunction with age-related metabolic and epigenetic changes and accumulation of dysfunctional mitochondria in the SN. In immortalised cell lines, or iPSC-derived neurons of foetal nature, the role of KAT8 and KANSL1 in mitophagy might be less detectable or compensated for by other mechanisms. It will thus be interesting to compare the epigenetic regulation of *PINK1* expression in different models of different ages.

However, whether the transcriptional role of KAT8 and KANSL1 explains the whole mitophagy phenotype remains to be confirmed. A study in 2016 showed that KAT8 and components of the NSL complex, including KANSL1, could partially localise at the mitochondria. The mitochondrial pool of KAT8 was shown to bind mtDNA and depletion of the NSL components reduced mtDNA expression and mitochondrial RNA synthesis, reduced mitochondrial membrane potential and impaired mitochondrial respiration (Chatterjee *et al.*, 2016). One possibility is that KAT8 and KANSL1 could affect mitochondrial health, and indirectly, PINK1 import,

processing and activity. Furthermore, mitochondria are hotspots of acetylation in cells (Baeza, Smallegan and Denu, 2016). While it is still unknown whether enzymatic activity is responsible for the acetylation detected on mitochondrial proteins, and indeed which KAT would be responsible for it (Narita, Weinert and Choudhary, 2019), it is possible that KAT8 could have other targets in the mitochondria than mtDNA, which could affect mitophagy. An intriguing hypothesis is that KAT8 could be involved in the acetylation of ubiquitin, which has been shown by mass spectrometry studies to be acetylated on 6 of its 7 lysines (Swatek and Komander, 2016). Acetylation of these lysine residues would affect formation of polyubiquitin chains by Parkin, but acetylation and other post translational modifications might interfere with each other in different ways than just competing for the same lysine residue. In particular, the cross talk between phosphorylation and acetylation is a key part of the regulation of several biological processes (Narita, Weinert and Choudhary, 2019). For example, acetylation promotes the mislocalisation, aggregation and hyperphosphorylation of TDP43, which is mutated in ALS (P. Wang *et al.*, 2017), and acetylation of the AD protein Tau, inhibits phosphorylation and reduces the formation of Tau aggregates (Cook *et al.*, 2014). Therefore, acetylation of ubiquitin could not only affect the formation of polyubiquitin chains, but also phosphorylation by PINK1, with downstream effects on the activation of mitophagy.

Unlike for the mitochondrial KATs, more is known about the enzymes responsible for the opposite reaction, deacetylation. Three sirtuins, SIRT3, SIRT4 and SIRT5, are NAD^+ -dependent deacetylases located at the mitochondria (van de Ven, Santos and Haigis, 2017). SIRT3, in particular, has been linked to the control of

metabolism in the mitochondria (Shimin *et al.*, 2010), is modulated by mitochondrial depolarisation (Yang *et al.*, 2016) and has been suggested to be protective for DA neurons (Shi *et al.*, 2017). Moreover, altered SIRT3 activity has been found in the brains of idiopathic PD patients (Toker *et al.*, 2021). The balance between acetylation and deacetylation events could therefore represent another aspect of the regulation of mitochondrial health, and thus quality control.

Finally, it would be interesting to investigate whether KAT8 and KANSL1 affect another aspect of PINK1 and Parkin activity in the cell, that is their role in inflammation and immunity. PINK1 and Parkin have been shown to inhibit the formation of MDVs involved in mitochondrial antigen presentation in response to treatment with heat shock or lipopolysaccharide, suggesting a role in the regulation of adaptive immunity (Matheoud *et al.*, 2016). Mice lacking PINK1 or Parkin generate a strong inflammation response after exhaustive exercise or mutations in mtDNA, mediated by the cGAS-STING pathway, which regulates the type I interferon response to the presence of double-stranded DNA in the cytoplasm (Sliter *et al.*, 2018). Neuroinflammation is a feature of PD (Poewe *et al.*, 2017), and KAT8 has been reported to be important for T-cell differentiation (Gupta *et al.*, 2013), regulation of type I interferon expression (Huai *et al.*, 2019) and promoting a pro-inflammatory state (denDekker *et al.*, 2020). KANSL1 has also been identified as a common genetic risk factor for both PD and autoimmune diseases (Witoelar *et al.*, 2017). Therefore, investigating whether KAT8 and KANSL1 affect PINK1 and Parkin-mediated immunity could open new strategies that target both mitophagy and neuroinflammation in PD.

KANSL1 is located on the 17q21 locus, known primarily for being the *MAPT* locus, of relevance for several neurodegenerative diseases, including AD and PSP. Using the high content mitophagy siRNA screen, I confirmed that out of the 32 ORFs in the locus, *KANSL1* was the only gene whose knockdown significantly reduced pUb(Ser65) levels. This is interesting, because *MAPT* has long been assumed to be the causal gene on this locus, due to genetic evidence that links this locus to increased risk of PD (Simón-Sánchez *et al.*, 2009) and some reports of tau aggregates in brains of PD patients, but functional evidence for a role of Tau in PD pathogenesis remained weak (Wray and Lewis, 2010). Recently, other groups studying the genetics of PD have proposed a role for *KANSL1* in driving PD risk at this locus (Dong *et al.*, 2018; Soto-Beasley *et al.*, 2020), short tandem repeats within KANSL1 are also associated with increased risk of PD (Bustos *et al.*, 2021) and reduced expression of *KANSL1* has been found in brains from PD and FTD patients (Ferrari *et al.*, 2017). These data do not exclude a possible role of any of the ORFs in PD, and indeed it has recently been suggested that other genes on this locus could be relevant in PD pathogenesis in astrocytes (Bowles *et al.*, 2021), but it strengthens the role of KANSL1 as a sporadic risk gene for PD by acting on mitophagy. The *MAPT* locus is a highly complex region to dissect with available methods. Functional screening of this region, potentially in different cell types, will help identify disease relevant genes. Long read sequencing will be necessary to identify hidden variation and resolve regions with duplications, inversions and repeats (Logsdon, Vollger and Eichler, 2020), which will be essential to understand how KANSL1 variation impacts PD risk and which variants to model in cell lines.

In the last part of the project, I focused on confirming the function of KAT8 and KANSL1 in a disease-relevant cell line. PINK1-dependent mitophagy has been mainly studied in immortalised cell lines, often overexpressing Parkin. These models have been useful to understand parts of the mechanism of mitophagy, and in this case high content screening, but other important aspects might be masked by the excessive levels of Parkin and/or by the different culture conditions and energy requirements than cells such as neurons. These details might have contributed to the initial controversy regarding the presence and relevance of mitophagy in neurons, with details such as the addition or not of antioxidants being cited early on as a potential reason for not detecting mitophagy (Joselin *et al.*, 2012). In this project, the direct comparison of two different maintenance media for iNeurons, in the attempt to generate more mature neurons, yielded interesting results with regards to mitophagy. iNeurons maintained in Brainphys were not able to induce mitophagy, as measured by accumulation of PINK1 and subsequent phosphorylation of mitochondrial ubiquitin. Whether this is actually due to the maturity levels of the different cultures, and whether this impacts their prevalent source of energy (oxidative phosphorylation or glycolysis), remains to be investigated. Neurons that are more active will require healthy mitochondria able to produce ATP and buffer calcium, and might be more susceptible to global mitochondrial damage. Overall, the striking difference in the activation of PINK1-dependent mitophagy between the two media types underlines the importance of understanding appropriate culture conditions, of finding physiologically relevant triggers of mitophagy to be used experimentally and well characterising the models used to study mitochondria-related pathways.

To model the effect of depletion of KAT8 and KANSL1 in neurons, I took advantage of the CRISPRi-i^{3}Neuron system developed by Tian and colleagues (Tian *et al.*, 2019). While the knockdown of PINK1 was highly efficient, the knockdown of KAT8 and KANSL1 was less successful. This was not unexpected, as both genes have been reported to be essential for cell survival, and obtaining KO cell lines using CRISPR/Cas9 has not been successful in our lab. Moreover, complete KO mice are not viable (Thomas *et al.*, 2008; Arbogast *et al.*, 2017), as well as KANSL1 KO iPSC lines (Linda *et al.*, 2021). Therefore, it is possible that the widespread cell death might have been due to excessive depletion of the proteins. This is problematic experimentally, as future research using this model will require finetuning of the knockdown, but also poses fundamental questions on how to better model how variation in these genes leads to PD. Given the lethality of complete knockouts of either protein, and that haploinsufficiency of KANSL1 causes a neurodevelopmental syndrome with no parkinsonism, it is probable that highly efficient CRISPRi-mediated knockdowns of KAT8 and KANSL1 are not likely to be a model of PD risk. The KAT8 SNPs are associated with a reduction in KAT8 protein in the brain, while some of the KANSL1 SNPs are predicted to be amino acid changes in the protein sequence (Soutar *et al.*, 2021). How this would lead to increased risk of PD is still unclear. Different levels of KAT8 or KANSL1, and different protein structures, might affect the formation of the NSL complex or their binding to DNA and other molecular partners, unbalance KAT8-regulated gene expression, or confer other preferred targets to KAT8-contaning complexes. Inefficient or lower NSL activity on a susceptible genetic background would therefore lead to reduced mitochondrial quality control, which predispose vulnerable neurons with high metabolic requirements to degeneration. Future strategies to investigate this are several. First of all, rescue experiments

introducing KANSL1 with the SNP mutations on a depleted background would help understand the impact of these changes associated with PD risk on the structure and activity of the NSL complex. This has proved challenging both because of the difficulty of knocking down KANSL1 to low levels, and the issues with overexpressing KANSL1 in SH-SY5Y cells. Other cell models, a better understanding of the structure of KANSL1 and more specific antibodies might help overcome these concerns. Other strategies could involve introducing these sequence mutations in model iPSC lines, as well as exploiting the rise in deep sequencing methods to identify patient cell lines with the different haplotypes of the 17q21 locus, which *KANSL1* is a part of. Setting up these systems would allow to answer whether KAT8 and KANSL1 do modulate mitophagy in disease-relevant lines, not only neurons but also glia. Use of the mitophagy reporters, and longitudinal high content imaging of cultures over time with physiological triggers of mitophagy, might enable detection of possibly rare events of mitochondrial degradation and whether the presence of the KAT8 and KANSL1 variants impairs these events, leading to increased cell death. Understanding of this mechanism in neurons could open novel therapeutic avenues for the modulation of mitophagy not only in familial, but also in sporadic PD, with connotations for other neurodegenerative diseases in which dysfunction of mitochondrial quality control pathways is increasingly identified (Chu, 2019).

Appendix

Plate map of the GWAS screen

Well Name	siRNA	Well Name	siRNA	Well Name	siRNA
A1	SCR	C9	KLHL7	F5	PARK2
A2	ATG14	C10	NUPL2	F6	VPS35
A3	PARK7	C11	SPPL2B	F7	CTSB
A4	INPP5F	C12	PINK1	F8	GPNMB
A5	NSF	D1	PINK1	F9	MAPT
A6	SLC41A1	D2	CCNT2	F10	PARK2
A7	ATG14	D3	GALC	F11	VPS35
A8	PARK7	D4	LRRK2	F12	PLK1
A9	INPP5F	D5	PDLIM2	G1	Non Transfected
A10	NSF	D6	STK39	G2	DDRGK1
A11	SLC41A1	D7	CCNT2	G3	HSD3B7
A12	SCR	D8	GALC	G4	NCKIPSD
B1	SCR	D9	LRRK2	G5	RAB29
B2	ATP13A2	D10	PDLIM2	G6	WDR6
B3	DNAJC13	D11	STK39	G7	DDRGK1
B4	KAT8	D12	PINK1	G8	HSD3B7
B5	NUCKS1	E1	PLK1	G9	NCKIPSD
B6	SNCA	E2	CD38	G10	RAB29
B7	ATP13A2	E3	GBA	G11	WDR6
B8	DNAJC13	E4	LSM7	G12	Non Transfected
B9	KAT8	E5	PM20D1	H1	Non Transfected
B10	NUCKS1	E6	VAMP4	H2	DGKQ
B11	SNCA	E7	CD38	H3	IDUA
B12	SCR	E8	GBA	H4	NEK1
C1	PINK1	E9	LSM7	H5	SH3GL2
C2	CAB39L	E10	PM20D1	H6	ZNF646
C3	FBXO7	E11	VAMP4	H7	DGKQ
C4	KLHL7	E12	PLK1	H8	IDUA
C5	NUPL2	F1	PLK1	H9	NEK1
C6	SPPL2B	F2	CTSB	H10	SH3GL2
C7	CAB39L	F3	GPNMB	H11	ZNF646
C8	FBXO7	F4	MAPT	H12	Non Transfected

p-values for figure 18C

Within each row, compare columns (simple effects within rows)

Number of families 8

Number of comparisons 3

Alpha 0.5

Dunnett's multiple comparisons test	Mean Diff.	95.00% CI of diff.	Significant?	Summary	Adjusted P Value
DMSO					
SCR vs. KAT8	0	-14.19 to 14.19	No	ns	>0.9999
SCR vs. KANSL1	0	-14.19 to 14.19	No	ns	>0.9999
SCR vs. PINK1	0	-14.19 to 14.19	No	ns	>0.9999
1 h					
SCR vs. KAT8	21	6.807 to 35.19	Yes	**	0.0017
SCR vs. KANSL1	30	15.81 to 44.19	Yes	****	<0.0001
SCR vs. PINK1	38	23.81 to 52.19	Yes	****	<0.0001
2 h					
SCR vs. KAT8	30	15.81 to 44.19	Yes	****	<0.0001
SCR vs. KANSL1	53	38.81 to 67.19	Yes	****	<0.0001
SCR vs. PINK1	71	56.81 to 85.19	Yes	****	<0.0001
3 h					
SCR vs. KAT8	33	18.81 to 47.19	Yes	****	<0.0001
SCR vs. KANSL1	51	36.81 to 65.19	Yes	****	<0.0001
SCR vs. PINK1	73	58.81 to 87.19	Yes	****	<0.0001
4 h					
SCR vs. KAT8	15	0.8065 to 29.19	Yes	*	0.0355
SCR vs. KANSL1	28	13.81 to 42.19	Yes	****	<0.0001
SCR vs. PINK1	49	34.81 to 63.19	Yes	****	<0.0001
5 h					
SCR vs. KAT8	9	-5.193 to 23.19	No	ns	0.307
SCR vs. KANSL1	21	6.807 to 35.19	Yes	**	0.0017
SCR vs. PINK1	39	24.81 to 53.19	Yes	****	<0.0001
6 h					
SCR vs. KAT8	14	-0.1935 to 28.19	No	ns	0.0542
SCR vs. KANSL1	24	9.807 to 38.19	Yes	***	0.0003
SCR vs. PINK1	42	27.81 to 56.19	Yes	****	<0.0001
7 h					
SCR vs. KAT8	19	4.807 to 33.19	Yes	**	0.0051
SCR vs. KANSL1	23	8.807 to 37.19	Yes	***	0.0005
SCR vs. PINK1	40	25.81 to 54.19	Yes	****	<0.0001

p-values for figure 22

Within each row, compare columns (simple effects within rows)

Number of families	5
Number of comparisons per family	3
Alpha	0.05

Dunnett's multiple comparisons test	Mean Diff.	95.00% CI of diff.	Below threshold?	Summary	Adjusted P Value
0 h					
SCR OA vs. KAT8 OA	-0.003343	-0.04335 to 0.03667	No	ns	0.9940
SCR OA vs. KANSL1 OA	-0.002681	-0.04269 to 0.03733	No	ns	0.9969
SCR OA vs. PINK1 OA	0.004262	-0.03575 to 0.04427	No	ns	0.9878
2 h					
SCR OA vs. KAT8 OA	0.04496	0.004950 to 0.08497	Yes	*	0.0243
SCR OA vs. KANSL1 OA	0.04991	0.009896 to 0.08992	Yes	*	0.0113
SCR OA vs. PINK1 OA	0.05799	0.01798 to 0.09800	Yes	**	0.0029
4 h					
SCR OA vs. KAT8 OA	0.06233	0.02232 to 0.1023	Yes	**	0.0014
SCR OA vs. KANSL1 OA	0.07349	0.03348 to 0.1135	Yes	***	0.0002
SCR OA vs. PINK1 OA	0.07958	0.03957 to 0.1196	Yes	****	<0.0001
6 h					
SCR OA vs. KAT8 OA	0.05593	0.01592 to 0.09594	Yes	**	0.0042
SCR OA vs. KANSL1 OA	0.06001	0.02000 to 0.1000	Yes	**	0.0021
SCR OA vs. PINK1 OA	0.05635	0.01634 to 0.09636	Yes	**	0.0039
8 h					
SCR OA vs. KAT8 OA	0.04123	0.001219 to 0.08124	Yes	*	0.0421
SCR OA vs. KANSL1 OA	0.03317	-0.006843 to 0.07318	No	ns	0.1231
SCR OA vs. PINK1 OA	0.02560	-0.01441 to 0.06561	No	ns	0.2876

References

Akhtar, A. and Becker, P. B. (2000) 'Activation of transcription through histone H4 acetylation by MOF, an acetyltransferase essential for dosage compensation in Drosophila', *Molecular Cell*, 5(2), pp. 367–375. doi: 10.1016/S1097-2765(00)80431-1.

Allen, G. F. G. *et al.* (2013) 'Loss of iron triggers PINK1/Parkin-independent mitophagy', *EMBO reports*. John Wiley & Sons, Ltd, 14(12), pp. 1127–1135. doi: https://doi.org/10.1038/embor.2013.168.

Arbogast, T. *et al.* (2017) 'Mouse models of 17q21.31 microdeletion and microduplication syndromes highlight the importance of Kansl1 for cognition', *PLoS Genetics*, 13(7), pp. 1–25. doi: 10.1371/journal.pgen.1006886.

Ardley, H. C. *et al.* (2003) 'Inhibition of proteasomal activity causes inclusion formation in neuronal and non-neuronal cells overexpressing Parkin.', *Molecular biology of the cell*, 14(11), pp. 4541–4556. doi: 10.1091/mbc.E03-02-0078.

Armstrong, M. J. and Okun, M. S. (2020) 'Diagnosis and Treatment of Parkinson Disease: A Review', *JAMA - Journal of the American Medical Association*, 323(6), pp. 548–560. doi: 10.1001/jama.2019.22360.

Ascherio, A. and Schwarzschild, M. A. (2016) 'The epidemiology of Parkinson's disease: risk factors and prevention', *The Lancet Neurology*. Elsevier Ltd, 15(12), pp. 1257–1272. doi: 10.1016/S1474-4422(16)30230-7.

Ashrafi, G. *et al.* (2014) 'Mitophagy of damaged mitochondria occurs locally in distal neuronal axons and requires PINK1 and Parkin', *Journal of Cell Biology*, 206(5), pp. 655–670. doi: 10.1083/jcb.201401070.

Auld, D. S. *et al.* (2004) 'Microplate Selection and Recommended Practices in High-

throughput Screening and Quantitative Biology', *Assay Guidance Manual*, (Md), pp. 1–50.

Baeza, J., Smallegan, M. J. and Denu, J. M. (2016) 'Mechanisms and Dynamics of Protein Acetylation in Mitochondria', *Trends in Biochemical Sciences*. Elsevier Ltd, 41(3), pp. 231–244. doi: 10.1016/j.tibs.2015.12.006.

Banerjee, R. *et al.* (2009) 'Mitochondrial dysfunction in the limelight of Parkinson's disease pathogenesis', *Biochimica et Biophysica Acta - Molecular Basis of Disease*. Elsevier B.V., 1792(7), pp. 651–663. doi: 10.1016/j.bbadis.2008.11.007.

Bardy, C. *et al.* (2015) 'Neuronal medium that supports basic synaptic functions and activity of human neurons in vitro', *Proceedings of the National Academy of Sciences*, 112(20), p. E2725 LP-E2734. doi: 10.1073/pnas.1504393112.

Barodia, S. K. *et al.* (2019) 'PINK1 phosphorylates ubiquitin predominantly in astrocytes', *npj Parkinson's Disease*. Springer US, 5(1). doi: 10.1038/s41531-019-0101-9.

Bartolome, F. *et al.* (2013) 'Pathogenic VCP Mutations Induce Mitochondrial Uncoupling and Reduced ATP Levels', *Neuron*, 78(1), pp. 57–64. doi: https://doi.org/10.1016/j.neuron.2013.02.028.

Bellot, G. *et al.* (2009) 'Hypoxia-Induced Autophagy Is Mediated through Hypoxia-Inducible Factor Induction of BNIP3 and BNIP3L via Their BH3 Domains', *Molecular and Cellular Biology*. American Society for Microbiology, 29(10), pp. 2570–2581. doi: 10.1128/MCB.00166-09.

Benayoun, B. A., Pollina, E. A. and Brunet, A. (2015) 'Epigenetic regulation of ageing: Linking environmental inputs to genomic stability', *Nature Reviews Molecular Cell Biology*. Nature Publishing Group, 16(10), pp. 593–610. doi: 10.1038/nrm4048.

Berenguer-Escuder, C. *et al.* (2020) 'Impaired mitochondrial-endoplasmic reticulum

interaction and mitophagy in Miro1-mutant neurons in Parkinson's disease', *Human Molecular Genetics*, 29(8), pp. 1353–1364. doi: 10.1093/hmg/ddaa066.

Billingsley, K. J. *et al.* (2019) 'Mitochondria function associated genes contribute to Parkinson's Disease risk and later age at onset', *npj Parkinson's Disease*, 5(1). doi: 10.1038/s41531-019-0080-x.

Bingol, B. *et al.* (2014) 'The mitochondrial deubiquitinase USP30 opposes parkin-mediated mitophagy', *Nature*. Nature Publishing Group, 510(7505), pp. 370–375. doi: 10.1038/nature13418.

Birmingham, A. *et al.* (2009) 'Statistical methods for analysis of high-throughput RNA interference screens', *Nature Methods*. Nature Publishing Group, 6(8), pp. 569–575. doi: 10.1038/nmeth.1351.

Blauwendraat, C., Nalls, M. A. and Singleton, A. B. (2020) 'The genetic architecture of Parkinson's disease', *The Lancet Neurology*. Elsevier Ltd, 19(2), pp. 170–178. doi: 10.1016/S1474-4422(19)30287-X.

Bolam, J. P. and Pissadaki, E. K. (2012) 'Living on the edge with too many mouths to feed: Why dopamine neurons die', *Movement Disorders*, 27(12), pp. 1478–1483. doi: 10.1002/mds.25135.

Bonello, F. *et al.* (2019) 'LRRK2 impairs PINK1/Parkin-dependent mitophagy via its kinase activity: pathologic insights into Parkinson's disease', *Human Molecular Genetics*, 28(10), pp. 1645–1660. doi: 10.1093/hmg/ddz004.

Bonifati, V. *et al.* (2003) 'Mutations in the DJ-1 Gene Associated with Autosomal Recessive Early-Onset Parkinsonism', *Science*. American Association for the Advancement of Science, 299(5604), pp. 256–259. doi: 10.1126/science.1077209.

Booth, H. D. E., Hirst, W. D. and Wade-Martins, R. (2017) 'The Role of Astrocyte Dysfunction in Parkinson's Disease Pathogenesis', *Trends in Neurosciences*.

Elsevier Ltd, 40(6), pp. 358–370. doi: 10.1016/j.tins.2017.04.001.

Bose, A. and Beal, M. F. (2016) ‘Mitochondrial dysfunction in Parkinson’s disease’, *Journal of Neurochemistry*, 139, pp. 216–231. doi: 10.1111/jnc.13731.

Bowles, K. R. *et al.* (2021) ‘17q21.31 sub-haplotypes underlying H1-associated risk for Parkinson’s disease are associated with LRRC37A/2 expression in astrocytes’, *bioRxiv*, p. 860668. doi: 10.1101/860668.

Braak, H. *et al.* (2003) ‘Staging of brain pathology related to sporadic Parkinson’s disease’, *Neurobiology of Aging*, 24(2), pp. 197–211. doi: https://doi.org/10.1016/S0197-4580(02)00065-9.

Braschi, E. *et al.* (2010) ‘Vps35 mediates vesicle transport between the mitochondria and peroxisomes’, *Current Biology*, 20(14), pp. 1310–1315. doi: 10.1016/j.cub.2010.05.066.

Van Der Brug, M. P. *et al.* (2015) ‘Parkinson’s disease: From human genetics to clinical trials’, *Science Translational Medicine*, 7(305). doi: 10.1126/scitranslmed.aaa8280.

Bruick, R. K. (2000) ‘Expression of the gene encoding the proapoptotic Nip3 protein is induced by hypoxia’, *Proceedings of the National Academy of Sciences*, 97(16), pp. 9082 LP – 9087. doi: 10.1073/pnas.97.16.9082.

Burchell, V. S. *et al.* (2013) ‘The Parkinson’s disease–linked proteins Fbxo7 and Parkin interact to mediate mitophagy’, *Nature Neuroscience*, 16(9), pp. 1257–1265. doi: 10.1038/nn.3489.

Bustos, B. I. *et al.* (2021) ‘Genome-wide contribution of common Short-Tandem Repeats to Parkinson’s Disease genetic risk’, *medRxiv*, p. 2021.07.01.21259645.

Cai, Q. *et al.* (2012) ‘Spatial parkin translocation and degradation of damaged mitochondria via mitophagy in live cortical neurons’, *Current Biology*. Elsevier Ltd,

22(6), pp. 545–552. doi: 10.1016/j.cub.2012.02.005.

Cai, Y. *et al.* (2010) 'Subunit Composition and Substrate Specificity of a MOF-containing Histone Acetyltransferase Distinct from the Male-specific Lethal (MSL) Complex', *Journal of Biological Chemistry*, 285(7), pp. 4268–4272. doi: 10.1074/jbc.C109.087981.

Carter, J. L., Halmai, J. A. N. M. and Fink, K. D. (2020) 'The iNs and Outs of Direct Reprogramming to Induced Neurons', *Frontiers in Genome Editing*, 2(September). doi: 10.3389/fgeed.2020.00007.

Chambers, S. M. *et al.* (2009) 'Highly efficient neural conversion of human ES and iPS cells by dual inhibition of SMAD signaling', *Nature Biotechnology*, 27(3), pp. 275–280. doi: 10.1038/nbt.1529.

Chan, N. C. *et al.* (2011) 'Broad activation of the ubiquitin-proteasome system by Parkin is critical for mitophagy', *Human Molecular Genetics*, 20(9), pp. 1726–1737. doi: 10.1093/hmg/ddr048.

Chang, D. *et al.* (2017) 'A meta-analysis of genome-wide association studies identifies 17 new Parkinson's disease risk loci.', *Nature genetics*. Nature Publishing Group, 49(10), pp. 1511–1516. doi: 10.1038/ng.3955.

Charvin, D. *et al.* (2018) 'Therapeutic strategies for Parkinson disease: Beyond dopaminergic drugs', *Nature Reviews Drug Discovery*. Nature Publishing Group, 17(11), pp. 804–822. doi: 10.1038/nrd.2018.136.

Chatterjee, A. *et al.* (2016) 'MOF Acetyl Transferase Regulates Transcription and Respiration in Mitochondria', *Cell*, 167(3), pp. 722-738.e23. doi: 10.1016/j.cell.2016.09.052.

Chaugule, V. K. *et al.* (2011) 'Autoregulation of Parkin activity through its ubiquitin-like domain', *The EMBO Journal*. John Wiley & Sons, Ltd, 30(14), pp. 2853–2867.

doi: https://doi.org/10.1038/emboj.2011.204.

Chen, G. *et al.* (2014) 'A Regulatory Signaling Loop Comprising the PGAM5 Phosphatase and CK2 Controls Receptor-Mediated Mitophagy', *Molecular Cell*. Elsevier, 54(3), pp. 362–377. doi: 10.1016/j.molcel.2014.02.034.

Cheng, X.-Y. *et al.* (2020) 'Human iPSCs derived astrocytes rescue rotenone-induced mitochondrial dysfunction and dopaminergic neurodegeneration in vitro by donating functional mitochondria', *Translational Neurodegeneration*, 9(1), p. 13. doi: 10.1186/s40035-020-00190-6.

Chu, C. T. (2019) 'Mechanisms of selective autophagy and mitophagy: Implications for neurodegenerative diseases', *Neurobiology of Disease*. Elsevier, 122(July 2018), pp. 23–34. doi: 10.1016/j.nbd.2018.07.015.

Clark, I. E. *et al.* (2006) 'Drosophila pink1 is required for mitochondrial function and interacts genetically with parkin', *Nature*, 441(7097), pp. 1162–1166. doi: 10.1038/nature04779.

Connolly, N. M. C. *et al.* (2018) *Guidelines on experimental methods to assess mitochondrial dysfunction in cellular models of neurodegenerative diseases*, *Cell Death and Differentiation*. Springer US. doi: 10.1038/s41418-017-0020-4.

Cook, C. *et al.* (2014) 'Acetylation of the KXGS motifs in tau is a critical determinant in modulation of tau aggregation and clearance', *Human Molecular Genetics*, 23(1), pp. 104–116. doi: 10.1093/hmg/ddt402.

Cornelissen, T. *et al.* (2018) 'Deficiency of parkin and PINK1 impairs age-dependent mitophagy in Drosophila'. doi: 10.7554/eLife.35878.001.

Creed, R. B. and Goldberg, M. S. (2018) 'New Developments in Genetic rat models of Parkinson's Disease', *Movement Disorders*, 33(5), pp. 717–729. doi: 10.1002/mds.27296.

Darios, F. *et al.* (2003) ‘Parkin prevents mitochondrial swelling and cytochrome c release in mitochondria-dependent cell death’, *Human Molecular Genetics*, 12(5), pp. 517–526. doi: 10.1093/hmg/ddg044.

Davis, C. H. O. *et al.* (2014) ‘Transcellular degradation of axonal mitochondria’, *Proceedings of the National Academy of Sciences of the United States of America*, 111(26), pp. 9633–9638. doi: 10.1073/pnas.1404651111.

Dawson, T. M., Ko, H. S. and Dawson, V. L. (2010) ‘Genetic animal models of Parkinson’s disease.’, *Neuron*. Elsevier Inc., 66(5), pp. 646–61. doi: 10.1016/j.neuron.2010.04.034.

Deas, E. *et al.* (2011) ‘PINK1 cleavage at position A103 by the mitochondrial protease PARL’, *Human Molecular Genetics*, 20(5), pp. 867–879. doi: 10.1093/hmg/ddq526.

denDekker, A. D. *et al.* (2020) ‘TNF-α regulates diabetic macrophage function through the histone acetyltransferase MOF’, *JCI Insight*. The American Society for Clinical Investigation, 5(5). doi: 10.1172/jci.insight.132306.

Dias, J. *et al.* (2014) ‘Structural analysis of the KANSL1/WDR5/ KANSL2 complex reveals that WDR5 is required for efficient assembly and chromatin targeting of the NSL complex’, *Genes and Development*, 28(9), pp. 929–942. doi: 10.1101/gad.240200.114.

Dickson, D. W. *et al.* (2009) ‘Neuropathological assessment of Parkinson’s disease: refining the diagnostic criteria’, *The Lancet Neurology*. Elsevier Ltd, 8(12), pp. 1150–1157. doi: 10.1016/S1474-4422(09)70238-8.

Dong, X. *et al.* (2018) ‘Enhancers active in dopamine neurons are a primary link between genetic variation and neuropsychiatric disease’, *Nature Neuroscience*, 21(10), pp. 1482–1492. doi: 10.1038/s41593-018-0223-0.

Dorsey, E. R. *et al.* (2018) ‘Global, regional, and national burden of Parkinson’s disease, 1990–2016: a systematic analysis for the Global Burden of Disease Study 2016’, *The Lancet Neurology*. Elsevier, 17(11), pp. 939–953. doi: 10.1016/S1474-4422(18)30295-3.

Dorval, T. *et al.* (2018) ‘Filling the drug discovery gap: is high-content screening the missing link?’, *Current Opinion in Pharmacology*. Elsevier Ltd, 42, pp. 40–45. doi: 10.1016/j.coph.2018.07.002.

Du, F. *et al.* (2017) ‘PINK1 signalling rescues amyloid pathology and mitochondrial dysfunction in Alzheimer’s disease’, *Brain*, 140(12), pp. 3233–3251. doi: 10.1093/brain/awx258.

Edwards, S. L. *et al.* (2013) ‘Beyond GWASs: Illuminating the dark road from association to function’, *American Journal of Human Genetics*. The American Society of Human Genetics, 93(5), pp. 779–797. doi: 10.1016/j.ajhg.2013.10.012.

Evans, C. S. and Holzbaur, E. L. F. (2020) ‘Degradation of engulfed mitochondria is rate-limiting in optineurin-mediated mitophagy in neurons’, *eLife*, 9, pp. 1–30. doi: 10.7554/eLife.50260.

Fairbrother-Browne, A. *et al.* (2021) ‘Mitochondrial-nuclear cross-talk in the human brain is modulated by cell type and perturbed in neurodegenerative disease’, *Communications Biology*. CRC Press, 4(1), p. 1262. doi: 10.1038/s42003-021-02792-w.

Feigin, V. L. *et al.* (2019) ‘Global, regional, and national burden of neurological disorders, 1990–2016: a systematic analysis for the Global Burden of Disease Study 2016’, *The Lancet Neurology*. Elsevier, 18(5), pp. 459–480. doi: 10.1016/S1474-4422(18)30499-X.

Fernandopulle, M. S. *et al.* (2018) ‘Transcription Factor–Mediated Differentiation of

Human iPSCs into Neurons', *Current Protocols in Cell Biology*, 79(1), p. e51. doi: https://doi.org/10.1002/cpcb.51.

Ferrari, R. *et al.* (2017) 'Genetic architecture of sporadic frontotemporal dementia and overlap with Alzheimer's and Parkinson's diseases', *Journal of Neurology, Neurosurgery and Psychiatry*, 88(2), pp. 152–164. doi: 10.1136/jnnp-2016-314411.

Ferrari, R. *et al.* (2018) 'Stratification of candidate genes for Parkinson's disease using weighted protein-protein interaction network analysis', *BMC Genomics*, 19(1), p. 452. doi: 10.1186/s12864-018-4804-9.

Fiesel, F. C. *et al.* (2015) '(Patho-)physiological relevance of <scp>PINK</scp> 1-dependent ubiquitin phosphorylation', *EMBO reports*, 16(9), pp. 1114–1130. doi: 10.15252/embr.201540514.

Fonzo, A. Di *et al.* (2009) 'FBXO7 mutations cause autosomal recessive, early-onset parkinsonian-pyramidal syndrome', *Neurology*, 72(3), pp. 240 LP – 245. doi: 10.1212/01.wnl.0000338144.10967.2b.

Füllgrabe, J. *et al.* (2013) 'The histone H4 lysine 16 acetyltransferase hMOF regulates the outcome of autophagy', *Nature*, 500(7463), pp. 468–471. doi: 10.1038/nature12313.

Gallagher, M. D. and Chen-Plotkin, A. S. (2018) 'The Post-GWAS Era: From Association to Function', *American Journal of Human Genetics*. American Society of Human Genetics, 102(5), pp. 717–730. doi: 10.1016/j.ajhg.2018.04.002.

Gandhi, S. *et al.* (2009) 'PINK1-Associated Parkinson's Disease Is Caused by Neuronal Vulnerability to Calcium-Induced Cell Death', *Molecular Cell*, 33(5), pp. 627–638. doi: 10.1016/j.molcel.2009.02.013.

Gao, F. *et al.* (2015) 'The mitochondrial protein BNIP3L is the substrate of PARK2 and mediates mitophagy in PINK1/PARK2 pathway', *Human Molecular Genetics*,

24(9), pp. 2528–2538. doi: 10.1093/hmg/ddv017.

Geisler, S. *et al.* (2010) 'PINK1/Parkin-mediated mitophagy is dependent on VDAC1 and p62/SQSTM1', *Nature Cell Biology*. doi: 10.1038/ncb2012.

Gilbert, L. A. *et al.* (2013) 'XCRISPR-mediated modular RNA-guided regulation of transcription in eukaryotes', *Cell*. Elsevier Inc., 154(2), p. 442. doi: 10.1016/j.cell.2013.06.044.

Gilbert, L. A. *et al.* (2014) 'Genome-Scale CRISPR-Mediated Control of Gene Repression and Activation', *Cell*. Elsevier Inc., 159(3), pp. 647–661. doi: 10.1016/j.cell.2014.09.029.

Giorgi, C., Marchi, S. and Pinton, P. (2018) 'The machineries, regulation and cellular functions of mitochondrial calcium', *Nature Reviews Molecular Cell Biology*. Springer US, 19(11), pp. 713–730. doi: 10.1038/s41580-018-0052-8.

Gladkova, C. *et al.* (2018) 'Mechanism of parkin activation by PINK1', *Nature*, 559(7714), pp. 410–414. doi: 10.1038/s41586-018-0224-x.

Goedert, M. *et al.* (2013) '100 years of Lewy pathology', *Nature Reviews Neurology*, 9(1), pp. 13–24. doi: 10.1038/nrneurol.2012.242.

González-Rodríguez, P. *et al.* (2021) 'Disruption of mitochondrial complex I induces progressive parkinsonism', *Nature*, (December 2020). doi: 10.1038/s41586-021-04059-0.

Greene, A. W. *et al.* (2012) 'Mitochondrial processing peptidase regulates PINK1 processing, import and Parkin recruitment', *EMBO Reports*. Nature Publishing Group, 13(4), pp. 378–385. doi: 10.1038/embor.2012.14.

Greene, J. C. *et al.* (2003) 'Mitochondrial pathology and apoptotic muscle degeneration in Drosophila parkin mutants', *Proceedings of the National Academy of Sciences*, 100(7), pp. 4078 LP – 4083. doi:

10.1073/pnas.0737556100.

Gupta, A. *et al.* (2005) 'Involvement of Human MOF in ATM Function', *Molecular and Cellular Biology*, 25(12), pp. 5292–5305. doi: 10.1128/mcb.25.12.5292-5305.2005.

Gupta, A. *et al.* (2013) 'T-cell-specific deletion of Mof blocks their differentiation and results in genomic instability in mice', *Mutagenesis*, 28(3), pp. 263–270. doi: 10.1093/mutage/ges080.

Hale, C. M. *et al.* (2016) 'Identification of modulators of autophagic flux in an image-based high content siRNA screen', *Autophagy*. Taylor & Francis, 12(4), pp. 713–726. doi: 10.1080/15548627.2016.1147669.

Hall, C. N. *et al.* (2012) 'Oxidative phosphorylation, not glycolysis, powers presynaptic and postsynaptic mechanisms underlying brain information processing', *Journal of Neuroscience*, 32(26), pp. 8940–8951. doi: 10.1523/JNEUROSCI.0026-12.2012.

Hamacher-Brady, A. *et al.* (2007) 'Response to myocardial ischemia/reperfusion injury involves Bnip3 and autophagy', *Cell Death & Differentiation*, 14(1), pp. 146–157. doi: 10.1038/sj.cdd.4401936.

Harding, O. *et al.* (2021) 'ALS- and FTD-associated missense mutations in TBK1 differentially disrupt mitophagy', *Proceedings of the National Academy of Sciences*, 118(24), p. e2025053118. doi: 10.1073/pnas.2025053118.

Harper, J. W., Ordureau, A. and Heo, J.-M. (2018) 'Building and decoding ubiquitin chains for mitophagy', *Nature Reviews Molecular Cell Biology*. Nature Publishing Group, 19(2), pp. 93–108. doi: 10.1038/nrm.2017.129.

Hasson, S. A. *et al.* (2013) 'High-content genome-wide RNAi screens identify regulators of parkin upstream of mitophagy', *Nature*. Nature Publishing Group, 504(7479), pp. 291–295. doi: 10.1038/nature12748.

Heo, J.-M. *et al.* (2015) 'The PINK1-PARKIN Mitochondrial Ubiquitylation Pathway Drives a Program of OPTN/NDP52 Recruitment and TBK1 Activation to Promote Mitophagy.', *Molecular cell*, 60(1), pp. 7–20. doi: 10.1016/j.molcel.2015.08.016.

Hernandez, D. G., Reed, X. and Singleton, A. B. (2016) 'Genetics in Parkinson disease: Mendelian versus non-Mendelian inheritance', *Journal of Neurochemistry*, 139, pp. 59–74. doi: 10.1111/jnc.13593.

Hilfiker, A. *et al.* (1997) 'mof, a putative acetyl transferase gene related to the Tip60 and MOZ human genes and to the SAS genes of yeast, is required for dosage compensation in Drosophila', *EMBO Journal*, 16(8), pp. 2054–2060. doi: 10.1093/emboj/16.8.2054.

Horlbeck, M. A. *et al.* (2016) 'Compact and highly active next-generation libraries for CRISPR-mediated gene repression and activation', *eLife*, 5(September2016), pp. 1–20. doi: 10.7554/eLife.19760.

Hoshino, A. *et al.* (2019) 'The ADP/ATP translocase drives mitophagy independent of nucleotide exchange', *Nature*. Springer US, 575(7782), pp. 375–379. doi: 10.1038/s41586-019-1667-4.

Hou, X. *et al.* (2018) 'Age- and disease-dependent increase of the mitophagy marker phospho-ubiquitin in normal aging and Lewy body disease', *Autophagy*. Taylor & Francis, 14(8), pp. 1404–1418. doi: 10.1080/15548627.2018.1461294.

Hsieh, C. H. *et al.* (2016) 'Functional Impairment in Miro Degradation and Mitophagy Is a Shared Feature in Familial and Sporadic Parkinson's Disease', *Cell Stem Cell*, 19(6), pp. 709–724. doi: 10.1016/j.stem.2016.08.002.

Huai, W. *et al.* (2019) 'KAT8 selectively inhibits antiviral immunity by acetylating IRF3', *Journal of Experimental Medicine*, 216(4), pp. 772–785. doi: 10.1084/jem.20181773.

Irrcher, I. *et al.* (2010) ‘Loss of the Parkinson’s disease-linked gene DJ-1 perturbs mitochondrial dynamics’, *Human Molecular Genetics*, 19(19), pp. 3734–3746. doi: 10.1093/hmg/ddq288.

Ivatt, R. M. *et al.* (2014) ‘Genome-wide RNAi screen identifies the Parkinson disease GWAS risk locus SREBF1 as a regulator of mitophagy’, *Proceedings of the National Academy of Sciences of the United States of America*, 111(23), pp. 8494–8499. doi: 10.1073/pnas.1321207111.

Jansen, I. E. *et al.* (2019) ‘Genome-wide meta-analysis identifies new loci and functional pathways influencing Alzheimer’s disease risk’, *Nature Genetics*. Springer US, 51(3), pp. 404–413. doi: 10.1038/s41588-018-0311-9.

Jin, S. M. *et al.* (2010) ‘Mitochondrial membrane potential regulates PINK1 import and proteolytic destabilization by PARL’, *Journal of Cell Biology*, 191(5), pp. 933–942. doi: 10.1083/jcb.201008084.

Jin, S. M. and Youle, R. J. (2013) ‘The accumulation of misfolded proteins in the mitochondrial matrix is sensed by PINK1 to induce PARK2/Parkin-mediated mitophagy of polarized mitochondria’, *Autophagy*, 9(11), pp. 1750–1757. doi: 10.4161/auto.26122.

Joselin, A. P. *et al.* (2012) ‘ROS-dependent regulation of parkin and DJ-1 localization during oxidative stress in neurons’, *Human Molecular Genetics*, 21(22), pp. 4888–4903. doi: 10.1093/hmg/dds325.

Jost, M. *et al.* (2020) ‘Titrating gene expression using libraries of systematically attenuated CRISPR guide RNAs’, *Nature Biotechnology*. Springer US, 38(3), pp. 355–364. doi: 10.1038/s41587-019-0387-5.

Jun, G. *et al.* (2016) ‘A novel Alzheimer disease locus located near the gene encoding tau protein’, *Molecular Psychiatry*, 21(1), pp. 108–117. doi:

10.1038/mp.2015.23.

Kalia, L. V and Lang, A. E. (2015) ‘Parkinson’s disease’, *The Lancet*. Elsevier Ltd, 386(9996), pp. 896–912. doi: 10.1016/S0140-6736(14)61393-3.

Kane, L. A. *et al.* (2014) ‘PINK1 phosphorylates ubiquitin to activate Parkin E3 ubiquitin ligase activity’, *Journal of Cell Biology*, 205(2), pp. 143–153. doi: 10.1083/jcb.201402104.

Kasten, M. *et al.* (2018) ‘Genotype-Phenotype Relations for the Parkinson’s Disease Genes Parkin, PINK1, DJ1: MDSGene Systematic Review’, *Movement Disorders*, 33(5), pp. 730–741. doi: 10.1002/mds.27352.

Katayama, H. *et al.* (2011) ‘A sensitive and quantitative technique for detecting autophagic events based on lysosomal delivery’, *Chemistry and Biology*. Elsevier Ltd, 18(8), pp. 1042–1052. doi: 10.1016/j.chembiol.2011.05.013.

Katayama, H. *et al.* (2020) ‘Visualizing and Modulating Mitophagy for Therapeutic Studies of Neurodegeneration’, *Cell*. Elsevier Inc., 0(0), pp. 1–12. doi: 10.1016/j.cell.2020.04.025.

Kazlauskaite, A. *et al.* (2014) ‘Parkin is activated by PINK1-dependent phosphorylation of ubiquitin at Ser65’, *Biochemical Journal*, 460(1), pp. 127–141. doi: 10.1042/BJ20140334.

Kazlauskaite, A. *et al.* (2015) ‘Binding to serine 65-phosphorylated ubiquitin primes Parkin for optimal PINK1-dependent phosphorylation and activation’, *EMBO reports*. John Wiley & Sons, Ltd, 16(8), pp. 939–954. doi: https://doi.org/10.15252/embr.201540352.

Khalil, B. *et al.* (2015) ‘PINK1-induced mitophagy promotes neuroprotection in Huntington’s disease’, *Cell Death and Disease*, 6(1), pp. 1–12. doi: 10.1038/cddis.2014.581.

Kia, D. A. *et al.* (2019) 'Integration of eQTL and Parkinson's disease GWAS data implicates 11 disease genes', *bioRxiv*, p. 627216. doi: 10.1101/627216.

Kim, N. C. *et al.* (2013) 'VCP Is Essential for Mitochondrial Quality Control by PINK1/Parkin and this Function Is Impaired by VCP Mutations', *Neuron*. Elsevier Inc., 78(1), pp. 65–80. doi: 10.1016/j.neuron.2013.02.029.

Kim, Y. Y. *et al.* (2019) 'Assessment of mitophagy in mt-Keima Drosophila revealed an essential role of the PINK1-Parkin pathway in mitophagy induction in vivo', *FASEB Journal*. John Wiley and Sons Inc., 33(9), pp. 9742–9751. doi: 10.1096/fj.201900073R.

Kitada, T. *et al.* (1998) 'Mutations in the parkin gene cause autosomal recessive juvenile parkinsonism', *Nature*, 392(6676), pp. 605–608. doi: 10.1038/33416.

Kleele, T. *et al.* (2021) 'Distinct fission signatures predict mitochondrial degradation or biogenesis', *Nature*. Springer US, 593(7859), pp. 435–439. doi: 10.1038/s41586-021-03510-6.

Klionsky, D. J. *et al.* (2021) 'Guidelines for the use and interpretation of assays for monitoring autophagy (4th edition)1', *Autophagy*. Taylor & Francis, 17(1), pp. 1–382. doi: 10.1080/15548627.2020.1797280.

Koentjoro, B., Park, J. S. and Sue, C. M. (2017) 'Nix restores mitophagy and mitochondrial function to protect against PINK1/Parkin-related Parkinson's disease', *Scientific Reports*. Nature Publishing Group, 7(September 2016), pp. 1–11. doi: 10.1038/srep44373.

Kondapalli, C. *et al.* (2012) 'PINK1 is activated by mitochondrial membrane potential depolarization and stimulates Parkin E3 ligase activity by phosphorylating Serine 65', *Open Biology*, 2(MAY). doi: 10.1098/rsob.120080.

Koolen, D. A. *et al.* (2012) 'Mutations in the chromatin modifier gene KANSL1 cause

the 17q21.31 microdeletion syndrome', *Nature Genetics*. Nature Publishing Group, 44(6), pp. 639–641. doi: 10.1038/ng.2262.

Kordower, J. H. *et al.* (2013) 'Disease duration and the integrity of the nigrostriatal system in Parkinson's disease', *Brain*, 136(8), pp. 2419–2431. doi: 10.1093/brain/awt192.

Korecka, J. A. *et al.* (2019) 'Mitochondrial clearance and maturation of autophagosomes are compromised in LRRK2 G2019S familial Parkinson's disease patient fibroblasts', *Human Molecular Genetics*, 28(19), pp. 3232–3243. doi: 10.1093/hmg/ddz126.

Koyano, F. *et al.* (2014) 'Ubiquitin is phosphorylated by PINK1 to activate parkin', *Nature*. doi: 10.1038/nature13392.

Koyano, F. *et al.* (2019) 'Parkin recruitment to impaired mitochondria for nonselective ubiquitylation is facilitated by MITOL', *Journal of Biological Chemistry*. Â© THE AUTHORS. Currently published by Elsevier Inc; originally published by American Society for Biochemistry and Molecular Biology., 294(26), pp. 10300–10314. doi: 10.1074/jbc.RA118.006302.

Krebiehl, G. *et al.* (2010) 'Reduced Basal Autophagy and Impaired Mitochondrial Dynamics Due to Loss of Parkinson's Disease-Associated Protein DJ-1', *PLOS ONE*. Public Library of Science, 5(2), p. e9367.

Kubo, S. *et al.* (2001) 'Parkin is associated with cellular vesicles', *Journal of Neurochemistry*. John Wiley & Sons, Ltd, 78(1), pp. 42–54. doi: https://doi.org/10.1046/j.1471-4159.2001.00364.x.

Kühlbrandt, W. (2015) 'Structure and function of mitochondrial membrane protein complexes', *BMC Biology*, 13(1), p. 89. doi: 10.1186/s12915-015-0201-x.

Kumar, A. *et al.* (2015) 'Disruption of the autoinhibited state primes the E3 ligase

parkin for activation and catalysis', *The EMBO Journal*. John Wiley & Sons, Ltd, 34(20), pp. 2506–2521. doi: https://doi.org/10.15252/embj.201592337.

Kumar, A. *et al.* (2017) 'Structure of PINK1 and mechanisms of Parkinson's disease-associated mutations', *eLife*. Edited by T. Hunter. eLife Sciences Publications, Ltd, 6, p. e29985. doi: 10.7554/eLife.29985.

Kuroda, Y. *et al.* (2006) 'Parkin enhances mitochondrial biogenesis in proliferating cells', *Human Molecular Genetics*, 15(6), pp. 883–895. doi: 10.1093/hmg/ddl006.

van Laar, V. S. *et al.* (2011) 'Bioenergetics of neurons inhibit the translocation response of Parkin following rapid mitochondrial depolarization', *Human Molecular Genetics*, 20(5), pp. 927–940. doi: 10.1093/hmg/ddq531.

Lai, Y.-C. Y. *et al.* (2015) 'Phosphoproteomic screening identifies Rab GTP ases as novel downstream targets of PINK 1', *The EMBO Journal*, 34(22), pp. 2840–2861. doi: 10.15252/embj.201591593.

Langston, J. *et al.* (1983) 'Chronic Parkinsonism in humans due to a product of meperidine-analog synthesis', *Science*, 219(4587), pp. 979–980. doi: 10.1126/science.6823561.

Lazarou, M. *et al.* (2015) 'The ubiquitin kinase PINK1 recruits autophagy receptors to induce mitophagy', *Nature*, 524(7565), pp. 309–314. doi: 10.1038/nature14893.

Lazo, O. M. and Schiavo, G. (2021) 'Rab10 regulates the sorting of internalised TrkB to retrograde axonal transport', *bioRxiv*, p. 2021.04.07.438771. doi: 10.1101/2021.04.07.438771.

Lee, B. E. *et al.* (2021) ' O- GlcNAcylation regulates dopamine neuron function, survival and degeneration in Parkinson disease ', *Brain*, 143(12), pp. 3699–3716. doi: 10.1093/brain/awaa320.

Lee, J. J. *et al.* (2018) 'Basal mitophagy is widespread in Drosophila but minimally

affected by loss of Pink1 or parkin', pp. 1–13. doi: 10.1083/jcb.201801044.

Lee, S., Zhang, C. and Liu, X. (2015) 'Role of glucose metabolism and ATP in maintaining PINK1 levels during Parkin-mediated mitochondrial damage responses', *Journal of Biological Chemistry*. © 2015 ASBMB. Currently published by Elsevier Inc; originally published by American Society for Biochemistry and Molecular Biology., 290(2), pp. 904–917. doi: 10.1074/jbc.M114.606798.

Lefebvre, V. *et al.* (2013) 'Genome-wide RNAi screen identifies ATPase inhibitory factor 1 (ATPIF1) as essential for PARK2 recruitment and mitophagy', *Autophagy*, 9(11), pp. 1770–1779. doi: 10.4161/auto.25413.

Lesage, S. *et al.* (2016) 'Loss of VPS13C Function in Autosomal-Recessive Parkinsonism Causes Mitochondrial Dysfunction and Increases PINK1/Parkin-Dependent Mitophagy', *American Journal of Human Genetics*, 98(3), pp. 500–513. doi: 10.1016/j.ajhg.2016.01.014.

Levine, P. M. *et al.* (2019) 'α-Synuclein O-GlcNAcylation alters aggregation and toxicity, revealing certain residues as potential inhibitors of Parkinson's disease', *Proceedings of the National Academy of Sciences of the United States of America*, 116(5), pp. 1511–1519. doi: 10.1073/pnas.1808845116.

Li, H. *et al.* (2021) 'Longitudinal tracking of neuronal mitochondria delineates PINK1/Parkin-dependent mechanisms of mitochondrial recycling and degradation', *Science Advances*, 7(32), p. eabf6580. doi: 10.1126/sciadv.abf6580.

Li, W. *et al.* (2008) 'Genome-Wide and Functional Annotation of Human E3 Ubiquitin Ligases Identifies MULAN, a Mitochondrial E3 that Regulates the Organelle's Dynamics and Signaling', *PLOS ONE*. Public Library of Science, 3(1), p. e1487.

Lin, H. C. *et al.* (2020) 'Ngn2 induces diverse neuronal lineages from human pluripotency', *bioRxiv*, pp. 1–13. doi: 10.1101/2020.11.19.389445.

Linda, K. *et al.* (2020) 'KANSL1 Deficiency Causes Neuronal Dysfunction by Oxidative Stress-Induced Autophagy', *bioRxiv*.

Linda, K. *et al.* (2021) 'Imbalanced autophagy causes synaptic deficits in a human model for neurodevelopmental disorders', *Autophagy*. Taylor & Francis, 00(00), pp. 1–20. doi: 10.1080/15548627.2021.1936777.

Liu, L. *et al.* (2012) 'Mitochondrial outer-membrane protein FUNDC1 mediates hypoxia-induced mitophagy in mammalian cells', *Nature Cell Biology*, 14(2), pp. 177–185. doi: 10.1038/ncb2422.

Liu, X. and Erikson, R. L. (2003) 'Polo-like kinase (Plk)1 depletion induces apoptosis in cancer cells', *Proceedings of the National Academy of Sciences of the United States of America*, 100(10), pp. 5789–5794. doi: 10.1073/pnas.1031523100.

Liu, Y. *et al.* (2021) 'Mt-Keima detects PINK1-PRKN mitophagy in vivo with greater sensitivity than mito-QC', *Autophagy*. Taylor & Francis, 00(00), pp. 1–10. doi: 10.1080/15548627.2021.1896924.

Logsdon, G. A., Vollger, M. R. and Eichler, E. E. (2020) 'Long-read human genome sequencing and its applications', *Nature Reviews Genetics*, 21(10), pp. 597–614. doi: 10.1038/s41576-020-0236-x.

López-Doménech, G. *et al.* (2021) 'Loss of neuronal Miro1 disrupts mitophagy and induces hyperactivation of the integrated stress response', *The EMBO Journal*, 40(14), pp. 1–20. doi: 10.15252/embj.2018100715.

Ludtmann, M. H. R. *et al.* (2018) 'α-synuclein oligomers interact with ATP synthase and open the permeability transition pore in Parkinson's disease', *Nature Communications*. Springer US, 9(1). doi: 10.1038/s41467-018-04422-2.

Malik, B. R., Godena, V. K. and Whitworth, A. J. (2015) 'VPS35 pathogenic mutations confer no dominant toxicity but partial loss of function in Drosophila and

genetically interact with parkin', *Human Molecular Genetics*, 24(21), pp. 6106–6117. doi: 10.1093/hmg/ddv322.

Marioni, R. E. *et al.* (2018) 'GWAS on family history of Alzheimer's disease', *Translational Psychiatry*. Springer US, 8(1), pp. 0–6. doi: 10.1038/s41398-018-0150-6.

Martín-Maestro, P. *et al.* (2017) 'Mitophagy failure in fibroblasts and iPSC-derived neurons of alzheimer's disease-associated presenilin 1 mutation', *Frontiers in Molecular Neuroscience*, 10(September), pp. 1–15. doi: 10.3389/fnmol.2017.00291.

Matheoud, D. *et al.* (2016) 'Parkinson's Disease-Related Proteins PINK1 and Parkin Repress Mitochondrial Antigen Presentation.', *Cell*, 166(2), pp. 314–327. doi: 10.1016/j.cell.2016.05.039.

Matsuda, N. *et al.* (2010) 'PINK1 stabilized by mitochondrial depolarization recruits Parkin to damaged mitochondria and activates latent Parkin for mitophagy', *Journal of Cell Biology*, 189(2), pp. 211–221. doi: 10.1083/jcb.200910140.

Matsuda, W. *et al.* (2009) 'Single Nigrostriatal Dopaminergic Neurons Form Widely Spread and Highly Dense Axonal Arborizations in the Neostriatum', *The Journal of Neuroscience*, 29(2), pp. 444 LP – 453. doi: 10.1523/JNEUROSCI.4029-08.2009.

McCoy, M. K. *et al.* (2014) 'Hexokinase activity is required for recruitment of parkin to depolarized mitochondria', *Human Molecular Genetics*, 23(1), pp. 145–156. doi: 10.1093/hmg/ddt407.

McLelland, G. L. *et al.* (2014) 'Parkin and PINK1 function in a vesicular trafficking pathway regulating mitochondrial quality control', *EMBO Journal*. doi: 10.1002/embj.201385902.

McWilliams, T. G. *et al.* (2016) 'mito-QC illuminates mitophagy and mitochondrial architecture in vivo', *Journal of Cell Biology*, 214(3), pp. 333–345. doi:

10.1083/jcb.201603039.

McWilliams, T. G. *et al.* (2018) ‘Basal Mitophagy Occurs Independently of PINK1 in Mouse Tissues of High Metabolic Demand’, *Cell Metabolism*, pp. 1–11. doi: 10.1016/j.cmet.2017.12.008.

McWilliams, T. G. and Muqit, M. M. (2017) ‘PINK1 and Parkin: emerging themes in mitochondrial homeostasis’, *Current Opinion in Cell Biology*. Elsevier Ltd, 45, pp. 83–91. doi: 10.1016/j.ceb.2017.03.013.

Meissner, C. *et al.* (2011) ‘The mitochondrial intramembrane protease PARL cleaves human Pink1 to regulate Pink1 trafficking’, *Journal of Neurochemistry*, 117(5), pp. 856–867. doi: 10.1111/j.1471-4159.2011.07253.x.

Mertens, J. *et al.* (2015) ‘Directly Reprogrammed Human Neurons Retain Aging-Associated Transcriptomic Signatures and Reveal Age-Related Nucleocytoplasmic Defects’, *Cell Stem Cell*, 17(6), pp. 705–718. doi: 10.1016/j.stem.2015.09.001.

Michel, M. A. *et al.* (2017) ‘Ubiquitin Linkage-Specific Affimers Reveal Insights into K6-Linked Ubiquitin Signaling’, *Molecular Cell*. Elsevier, 68(1), pp. 233-246.e5. doi: 10.1016/j.molcel.2017.08.020.

Mohr, S. E. *et al.* (2014) ‘RNAi screening comes of age: Improved techniques and complementary approaches’, *Nature Reviews Molecular Cell Biology*. Nature Publishing Group, 15(9), pp. 591–600. doi: 10.1038/nrm3860.

Moore, A. S. and Holzbaur, E. L. F. (2016) ‘Dynamic recruitment and activation of ALS-associated TBK1 with its target optineurin are required for efficient mitophagy’, *Proceedings of the National Academy of Sciences of the United States of America*, 113(24), pp. E3349–E3358. doi: 10.1073/pnas.1523810113.

Morais, V. A. *et al.* (2009) ‘Parkinson’s disease mutations in PINK1 result in decreased Complex I activity and deficient synaptic function’, *EMBO Molecular*

Medicine, 1(2), pp. 99–111. doi: 10.1002/emmm.200900006.

Morales, I. *et al.* (2020) 'Neuroglial transmitophagy and Parkinson's disease', *Glia*, (February), pp. 1–23. doi: 10.1002/glia.23839.

Mot, A. I. *et al.* (2016) 'Circumventing the Crabtree Effect: A method to induce lactate consumption and increase oxidative phosphorylation in cell culture', *International Journal of Biochemistry and Cell Biology*. Elsevier Ltd, 79, pp. 128–138. doi: 10.1016/j.biocel.2016.08.029.

Murakami, K. *et al.* (2021) 'OGT Regulates Hematopoietic Stem Cell Maintenance via PINK1-Dependent Mitophagy', *Cell Reports*. ElsevierCompany., 34(1), p. 108579. doi: 10.1016/j.celrep.2020.108579.

Murphy, M. P. and Hartley, R. C. (2018) 'Mitochondria as a therapeutic target for common pathologies', *Nature Reviews Drug Discovery*. Nature Publishing Group, 17(12), pp. 865–886. doi: 10.1038/nrd.2018.174.

Nalls, M. A. *et al.* (2014) 'Large-scale meta-analysis of genome-wide association data identifies six new risk loci for Parkinson's disease', *Nature Genetics*. Nature Publishing Group, 46(9), pp. 989–993. doi: 10.1038/ng.3043.

Nalls, M. A. *et al.* (2019) 'Identification of novel risk loci, causal insights, and heritable risk for Parkinson's disease: a meta-analysis of genome-wide association studies', *The Lancet Neurology*, 18(12), pp. 1091–1102. doi: 10.1016/S1474-4422(19)30320-5.

Narendra, D. *et al.* (2008) 'Parkin is recruited selectively to impaired mitochondria and promotes their autophagy', *Journal of Cell Biology*, 183(5), pp. 795–803. doi: 10.1083/jcb.200809125.

Narendra, D. P., Kane, L. A., *et al.* (2010) 'p62/SQSTM1 is required for Parkin-induced mitochondrial clustering but not mitophagy; VDAC1 is dispensable for both',

Autophagy, 6(8), pp. 1090–1106. doi: 10.4161/auto.6.8.13426.

Narendra, D. P., Jin, S. M., *et al.* (2010) 'PINK1 Is Selectively Stabilized on Impaired Mitochondria to Activate Parkin', *PLoS Biology*. Edited by D. R. Green, 8(1), p. e1000298. doi: 10.1371/journal.pbio.1000298.

Narita, T., Weinert, B. T. and Choudhary, C. (2019) 'Functions and mechanisms of non-histone protein acetylation', *Nature Reviews Molecular Cell Biology*. Springer US, 20(3), pp. 156–174. doi: 10.1038/s41580-018-0081-3.

Nativio, R. *et al.* (2018) 'Dysregulation of the epigenetic landscape of normal aging in Alzheimer's disease', *Nature Neuroscience*, 21(4), pp. 497–505. doi: 10.1038/s41593-018-0101-9.

Neal, K. C. *et al.* (2000) 'A new human member of the MYST family of histone acetyl transferases with high sequence similarity to Drosophila MOF', *Biochimica et Biophysica Acta - Gene Structure and Expression*, 1490(1–2), pp. 170–174. doi: 10.1016/S0167-4781(99)00211-0.

Nelson, M. R. *et al.* (2015) 'The support of human genetic evidence for approved drug indications', *Nature Genetics*. Nature Publishing Group, 47(8), pp. 856–860. doi: 10.1038/ng.3314.

Neuspiel, M. *et al.* (2008) 'Cargo-Selected Transport from the Mitochondria to Peroxisomes Is Mediated by Vesicular Carriers', *Current Biology*, 18(2), pp. 102–108. doi: https://doi.org/10.1016/j.cub.2007.12.038.

Noda, S. *et al.* (2020) 'Loss of Parkin contributes to mitochondrial turnover and dopaminergic neuronal loss in aged mice', *Neurobiology of Disease*, 136, p. 104717. doi: https://doi.org/10.1016/j.nbd.2019.104717.

Novak, I. *et al.* (2010) 'Nix is a selective autophagy receptor for mitochondrial clearance', *EMBO reports*. John Wiley & Sons, Ltd, 11(1), pp. 45–51. doi:

https://doi.org/10.1038/embor.2009.256.

Oh, C.-K. *et al.* (2017) 'S-Nitrosylation of PINK1 Attenuates PINK1/Parkin-Dependent Mitophagy in hiPSC-Based Parkinson's Disease Models', *Cell Reports*. Elsevier B.V., 21(8), pp. 2171–2182. doi: 10.1016/j.celrep.2017.10.068.

Okatsu, K. *et al.* (2012) 'PINK1 autophosphorylation upon membrane potential dissipation is essential for Parkin recruitment to damaged mitochondria', *Nature Communications*. Nature Publishing Group, 3, pp. 1–7. doi: 10.1038/ncomms2016.

Okatsu, K. *et al.* (2015) 'Phosphorylated ubiquitin chain is the genuine Parkin receptor', *Journal of Cell Biology*, 209(1), pp. 111–128. doi: 10.1083/jcb.201410050.

Olgiati, S. *et al.* (2016) 'DNAJC6 Mutations Associated With Early-Onset Parkinson's Disease', *Annals of Neurology*. John Wiley & Sons, Ltd, 79(2), pp. 244–256. doi: https://doi.org/10.1002/ana.24553.

Onishi, M. *et al.* (2021) 'Molecular mechanisms and physiological functions of mitophagy.', *The EMBO journal*, p. e104705. doi: 10.15252/embj.2020104705.

Ordureau, A. *et al.* (2014) 'Quantitative Proteomics Reveal a Feedforward Mechanism for Mitochondrial PARKIN Translocation and Ubiquitin Chain Synthesis', *Molecular Cell*, 56(3), pp. 360–375. doi: 10.1016/j.molcel.2014.09.007.

Ordureau, A. *et al.* (2018) 'Dynamics of PARKIN-Dependent Mitochondrial Ubiquitylation in Induced Neurons and Model Systems Revealed by Digital Snapshot Proteomics', *Molecular Cell*. Elsevier Inc., 70(2), pp. 211-227.e8. doi: 10.1016/j.molcel.2018.03.012.

Ordureau, A. *et al.* (2020) 'Global Landscape and Dynamics of Parkin and USP30-Dependent Ubiquitylomes in iNeurons during Mitophagic Signaling', *Molecular Cell*. Elsevier Inc., 77(5), pp. 1124-1142.e10. doi: 10.1016/j.molcel.2019.11.013.

Pacelli, C. *et al.* (2015) 'Elevated Mitochondrial Bioenergetics and Axonal

Arborization Size Are Key Contributors to the Vulnerability of Dopamine Neurons', *Current Biology*, 25(18), pp. 2349–2360. doi: 10.1016/j.cub.2015.07.050.

Padman, B. S. *et al.* (2013) 'The protonophore CCCP interferes with lysosomal degradation of autophagic cargo in yeast and mammalian cells', *Autophagy*. Taylor & Francis, 9(11), pp. 1862–1875. doi: 10.4161/auto.26557.

Paisan-Ruiz, C. *et al.* (2009) 'Characterization of PLA2G6 as a locus for dystonia-parkinsonism', *Annals of Neurology*. John Wiley & Sons, Ltd, 65(1), pp. 19–23. doi: https://doi.org/10.1002/ana.21415.

Pang, Z. P. *et al.* (2011) 'Induction of human neuronal cells by defined transcription factors', *Nature*, 476(7359), pp. 220–223. doi: 10.1038/nature10202.

Park, J. *et al.* (2006) 'Mitochondrial dysfunction in Drosophila PINK1 mutants is complemented by parkin', *Nature*, 441(7097), pp. 1157–1161. doi: 10.1038/nature04788.

Paul, S. and Pickrell, A. M. (2021) 'Hidden phenotypes of PINK1/Parkin knockout mice', *Biochimica et Biophysica Acta (BBA) - General Subjects*. Elsevier B.V., 1865(6), p. 129871. doi: 10.1016/j.bbagen.2021.129871.

Peleg, S. *et al.* (2016) 'The Metabolic Impact on Histone Acetylation and Transcription in Ageing', *Trends in Biochemical Sciences*. Elsevier Ltd, 41(8), pp. 700–711. doi: 10.1016/j.tibs.2016.05.008.

Phu, L. *et al.* (2020) 'Dynamic Regulation of Mitochondrial Import by the Ubiquitin System', *Molecular Cell*. Elsevier Inc., 77(5), pp. 1107-1123.e10. doi: 10.1016/j.molcel.2020.02.012.

Pickrell, A. M. *et al.* (2015) 'Endogenous Parkin Preserves Dopaminergic Substantia Nigral Neurons following Mitochondrial DNA Mutagenic Stress', *Neuron*, 87(2), pp. 371–381. doi: 10.1016/j.neuron.2015.06.034.

Pickrell, A. M. and Youle, R. J. (2015) 'The roles of PINK1, Parkin, and mitochondrial fidelity in parkinson's disease', *Neuron*. doi: 10.1016/j.neuron.2014.12.007.

Pittman, A. M., Fung, H. C. and de Silva, R. (2006) 'Untangling the tau gene association with neurodegenerative disorders', *Human Molecular Genetics*, 15(SUPPL. 2), pp. 188–195. doi: 10.1093/hmg/ddl190.

Poewe, W. *et al.* (2017) 'Parkinson disease', *Nature Reviews Disease Primers*, 3(1), p. 17013. doi: 10.1038/nrdp.2017.13.

Polymeropoulos, M. H. *et al.* (1996) 'Mapping of a gene for Parkinson's disease to chromosome 4q21-q23', *Science*, 274(5290), pp. 1197–1199. doi: 10.1126/science.274.5290.1197.

Polymeropoulos, M. H. *et al.* (1997) 'Mutation in the α-synuclein gene identified in families with Parkinson's disease', *Science*, 276(5321), pp. 2045–2047. doi: 10.1126/science.276.5321.2045.

Potting, C. *et al.* (2017) 'Genome-wide CRISPR screen for PARKIN regulators reveals transcriptional repression as a determinant of mitophagy', *Proceedings of the National Academy of Sciences*, p. 201711023. doi: 10.1073/pnas.1711023115.

Puri, R. *et al.* (2019) 'Mul1 restrains Parkin-mediated mitophagy in mature neurons by maintaining ER-mitochondrial contacts', *Nature Communications*. Springer US, 10(1), pp. 1–19. doi: 10.1038/s41467-019-11636-5.

Quadri, M. *et al.* (2013) 'Mutation in the SYNJ1 Gene Associated with Autosomal Recessive, Early-Onset Parkinsonism', *Human Mutation*. John Wiley & Sons, Ltd, 34(9), pp. 1208–1215. doi: https://doi.org/10.1002/humu.22373.

Quirós, P. M., Langer, T. and López-Otín, C. (2015) 'New roles for mitochondrial proteases in health, ageing and disease', *Nature Reviews Molecular Cell Biology*. Nature Publishing Group, 16(6), pp. 345–359. doi: 10.1038/nrm3984.

Radzisheuskaya, A. *et al.* (2021) ‘Complex-dependent histone acetyltransferase activity of KAT8 determines its role in transcription and cellular homeostasis’, *Molecular Cell*. Elsevier Inc., pp. 1–17. doi: 10.1016/j.molcel.2021.02.012.

Rakovic, A. *et al.* (2013) ‘Phosphatase and tensin homolog (PTEN)-induced Putative Kinase 1 (PINK1)-dependent ubiquitination of endogenous parkin attenuates mitophagy: Study in human primary fibroblasts and induced pluripotent stem cell-derived neurons’, *Journal of Biological Chemistry*, 288(4), pp. 2223–2237. doi: 10.1074/jbc.M112.391680.

Rakovic, A. *et al.* (2019) ‘PINK1-dependent mitophagy is driven by the UPS and can occur independently of LC3 conversion’, *Cell Death and Differentiation*. Springer US, 26(8), pp. 1428–1441. doi: 10.1038/s41418-018-0219-z.

Ramirez, A. *et al.* (2006) ‘Hereditary parkinsonism with dementia is caused by mutations in ATP13A2, encoding a lysosomal type 5 P-type ATPase’, *Nature Genetics*, 38(10), pp. 1184–1191. doi: 10.1038/ng1884.

Del Rey, N. L. G. *et al.* (2018) ‘Advances in parkinson’s disease: 200 years later’, *Frontiers in Neuroanatomy*, 12(December), pp. 1–14. doi: 10.3389/fnana.2018.00113.

Robak, L. A. *et al.* (2017) ‘Excessive burden of lysosomal storage disorder gene variants in Parkinson’s disease’, *Brain*, 140(12), pp. 3191–3203. doi: 10.1093/brain/awx285.

Roberts, R. F. *et al.* (2021) ‘Proteomic Profiling of Mitochondrial-Derived Vesicles in Brain Reveals Enrichment of Respiratory Complex Sub-assemblies and Small TIM Chaperones’, *Journal of Proteome Research*, 20(1), pp. 506–517. doi: 10.1021/acs.jproteome.0c00506.

Ryan, T. A. *et al.* (2020) ‘Tollip coordinates Parkin-dependent trafficking of

mitochondrial-derived vesicles', *The EMBO Journal*, pp. 1–21. doi: 10.15252/embj.2019102539.

Sandoval, H. *et al.* (2008) 'Essential role for Nix in autophagic maturation of erythroid cells', *Nature*, 454(7201), pp. 232–235. doi: 10.1038/nature07006.

Sarraf, S. A. *et al.* (2013) 'Landscape of the PARKIN-dependent ubiquitylome in response to mitochondrial depolarization', *Nature*. Nature Publishing Group, 496(7445), pp. 372–376. doi: 10.1038/nature12043.

Sauvé, V. *et al.* (2015) 'A Ubl/ubiquitin switch in the activation of Parkin', *The EMBO Journal*, 34(20), pp. 2492–2505. doi: 10.15252/embj.201592237.

Schmidt, O., Pfanner, N. and Meisinger, C. (2010) 'Mitochondrial protein import: from proteomics to functional mechanisms', *Nature Reviews Molecular Cell Biology*, 11(9), pp. 655–667. doi: 10.1038/nrm2959.

Schubert, A. F. *et al.* (2017) 'Structure of PINK1 in complex with its substrate ubiquitin', *Nature*. Nature Publishing Group, pp. 1–28. doi: 10.1038/nature24645.

Schwarten, M. *et al.* (2009) 'Nix directly binds to GABARAP: A possible crosstalk between apoptosis and autophagy', *Autophagy*. Taylor & Francis, 5(5), pp. 690–698. doi: 10.4161/auto.5.5.8494.

Schwartzentruber, A. *et al.* (2020) 'Oxidative switch drives mitophagy defects in dopaminergic parkin mutant patient neurons', *Scientific Reports*. Nature Publishing Group UK, 10(1), pp. 1–14. doi: 10.1038/s41598-020-72345-4.

Schweers, R. L. *et al.* (2007) 'NIX is required for programmed mitochondrial clearance during reticulocyte maturation', *Proceedings of the National Academy of Sciences*, 104(49), pp. 19500 LP – 19505. doi: 10.1073/pnas.0708818104.

Scott, H. L. *et al.* (2020) 'A dual druggable genome-wide siRNA and compound library screening approach identifies modulators of parkin recruitment to

mitochondria', *Journal of Biological Chemistry*, 295(10), pp. 3285–3300. doi: 10.1074/jbc.RA119.009699.

Seibler, P. *et al.* (2011) 'Mitochondrial parkin recruitment is impaired in neurons derived from mutant PINK1 induced pluripotent stem cells', *Journal of Neuroscience*, 31(16), pp. 5970–5976. doi: 10.1523/JNEUROSCI.4441-10.2011.

Shahmoradian, S. H. *et al.* (2019) 'Lewy pathology in Parkinson's disease consists of crowded organelles and lipid membranes', *Nature Neuroscience*, 22(7), pp. 1099–1109. doi: 10.1038/s41593-019-0423-2.

Shaltouki, A. *et al.* (2018) 'Alpha-synuclein delays mitophagy and targeting Miro rescues neuron loss in Parkinson's models', *Acta Neuropathologica*. Springer Berlin Heidelberg, (0123456789), pp. 1–14. doi: 10.1007/s00401-018-1873-4.

Sharma, S. and Rao, A. (2009) 'RNAi screening: Tips and techniques', *Nature Immunology*. Nature Publishing Group, 10(8), pp. 799–804. doi: 10.1038/ni0809-799.

Sheikh, B. N. and Akhtar, A. (2019) 'The many lives of KATs — detectors, integrators and modulators of the cellular environment', *Nature Reviews Genetics*. Springer US, 20(January). doi: 10.1038/s41576-018-0072-4.

Sheikh, B. N., Guhathakurta, S. and Akhtar, A. (2019) ' The non-specific lethal (NSL) complex at the crossroads of transcriptional control and cellular homeostasis ', *EMBO reports*, 20(7). doi: 10.15252/embr.201847630.

Shi, H. *et al.* (2017) 'Sirt3 protects dopaminergic neurons from mitochondrial oxidative stress', *Human Molecular Genetics*, 26(10), pp. 1915–1926. doi: 10.1093/hmg/ddx100.

Shi, Y. *et al.* (2012) 'Human cerebral cortex development from pluripotent stem cells to functional excitatory synapses', *Nature Neuroscience*. Nature Publishing Group, 15(3), pp. 477–486. doi: 10.1038/nn.3041.

Shi, Y., Kirwan, P. and Livesey, F. J. (2012) 'Directed differentiation of human pluripotent stem cells to cerebral cortex neurons and neural networks', *Nature Protocols*, 7(10), pp. 1836–1846. doi: 10.1038/nprot.2012.116.

Shiba-Fukushima, K. *et al.* (2012) 'PINK1-mediated phosphorylation of the Parkin ubiquitin-like domain primes mitochondrial translocation of Parkin and regulates mitophagy', *Scientific Reports*, 2(1), p. 1002. doi: 10.1038/srep01002.

Shiba-Fukushima, K. *et al.* (2014) 'Phosphorylation of Mitochondrial Polyubiquitin by PINK1 Promotes Parkin Mitochondrial Tethering', *PLoS Genetics*, 10(12). doi: 10.1371/journal.pgen.1004861.

Shiba-Fukushima, K. *et al.* (2017) 'Evidence that phosphorylated ubiquitin signaling is involved in the etiology of Parkinson's disease', *Human Molecular Genetics*, 26(16), pp. 3172–3185. doi: 10.1093/hmg/ddx201.

Shimin, Z. *et al.* (2010) 'Regulation of Cellular Metabolism by Protein Lysine Acetylation', *Science*. American Association for the Advancement of Science, 327(5968), pp. 1000–1004. doi: 10.1126/science.1179689.

Shimura, H. *et al.* (1999) 'Immunohistochemical and subcellular localization of parkin protein: Absence of protein in autosomal recessive juvenile parkinsonism patients', *Annals of Neurology*. John Wiley & Sons, Ltd, 45(5), pp. 668–672. doi: https://doi.org/10.1002/1531-8249(199905)45:5<668::AID-ANA19>3.0.CO;2-Z.

Simón-Sánchez, J. *et al.* (2009) 'Genome-wide association study reveals genetic risk underlying Parkinson's disease', *Nature Genetics*. Nature Publishing Group, 41(12), pp. 1308–1312. doi: 10.1038/ng.487.

Simon, R. P. *et al.* (2016) 'KATching-Up on Small Molecule Modulators of Lysine Acetyltransferases', *Journal of Medicinal Chemistry*, 59(4), pp. 1249–1270. doi: 10.1021/acs.jmedchem.5b01502.

Singh, F. and Ganley, I. G. (2021) ‘Parkinson’s disease and mitophagy: An emerging role for LRRK2’, *Biochemical Society Transactions*, 49(2), pp. 551–562. doi: 10.1042/BST20190236.

Singleton, A. B. *et al.* (2003) ‘α-Synuclein Locus Triplication Causes Parkinson’s Disease’, *Science*. American Association for the Advancement of Science, 302(5646), pp. 841–841. doi: 10.1126/science.1090278.

Singleton, A. and Hardy, J. (2019) ‘Progress in the Genetic Analysis of Parkinson’s Disease’, *Human Molecular Genetics*, (2), pp. 1–14. doi: 10.1093/hmg/ddz183.

Sliter, D. A. *et al.* (2018) ‘Parkin and PINK1 mitigate STING-induced inflammation’, *Nature*. Springer US, 561(7722), pp. 258–262. doi: 10.1038/s41586-018-0448-9.

Smith, E. R. *et al.* (2005) ‘A Human Protein Complex Homologous to the Drosophila MSL Complex Is Responsible for the Majority of Histone H4 Acetylation at Lysine 16’, *Molecular and Cellular Biology*, 25(21), pp. 9175–9188. doi: 10.1128/MCB.25.21.9175-9188.2005.

Snijder, B. *et al.* (2012) ‘Single-cell analysis of population context advances RNAi screening at multiple levels’, *Molecular Systems Biology*, 8(579). doi: 10.1038/msb.2012.9.

Son, S. M. *et al.* (2021) ‘Autophagy regulation by acetylation—implications for neurodegenerative diseases’, *Experimental and Molecular Medicine*. Springer US, 53(1), pp. 30–41. doi: 10.1038/s12276-021-00556-4.

Sonninen, T.-M. *et al.* (2020) ‘Metabolic alterations in Parkinson’s disease astrocytes’, *Scientific Reports*, 10(1), p. 14474. doi: 10.1038/s41598-020-71329-8.

Sorrentino, V. *et al.* (2017) ‘Enhancing mitochondrial proteostasis reduces amyloid-β proteotoxicity’, *Nature*. Nature Publishing Group, 552(7684), pp. 187–193. doi: 10.1038/nature25143.

Sorrentino, V., Menzies, K. J. and Auwerx, J. (2018) 'Repairing Mitochondrial Dysfunction in Disease', *Annual Review of Pharmacology and Toxicology*, 58, pp. 353–389. doi: 10.1146/annurev-pharmtox-010716-104908.

Soto-Beasley, A. I. *et al.* (2020) 'Screening non-MAPT genes of the Chr17q21 H1 haplotype in Parkinson's disease', *Parkinsonism & Related Disorders*. Elsevier Ltd, 78, pp. 138–144. doi: 10.1016/j.parkreldis.2020.07.022.

Soubannier, V., McLelland, G. L., *et al.* (2012) 'A vesicular transport pathway shuttles cargo from mitochondria to lysosomes', *Current Biology*. Elsevier Ltd, 22(2), pp. 135–141. doi: 10.1016/j.cub.2011.11.057.

Soubannier, V., Rippstein, P., *et al.* (2012) 'Reconstitution of Mitochondria Derived Vesicle Formation Demonstrates Selective Enrichment of Oxidized Cargo', *PLoS ONE*, 7(12). doi: 10.1371/journal.pone.0052830.

Soutar, M. P. M. *et al.* (2018) 'AKT signalling selectively regulates PINK1 mitophagy in SHSY5Y cells and human iPSC-derived neurons', *Scientific Reports*, 8(1), p. 8855. doi: 10.1038/s41598-018-26949-6.

Soutar, M. P. M. *et al.* (2019) 'FBS/BSA media concentration determines CCCP's ability to depolarize mitochondria and activate PINK1-PRKN mitophagy', *Autophagy*. Taylor & Francis, 15(11), pp. 2002–2011. doi: 10.1080/15548627.2019.1603549.

Soutar, M. P. M. *et al.* (2021) 'Regulation of mitophagy by the NSL complex underlies genetic risk for Parkinson's disease at Chr16q11.2 and on the MAPT H1 allele', *bioRxiv*, p. 2020.01.06.896241. doi: 10.1101/2020.01.06.896241.

Sowter, H. M. *et al.* (2001) 'HIF-1-dependent Regulation of Hypoxic Induction of the Cell Death Factors BNIP3 and NIX in Human Tumors', *Cancer Research*, 61(18), pp. 6669 LP – 6673.

Spillantini, M. G. *et al.* (1997) 'α-Synuclein in Lewy bodies', *Nature*, 388(6645), pp.

839–840. doi: 10.1038/42166.

Spinelli, J. B. and Haigis, M. C. (2018) ‘The multifaceted contributions of mitochondria to cellular metabolism’, *Nature Cell Biology*. Springer US, 20(7), pp. 745–754. doi: 10.1038/s41556-018-0124-1.

Sposito, T. *et al.* (2015) ‘Developmental regulation of tau splicing is disrupted in stem cell-derived neurons from frontotemporal dementia patients with the 10 + 16 splice-site mutation in MAPT’, *Human Molecular Genetics*, 24(18), pp. 5260–5269. doi: 10.1093/hmg/ddv246.

Stathakos, P. *et al.* (2020) ‘A monolayer hiPSC culture system for autophagy/mitophagy studies in human dopaminergic neurons’, *Autophagy*. Taylor & Francis, 00(00), pp. 1–17. doi: 10.1080/15548627.2020.1739441.

Stefansson, H. *et al.* (2005) ‘A common inversion under selection in Europeans’, *Nature Genetics*, 37(2), pp. 129–137. doi: 10.1038/ng1508.

Sugiura, A. *et al.* (2014) ‘A new pathway for mitochondrial quality control: mitochondrial-derived vesicles’, *The EMBO Journal*, 33(19), pp. 2142–2156. doi: 10.15252/embj.201488104.

Sun, N. *et al.* (2015) ‘Measuring In Vivo Mitophagy’, *Molecular Cell*, 60(4), pp. 685–696. doi: 10.1016/j.molcel.2015.10.009.

Surmeier, D. J. *et al.* (2011) ‘The Origins of Oxidant Stress in Parkinson’s Disease and Therapeutic Strategies’, *Antioxidants & Redox Signaling*. Mary Ann Liebert, Inc., publishers, 14(7), pp. 1289–1301. doi: 10.1089/ars.2010.3521.

Suzuki, S. *et al.* (2017) ‘Efficient induction of dopaminergic neuron differentiation from induced pluripotent stem cells reveals impaired mitophagy in PARK2 neurons’, *Biochemical and Biophysical Research Communications*. Elsevier Ltd, 483(1), pp. 88–93. doi: 10.1016/j.bbrc.2016.12.188.

Swatek, K. N. and Komander, D. (2016) 'Ubiquitin modifications', *Cell Research*. Nature Publishing Group, 26(4), pp. 399–422. doi: 10.1038/cr.2016.39.

Taipale, M. *et al.* (2005) 'hMOF Histone Acetyltransferase Is Required for Histone H4 Lysine 16 Acetylation in Mammalian Cells', *Molecular and Cellular Biology*, 25(15), pp. 6798–6810. doi: 10.1128/mcb.25.15.6798-6810.2005.

Tanaka, A. *et al.* (2010) 'Proteasome and p97 mediate mitophagy and degradation of mitofusins induced by Parkin', *Journal of Cell Biology*, 191(7), pp. 1367–1380. doi: 10.1083/jcb.201007013.

Tanner, C. M. *et al.* (2011) 'Rotenone, paraquat, and Parkinson's disease', *Environmental Health Perspectives*, 119(6), pp. 866–872. doi: 10.1289/ehp.1002839.

Taylor, E. B. and Rutter, J. (2011) 'Mitochondrial quality control by the ubiquitin-proteasome system', *Biochemical Society Transactions*, 39(5), pp. 1509–1513. doi: 10.1042/BST0391509.

Thenganatt, M. A. and Jankovic, J. (2014) 'Parkinson Disease Subtypes', *JAMA Neurology*, 71(4), pp. 499–504. doi: 10.1001/jamaneurol.2013.6233.

Thomas, K. J. *et al.* (2011) 'DJ-1 acts in parallel to the PINK1/parkin pathway to control mitochondrial function and autophagy', *Human Molecular Genetics*, 20(1), pp. 40–50. doi: 10.1093/hmg/ddq430.

Thomas, T. *et al.* (2008) 'Mof (MYST1 or KAT8) Is Essential for Progression of Embryonic Development Past the Blastocyst Stage and Required for Normal Chromatin Architecture', *Molecular and Cellular Biology*, 28(16), pp. 5093–5105. doi: 10.1128/mcb.02202-07.

Tian, R. *et al.* (2019) 'CRISPR Interference-Based Platform for Multimodal Genetic Screens in Human iPSC-Derived Neurons', *Neuron*. Elsevier Inc., 104(2), pp. 239-255.e12. doi: 10.1016/j.neuron.2019.07.014.

Toker, L. *et al.* (2021) ‘Genome-wide histone acetylation analysis reveals altered transcriptional regulation in the Parkinson’s disease brain’, *Molecular Neurodegeneration*. Molecular Neurodegeneration, 16(1), pp. 1–20. doi: 10.1186/s13024-021-00450-7.

Trinh, J. and Farrer, M. (2013) ‘Advances in the genetics of Parkinson disease’, *Nature Reviews Neurology*. Nature Publishing Group, 9(8), pp. 445–454. doi: 10.1038/nrneurol.2013.132.

Tsefou, E. *et al.* (2021) ‘Investigation of USP30 inhibition to enhance Parkin-mediated mitophagy : tools and approaches’, pp. 1–34.

Uesugi, R. *et al.* (2021) ‘Labeling and Measuring Stressed Mitochondria Using a PINK1-Based Ratiometric Fluorescent Sensor’, *Journal of Biological Chemistry*. Elsevier B.V, 297(5), p. 101279. doi: 10.1016/j.jbc.2021.101279.

Usher, J. L. *et al.* (2021) ‘Parkin drives pS65-Ub turnover independently of canonical autophagy in Drosophila’, *bioRxiv*, 3(2), p. 2021.06.10.447841. doi: 10.1101/2021.06.10.447841.

Valente, E. M. *et al.* (2004) ‘Hereditary early-onset Parkinson’s disease caused by mutations in PINK1’, *Science*, 304(5674), pp. 1158–1160. doi: 10.1126/science.1096284.

van de Ven, R. A. H., Santos, D. and Haigis, M. C. (2017) ‘Mitochondrial Sirtuins and Molecular Mechanisms of Aging’, *Trends in Molecular Medicine*. Elsevier Ltd, 23(4), pp. 320–331. doi: 10.1016/j.molmed.2017.02.005.

Vierbuchen, T. *et al.* (2010) ‘Direct conversion of fibroblasts to functional neurons by defined factors’, *Nature*, 463(7284), pp. 1035–1041. doi: 10.1038/nature08797.

Vilariño-Güell, C. *et al.* (2011) ‘VPS35 Mutations in Parkinson Disease’, *The American Journal of Human Genetics*. Elsevier, 89(1), pp. 162–167. doi:

10.1016/j.ajhg.2011.06.001.

Vives-Bauza, C. *et al.* (2010) 'PINK1-dependent recruitment of Parkin to mitochondria in mitophagy', *Proceedings of the National Academy of Sciences*, 107(1), pp. 378–383. doi: 10.1073/pnas.0911187107.

Wagner, G. R. and Payne, R. M. (2013) 'Widespread and enzyme-independent Nε-acetylation and Nε-succinylation of proteins in the chemical conditions of the mitochondrial matrix', *Journal of Biological Chemistry*. Â© 2013 ASBMB. Currently published by Elsevier Inc; originally published by American Society for Biochemistry and Molecular Biology., 288(40), pp. 29036–29045. doi: 10.1074/jbc.M113.486753.

Wang, C. *et al.* (2017) 'Scalable Production of iPSC-Derived Human Neurons to Identify Tau-Lowering Compounds by High-Content Screening', *Stem Cell Reports*. ElsevierCompany., 9(4), pp. 1221–1233. doi: 10.1016/j.stemcr.2017.08.019.

Wang, C. *et al.* (2019) 'Reciprocal Roles of Tom7 and OMA1 during Mitochondrial Import and Activation of PINK1', *Molecular Cell*. Elsevier Inc., pp. 1–16. doi: 10.1016/j.molcel.2019.01.002.

Wang, P. *et al.* (2017) 'Acetylation-induced TDP-43 pathology is suppressed by an HSF1-dependent chaperone program', *Nature Communications*. Springer US, 8(1), pp. 1–15. doi: 10.1038/s41467-017-00088-4.

Wani, W. Y. *et al.* (2017) 'O-GlcNAc regulation of autophagy and α-synuclein homeostasis; Implications for Parkinson's disease', *Molecular Brain*. Molecular Brain, 10(1), pp. 14–17. doi: 10.1186/s13041-017-0311-1.

Watzlawik, J. O. *et al.* (2020) 'Sensitive ELISA-based detection method for the mitophagy marker p-S65-Ub in human cells, autopsy brain, and blood samples', *Autophagy*. Taylor & Francis, 00(00), pp. 1–16. doi: 10.1080/15548627.2020.1834712.

Wauer, T. *et al.* (2015) ‘Mechanism of phospho-ubiquitin-induced PARKIN activation’, *Nature*, 524(7565), pp. 370–374. doi: 10.1038/nature14879.

Wauer, T. and Komander, D. (2013) ‘Structure of the human Parkin ligase domain in an autoinhibited state’, *The EMBO Journal*. John Wiley & Sons, Ltd, 32(15), pp. 2099–2112. doi: https://doi.org/10.1038/emboj.2013.125.

Wauters, F. *et al.* (2020) ‘LRRK2 mutations impair depolarization-induced mitophagy through inhibition of mitochondrial accumulation of RAB10’, *Autophagy*. Taylor & Francis, 16(2), pp. 203–222. doi: 10.1080/15548627.2019.1603548.

Whitworth, A. J. *et al.* (2005) ‘Increased glutathione S-transferase activity rescues dopaminergic neuron loss in a Drosophila model of Parkinson’s disease’, *Proceedings of the National Academy of Sciences of the United States of America*, 102(22), pp. 8024–8029. doi: 10.1073/pnas.0501078102.

Whitworth, A. J. and Pallanck, L. J. (2017) ‘PINK1/Parkin mitophagy and neurodegeneration—what do we really know in vivo?’, *Current Opinion in Genetics and Development*. Elsevier Ltd, 44, pp. 47–53. doi: 10.1016/j.gde.2017.01.016.

Williams, E. T. *et al.* (2018) ‘Parkin mediates the ubiquitination of VPS35 and modulates retromer-dependent endosomal sorting’, *Human Molecular Genetics*, 27(18), pp. 3189–3205. doi: 10.1093/hmg/ddy224.

Witoelar, A. *et al.* (2017) ‘Genome-wide pleiotropy between Parkinson disease and autoimmune diseases’, *JAMA Neurology*, 74(7), pp. 780–792. doi: 10.1001/jamaneurol.2017.0469.

Wong, Y. C. and Holzbaur, E. L. F. (2014) ‘Optineurin is an autophagy receptor for damaged mitochondria in parkin-mediated mitophagy that is disrupted by an ALS-linked mutation’, *Proceedings of the National Academy of Sciences*, 111(42), p. E4439 LP-E4448. doi: 10.1073/pnas.1405752111.

Wood-Kaczmar, A. *et al.* (2008) 'PINK1 is necessary for long term survival and mitochondrial function in human dopaminergic neurons', *PLoS ONE*, 3(6). doi: 10.1371/journal.pone.0002455.

Wray, S. and Lewis, P. A. (2010) 'A tangled web - tau and sporadic Parkinson's disease', *Frontiers in Psychiatry*, 1(DEC), pp. 1–7. doi: 10.3389/fpsyt.2010.00150.

Xicoy, H., Wieringa, B. and Martens, G. J. M. (2017) 'The SH-SY5Y cell line in Parkinson's disease research: a systematic review', *Molecular Neurodegeneration*. Molecular Neurodegeneration, 12(1), pp. 1–11. doi: 10.1186/s13024-017-0149-0.

Yamano, K. and Youle, R. J. (2013) 'PINK1 is degraded through the N-end rule pathway', *Autophagy*, 9(11), pp. 1758–1769. doi: 10.4161/auto.24633.

Yang, W. *et al.* (2016) 'Mitochondrial Sirtuin Network Reveals Dynamic SIRT3-Dependent Deacetylation in Response to Membrane Depolarization', *Cell*, 167(4), pp. 985-1000.e21. doi: 10.1016/j.cell.2016.10.016.

Yang, Y. *et al.* (2006) 'Mitochondrial pathology and muscle and dopaminergic neuron degeneration caused by inactivation of Drosophila Pink1 is rescued by Parkin', *Proceedings of the National Academy of Sciences*, 103(28), pp. 10793 LP – 10798. doi: 10.1073/pnas.0602493103.

Yi, W. *et al.* (2019) 'The landscape of Parkin variants reveals pathogenic mechanisms and therapeutic targets in Parkinson's disease', *Human Molecular Genetics*, 28(17), pp. 2811–2825. doi: 10.1093/hmg/ddz080.

Yoshii, S. R. *et al.* (2011) 'Parkin mediates proteasome-dependent protein degradation and rupture of the outer mitochondrial membrane', *Journal of Biological Chemistry*. Â© 2011 ASBMB. Currently published by Elsevier Inc; originally published by American Society for Biochemistry and Molecular Biology., 286(22), pp. 19630–19640. doi: 10.1074/jbc.M110.209338.

Zhang, J. and Ney, P. A. (2009) 'Role of BNIP3 and NIX in cell death, autophagy, and mitophagy', *Cell Death and Differentiation*. Nature Publishing Group, 16(7), pp. 939–946. doi: 10.1038/cdd.2009.16.

Zhang, T. *et al.* (2016) 'BNIP3 protein suppresses PINK1 kinase proteolytic cleavage to promote mitophagy', *Journal of Biological Chemistry*, 291(41), pp. 21616–21629. doi: 10.1074/jbc.M116.733410.

Zhang, Y. *et al.* (2013) 'Rapid single-step induction of functional neurons from human pluripotent stem cells', *Neuron*, 78(5), pp. 785–798. doi: 10.1016/j.neuron.2013.05.029.

Zhao, Q. *et al.* (2002) 'A mitochondrial specific stress response in mammalian cells', *EMBO Journal*, 21(17), pp. 4411–4419. doi: 10.1093/emboj/cdf445.

Zhou, D. *et al.* (2019) 'PGRN acts as a novel regulator of mitochondrial homeostasis by facilitating mitophagy and mitochondrial biogenesis to prevent podocyte injury in diabetic nephropathy', *Cell Death and Disease*, 10(7). doi: 10.1038/s41419-019-1754-3.

Zhu, Y. *et al.* (2013) 'Modulation of Serines 17 and 24 in the LC3-interacting Region of Bnip3 Determines Pro-survival Mitophagy versus Apoptosis * ', *Journal of Biological Chemistry*. Elsevier, 288(2), pp. 1099–1113. doi: 10.1074/jbc.M112.399345.

Zimprich, A. *et al.* (2004) 'Mutations in LRRK2 Cause Autosomal-Dominant Parkinsonism with Pleomorphic Pathology', *Neuron*. Elsevier, 44(4), pp. 601–607. doi: 10.1016/j.neuron.2004.11.005.

Zimprich, A. *et al.* (2011) 'A Mutation in VPS35, Encoding a Subunit of the Retromer Complex, Causes Late-Onset Parkinson Disease', *The American Journal of Human Genetics*. Elsevier, 89(1), pp. 168–175. doi: 10.1016/j.ajhg.2011.06.008.

Zollino, M. *et al.* (2012) ‘Mutations in KANSL1 cause the 17q21.31 microdeletion syndrome phenotype’, *Nature Genetics*. Nature Publishing Group, 44(6), pp. 636–638. doi: 10.1038/ng.2257.